CRCLEME
Cooperative Research Centre for
Landscape Environments
and Mineral Exploration

OPEN FILE
REPORT
SERIES

CSIRO

AMIRA
Australian Mineral Industries Research Association Limited ACN 004 448 266

GENESIS, CLASSIFICATION AND ATLAS OF FERRUGINOUS MATERIALS, YILGARN CRATON

R.R. Anand, M.D. Paine and R.E. Smith

CRC LEME OPEN FILE REPORT 73
April 2002

CRCLEME
Cooperative Research Centre for
Landscape Environments
and Mineral Exploration

OPEN FILE
REPORT
SERIES

CSIRO

AMIRA
Australian Mineral Industries Research Association Limited ACN 004 448 266

GENESIS, CLASSIFICATION AND ATLAS OF FERRUGINOUS MATERIALS, YILGARN CRATON

R.R. Anand, M.D. Paine and R.E. Smith

CRC LEME OPEN FILE REPORT 73
April 2002

RESEARCH ARISING FROM CSIRO/AMIRA YILGARN REGOLITH GEOCHEMISTRY PROJECTS 1987-1993

In 1987, CSIRO commenced a series of multi-client research projects in regolith geology and geochemistry which were sponsored by companies in the Australian mining industry, through the Australian Mineral Industries Research Association Limited (AMIRA). The initial research program, "Exploration for concealed gold deposits, Yilgarn Block, Western Australia" had the aim of developing improved geological, geochemical and geophysical methods for mineral exploration that would facilitate the location of blind, buried or deeply weathered gold deposits. The program commenced with the following projects:

P240: Laterite geochemistry for detecting concealed mineral deposits (1987-1991). Leader: Dr R.E. Smith.

Its scope was development of methods for sampling and interpretation of multi-element laterite geochemistry data and application of multi-element techniques to gold and polymetallic mineral exploration in weathered terrain. The project emphasised viewing laterite geochemical dispersion patterns in their regolith-landform context at local and district scales. It was supported by 30 companies.

P241: Gold and associated elements in the regolith - dispersion processes and implications for exploration (1987-1991). Leader: Dr C.R.M. Butt.

The project investigated the distribution of ore and indicator elements in the regolith. It included studies of the mineralogical and geochemical characteristics of weathered ore deposits and wall rocks, and the chemical controls on element dispersion and concentration during regolith evolution. This was to increase the effectiveness of geochemical exploration in weathered terrain through improved understanding of weathering processes. It was supported by 26 companies.

These projects represented 'an opportunity for the mineral industry to participate in a multi-disciplinary program of geoscience research aimed at developing new geological, geochemical and geophysical methods for exploration in deeply weathered Archaean terrains'. This initiative recognised the unique opportunities, created by exploration and open-cut mining, to conduct detailed studies of the weathered zone, with particular emphasis on the near-surface expression of gold mineralisation. The skills of existing and specially recruited research staff from the Floreat Park and North Ryde laboratories (of the then Divisions of Minerals and Geochemistry, and Mineral Physics and Mineralogy, subsequently Exploration Geoscience and later Exploration and Mining) were integrated to form a task force with expertise in geology, mineralogy, geochemistry and geophysics. Several staff participated in more than one project. Following completion of the original projects, two continuation projects were developed.

P240A: Geochemical exploration in complex lateritic environments of the Yilgarn Craton, Western Australia (1991-1993). Leaders: Drs R.E. Smith and R.R. Anand.

The approach of viewing geochemical dispersion within a well-controlled and well-understood regolith-landform and bedrock framework at detailed and district scales continued. In this extension, focus was particularly on areas of transported cover and on more complex lateritic environments typified by the Kalgoorlie regional study. This was supported by 17 companies.

P241A: Gold and associated elements in the regolith - dispersion processes and implications for exploration (1991-1993). Leader: Dr. C.R.M. Butt.

The significance of gold mobilisation under present-day conditions, particularly the important relationship with pedogenic carbonate, was investigated further. In addition, attention was focused on the recognition of primary lithologies from their weathered equivalents. This project was supported by 14 companies. Although the confidentiality periods of the above research projects have expired, the last in December 1994, they have not been made public until now. Publishing the reports through the CRC LEME Report Series is seen as an appropriate means of doing this. By making available the results of the research and the authors' interpretations, it is hoped that the reports will provide source data for future research and be useful for teaching. CRC LEME acknowledges the Australian Mineral Industries Research Association and CSIRO Division of Exploration and Mining for authorisation to publish these reports. It is intended that publication of the reports will be a substantial additional factor in transferring technology to aid the Australian mineral industry. Most reports related to the above research projects were published as CRC LEME Open File Reports Series (Nos 1-74), with an index (Report 75), by June 1999.

This report (CRC LEME Open File Report 73) is a complete rewrite of the original concept of CSIRO Division of Exploration Geoscience Restricted Report 60R, first issued in 1989, which formed part of the CSIRO/AMIRA Project P240. Consequently, Report EG60R has not been republished and is replaced by this one.

Copies of this publication can be obtained from:

The Publication Officer, c/- CRC LEME, CSIRO Exploration and Mining, P.O. Box 1130, Bentley, WA 6102, Australia.
Information on other publications in this series may be obtained from the above or from http://leme.anu.edu.au/

Cataloguing-in-Publication:
Anand, R.R.
Genesis, classification and atlas of ferruginous materials, Yilgarn Craton.
ISBN 0 642 28270 6
1. Geochemistry 2. Laterite - Western Australia
I. Paine, M.D. II. Smith, R.E. II. Title
CRC LEME Open File Report 73.
ISSN 1329-4768

TABLE OF CONTENTS

PREFACE AND EXECUTIVE SUMMARY

This report builds upon an earlier Atlas developed during the CSIRO/AMIRA Laterite Geochemistry project (1987-1991). The report fulfils an objective of the Cooperative Research Centre for Landscape Evolution and Mineral exploration (CRC LEME) Applications Group which was to prepare an Atlas of Ferruginous Materials to illustrate the morphology, composition and origin of ferruginous materials.

The report begins with the discussion on usage of the term 'laterite' and a summary of preferred lateritic profile terminology. This is followed by a discussion of the evolution of principal ferruginous materials and sources of Fe in duricrusts. Subsequent chapters discuss pisolith classification and review some classification schemes of ferruginous duricrust. The final chapter proposes a classification scheme of ferruginous materials.

The Atlas is based on the proposed classification scheme and is suitable for the field identification and classification of ferruginous materials. It contains detailed descriptions of the principal ferruginous materials including ferruginous saprolite, ferruginous clays, ferruginous mottles, lateritic residuum, ferricrete and iron segregations. Field relationships, microfabrics, mineralogical and chemical compositions are illustrated for each type.

R.R. Anand

Project Leader

1.0 INTRODUCTION

In Australia, exploration is hindered by a thick regolith[1], much of it produced by long and intense weathering. Concealed mineral deposits, like the bedrocks that host them, tend to be highly weathered and their appearance, mineralogy and chemistry are greatly altered. The same weathering processes, however, can result in geochemical dispersion patterns that, although weak, can form characteristic geochemical anomalies. In many situations, the geochemical anomaly arising from an ore deposit can be larger than the ore deposit itself, thus providing a larger target.

Ferruginous materials are abundant and widespread in the deeply weathered landscapes of the inter-tropical belt, particularly on the continental landmasses between latitude 35° N and 35° S. These take the form of crusts, gravels and diverse impregnations that are generally the products of complex chemical and mechanical weathering over long periods of geological time. Ferruginous duricrusts have been generally described as constituents of a deep weathering profile consisting of parent rock, saprolite, mottled zone and ferruginous duricrust. They are extensively used as a geochemical sampling medium in mineral exploration in many deeply weathered terrains around the world. Costa *et al* (1999) noted that, in the Brazilian Amazon, the 'laterites' offer practically the only geochemical sampling medium available for mineral exploration. Where profiles are capped with ferruginous duricrust, the upper saprolitic horizons are strongly leached, and lateral dispersion of most target and pathfinder elements is commonly very extensive, resulting in marked depletion of the elements and restricted anomalies. However, low-level anomalies may be present in the overlying ferruginous zone, either as pathfinder elements in resistant minerals, or as metals such as As, Au, Bi, Cu and Mo, bound to or contained within Fe oxides. Such anomalies have been reported in ferruginous duricrusts of Western Australia (e.g., Smith and Perdrix, 1983; Smith *et al.*, 1992; Anand *et al.*, 1993), Africa (Freyssinet *et al.*, 1989), India (Nair *et al.*, 1987) and South and Central America (Costa, 1993).

There is controversy over whether ferruginous duricrusts have formed *in situ* from the weathering of underlying bedrocks or developed in sediments (McFarlane, 1976; Milnes *et al.*, 1985; Nahon, 1986; Bourman *et al.*, 1987; Bardossy and Aleva, 1990; Ollier and Galloway, 1990; Anand, 1995; Anand, 1998). According to McFarlane (1976) and Nahon (1986), ferruginous duricrusts have formed *in situ* and their progressive formation can be traced from subsurface zones within the weathering profile through to the surface. Other authors (Ollier and Galloway, 1990) argue that ferruginous duricrust formed in transported materials in ancient alluvial channel systems, but now occupies high ground by virtue of relief inversion. Another view (Glassford and Semeniuk, 1995) is that duricrusts, in the eastern Yilgarn, are, in part, aeolian deposits. Brimhall *et al.* (1991) also advocate significant aeolian input to the bauxitic profiles of the Darling Range.

Some ferruginous duricrusts have certainly formed in colluvium, alluvium and aeolian materials (Anand, 1995; Anand, 1998). Consequently the geochemical relationship to mineralisation and bedrock, and the mechanisms of concentration of elements may differ according to the origin of these ferruginous materials. Ferruginous materials are postulated to concentrate Au and trace elements by at least three mechanisms, namely (a) residual accumulation, (b) local upward solution transport and precipitation of elements and (c) lateral solution transport and precipitation of elements on or in Fe oxides. All these mechanisms may operate to some extent in a particular setting, but the degree to which a particular mechanism dominates is governed by the nature of the material ferruginised, the timing of ferruginisation, characteristics of groundwater and the topographic setting.

---

[1] *Regolith is defined as the entire unconsolidated and secondarily recemented cover that overlies more coherent bedrock and has been formed by weathering, erosion, transport and/or deposition of older material. It includes fractured and weathered basement rocks, saprolites, soils, organic accumulations, glacial deposits, colluvium, alluvium, evaporitic sediments and aeolian deposits.*

Over the last 20 years in Australia, regional-and local-scale regolith and landscape models have provided a framework for the assessment of ferruginous regolith materials, particularly in the Yilgarn Craton. This Atlas provides an overview of the types of ferruginous materials found on the Yilgarn Craton, proposes environments for their formation and presents a scheme for their classification. It documents examples of the main types of ferruginous materials and provides distribution information, mineralogy and chemical compositions. The concepts and interpretations presented here draw from extensive studies of many districts and sites conducted as a component of several projects. The sites discussed in the text are shown in Figure 1.1.

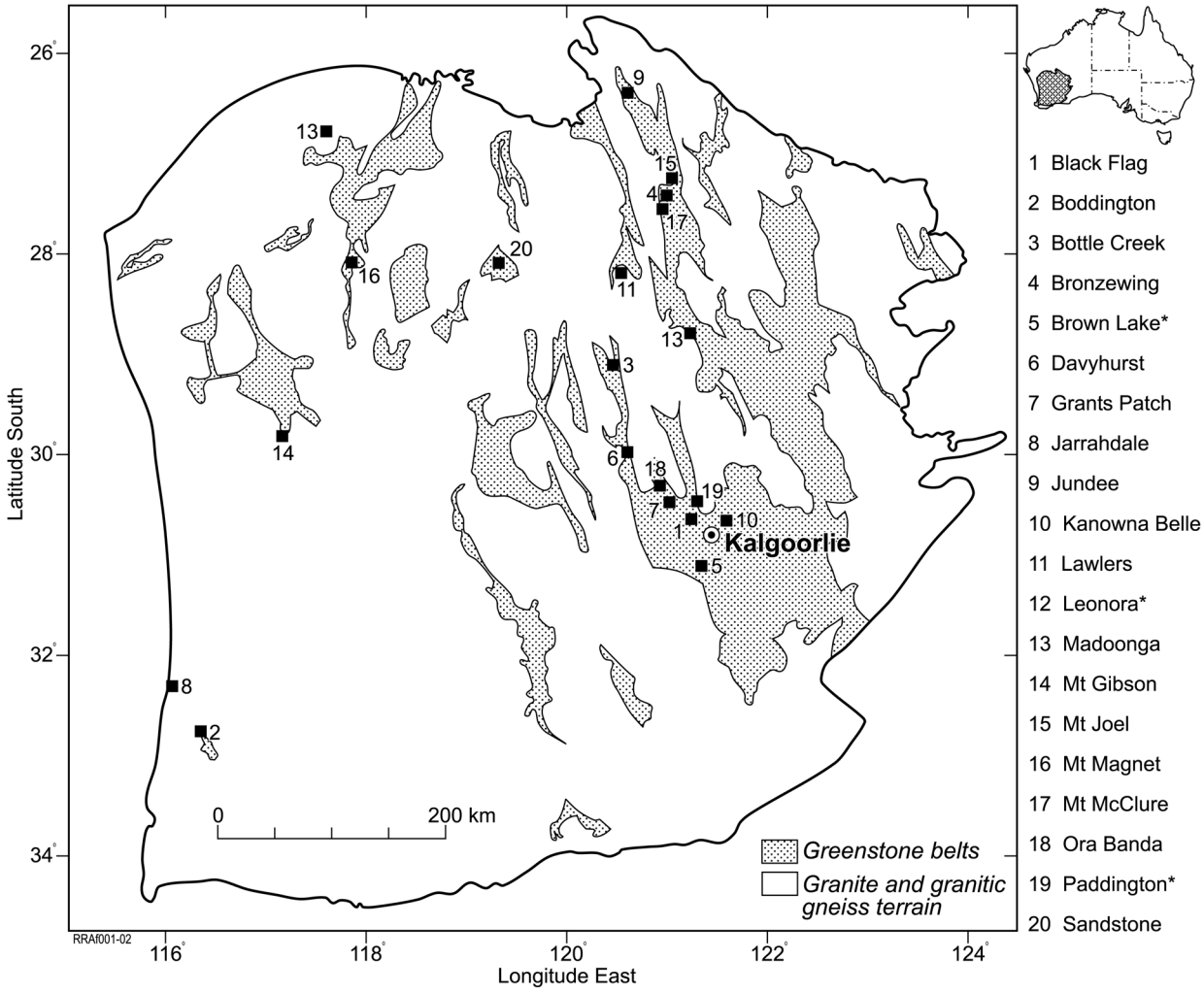

Figure 1.1 Location of the sites as referred to in the text. Gross bedrock geology of the Yilgarn Craton is also shown. Many sites are open cut goldmine exposures through the regolith. Local scale study sites are indicated with a (*) the remainder are district scale studies.

2.0 THE USAGE OF THE TERM 'LATERITE'

Laterites have been described in different ways and for different purposes; for pedologists they are soils, for engineers they are building materials or foundations and for geologists they are rocks or sample media. Table 2.1 lists some alternative terms and local names.

Table 2.1 A selection of terms for laterite (modified after Charman, 1988)

Brickstone (India)
Cabook (Ceylon)
Canga (Brazil)
Carapace (France)
Cuirasse (France)
Eisenkruste (Germany)
Ferricrete (Australia, Southern Africa, France)
Iron Clay (India)
Ironstone (Nigeria)
Krusteneisensteine (Germany)
Laterite (India, Australia)
Mantle rock (Ghana)
Moco de hierro (Venezuela)
Murram (East Africa)
Picarra (Brazil)
Pisolite (Australia)
Plinthite (USA)

The term 'laterite' was originally applied to Fe-rich material in Kerala (India) by Buchanan, 1807. It was sufficiently consolidated to be cut into building blocks (Figure 2.1), which hardened on exposure. However, the laterites of Kerala would now be regarded as vermiform mottles in saprolite. The crust is a separate entity largely used in Kerala for dry-stone walling. The extensive literature on 'laterite', since Buchanan, has produced a range of terms describing ferruginous duricrust. Ollier and Rajguru (1991) observed that 'laterite' is used to refer to both the indurated, mottled saprolite, as well as to concretionary material and, in Africa, to nodular and pisolitic material. In some African dialects, surficial materials that are generally red are called brick earth (Maignien, 1966) and the term 'laterite' refers to blocks used in construction (Prescott and Pendleton, 1952, in McFarlane, 1976).

McFarlane (1976) adopted the definition of Sivarajasingham *et al.* (1962) "laterites are highly weathered material, depleted in alkalis and alkaline earths, composed principally of secondary oxides and oxyhydroxides of iron (goethite, hematite, maghemite) and hydroxides of aluminium (gibbsite). These oxides may incorporate other minerals including clays and other secondary minerals (kaolinite, anatase), resistant primary minerals (quartz, zircon) and weatherable primary minerals (ilmenite, muscovite). According to Schellman (1983), laterites are products of intense subaerial rock weathering whose Fe and/or Al content is higher and Si content is lower than in merely kaolinised parent rocks. They consist of goethite, hematite, gibbsite, kaolinite and quartz. It is clear that Schellman's definition embraces anything more weathered than saprolite. Aleva (1986) includes only duricrust above mottled zone as 'laterite' whereas Millot (1964) grouped mottled zone and duricrust as 'laterite'. The term 'laterite' is used by some authors to refer to the whole weathering profile (ferruginous zone, mottled zone, saprolite) but the restricted usage, applying to the ferruginous/aluminous horizon only of such a profile, is more common.

Recently, a new view of 'laterite' has emerged. For example, Ollier (1991) preferred to define 'laterite' as reddish coloured mottled saprolite in a deep weathering profile. Several authors (Milnes *et al.*, 1985; Ollier and Galloway, 1990; Ollier, 1991) argued that the term 'laterite' should be abandoned, replacing it with 'ferricrete'. The term 'ferricrete' was originally used by Lamplugh (1902) to describe a ferruginous conglomerate of surficial sands and gravels cemented by Fe 'salts'. Subsequently it has been extended to include all Fe-cemented and indurated surface crusts and sub-surface horizons (e.g., Bourman, 1993) but provides little information about the materials which have been ferruginised. Hence, this term is also very general and imprecise. Furthermore, some authors (e.g., Ollier and Galloway, 1990) suggest that no relationship exists between the ferricrete and underlying saprolite zones, generally considered by others to be genetically linked to the 'laterite' as part of a 'complete' laterite profile (McFarlane, 1976; Nahon, 1986; Bardossy and Aleva, 1990; Nahon and Tardy, 1992). Laterite is perhaps best considered as an informal term and is used as a descriptor or adjective i.e. lateritic (Eggleton, 2001).

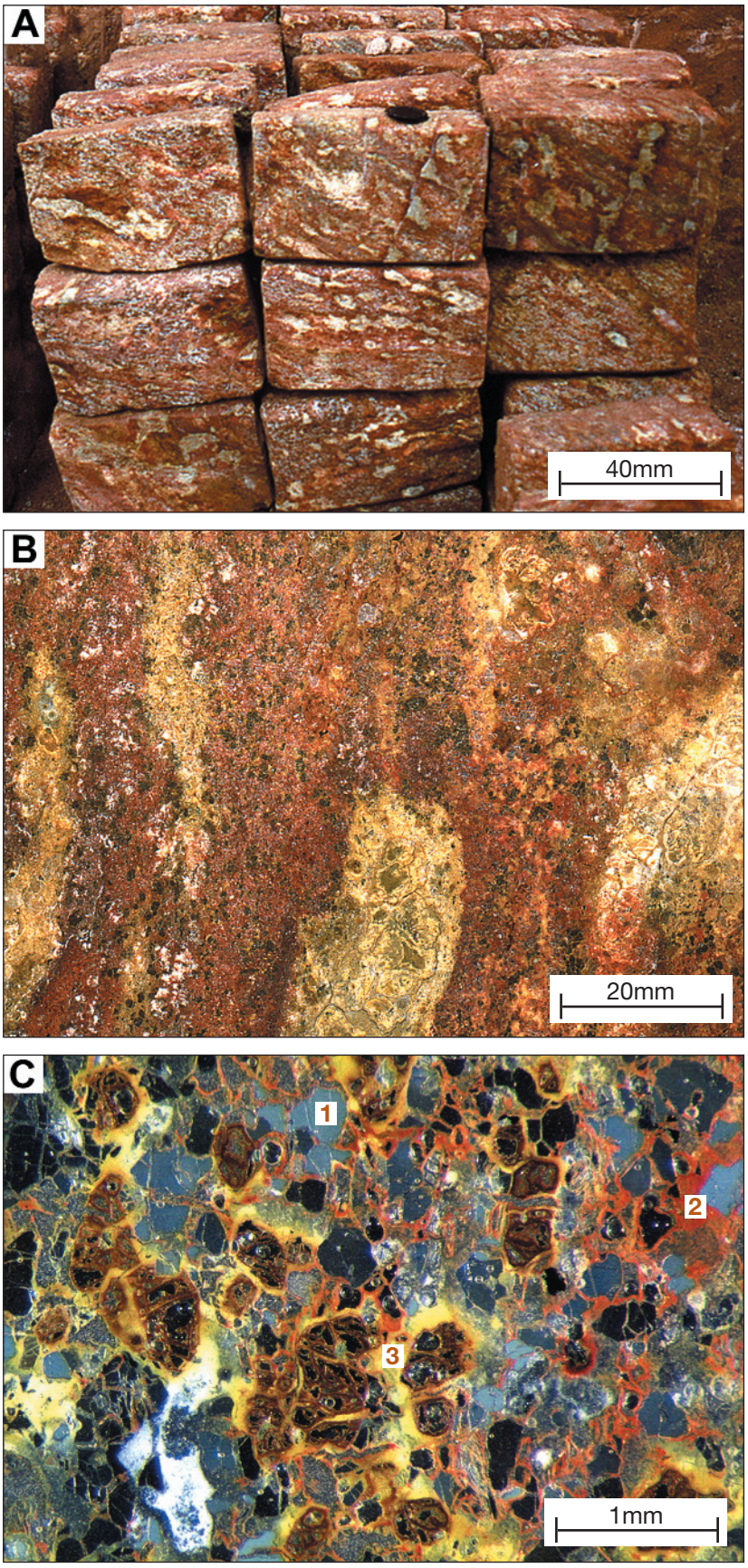

Chemical composition (XRF)

	Weight %
SiO_2%	53.3
Al_2O_3%	29.2
Fe_2O_3%	4.3
MgO%	0.15
Na_2O%	0.02
K_2O%	0.22
TiO_2%	0.72
LOI%	11.3
Total%	99.21
Cr	79 ppm
V	88 ppm
Ni	76 ppm
Zr	178 ppm

Figure 2.1 **The original "Laterite" from Kerala, India. (A) Laterite 'bricks' awaiting use, Angadipuram, Kerala. In the terminology of this atlas the specimen would be described as vermiform mottles in saprolite. (B) Close up photograph of a hand specimen showing elongate, vermiform orange to red mottles in a kaolinitic matrix. (C) A photomicrograph showing disagreggated angular to sub rounded quartz grains (1) set in hematitic clays (2). Goethite (3) forms a diffuse rim around some opaque minerals and quartz.**

3.0 PREFERRED LATERITIC PROFILE TERMINOLOGY

The study of regolith materials spans many disciplines of the earth sciences. Thus, many of the terms are used in different senses by the different disciplines. Some terms used herein are defined from the perspective of regolith geology and most of their definitions are given in Eggleton (2001).

The terminology for an idealised lateritic profile is summarised in Figure 3.1. A 'typical' deep weathering lateritic profile, described by Anand and Butt (1988), comprises fresh bedrock grading upwards into saprock, saprolite, a clay-rich (plasmic) or sand-rich (arenose) zone, a mottled zone and a lateritic residuum. The terminology used by other workers (Nahon and Tardy, 1992; Ollier and Galloway, 1990; Aleva, 1994; Millot, 1964) is also compared in Figure 3.1 to demonstrate the equivalence between different profile terminologies adopted in this Atlas and the related literature. The profile consists of two major components, the saprolith and the pedolith that are distinguished by their fabrics. The base of the saprolith is the boundary with fresh rock which forms the weathering front. The boundary between the *saprolith* and *pedolith* is termed the pedoplasmation front.

The *saprolith* is generally the lower part of the regolith that has retained the fabric originally expressed by the arrangement of the primary mineral constituents of the parent material. There are two major saprolith horizons, saprock and saprolite. *Saprock* is a compact, slightly weathered rock of low porosity (Trescases, 1992) with less than 20% of the weatherable minerals altered. Weathering occurs along mineral boundaries and intra-mineral fissures, along cleavages, shears, joints and fractures or affect only a few minerals. The first

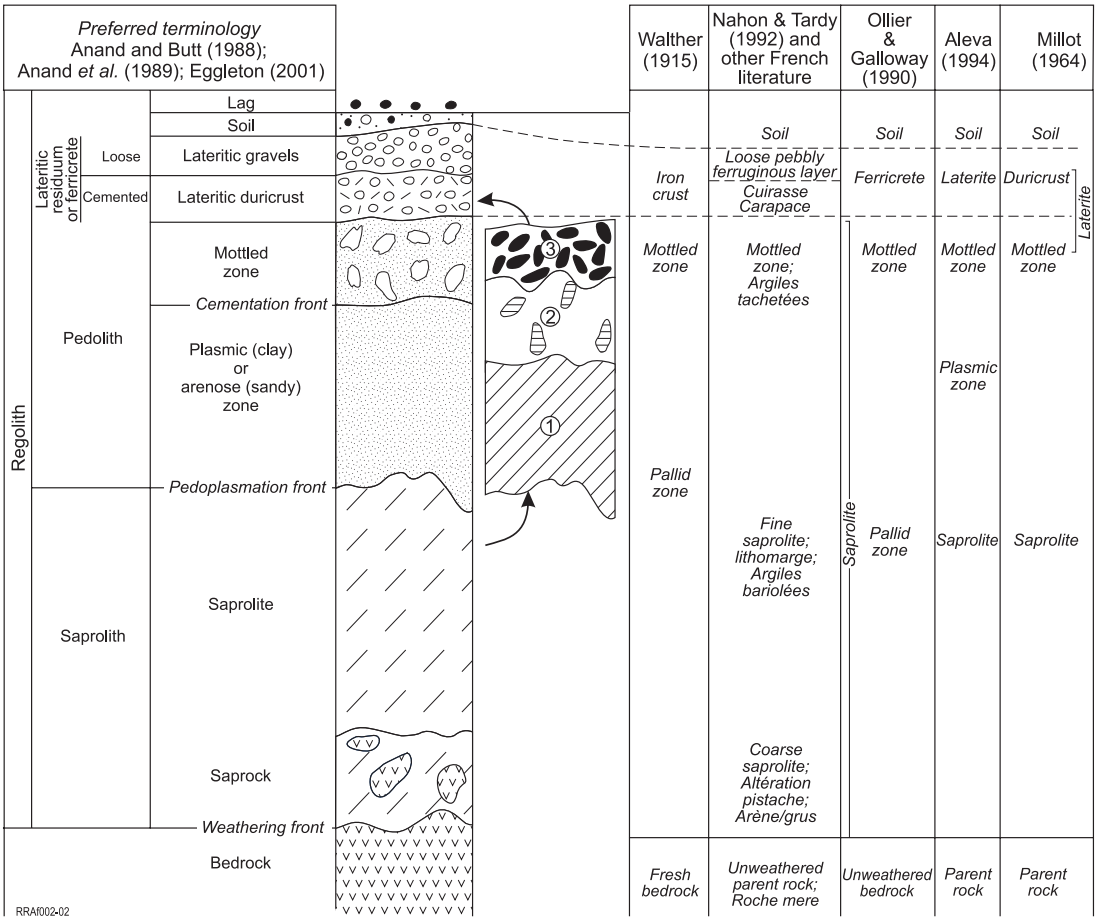

Figure 3.1 Comparisons of common terminologies for a deeply weathered profile.

signs of weathering are generally oxidation of sulphides and some easily weathered iron bearing silicates or breakdown of plagioclase feldspar to clay. The upper and lower boundaries of saprock may be sharp or gradational; it may vary markedly in depth and thickness over short distances with only minor lithological changes. It may not be possible to determine the upper boundary of saprock without petrographic study because it is difficult to determine the proportion of *weatherable* minerals in a hand specimen. *Saprolite* is weathered bedrock in which the fabric of the parent rock, originally expressed by the arrangement of primary minerals comprising the rock, is retained. Compared to saprock, saprolite has more than 20% of the weatherable materials altered. The saprolite is a product of a nearly iso-volumetric weathering, as also shown by quartz veins and corestones continuing undeflected from bedrock to the top of saprolite. The primary minerals can be pseudomorphically replaced by weathering products, retaining the fabric and structure of the parent rock. In the upper saprolite, most of the weatherable minerals have been altered to kaolinite, goethite and hematite; only quartz, zircon, chromite and other resistant minerals, remain unaffected. Saprolite may progressively lose its fabric upwards as the proportion of clay increases and cementation by secondary silica, aluminosilicates and, by Fe oxides increases. However, Fe oxides may preserve the fabric in places. Where Fe accumulation occurs without loss of the saprolitic fabric, the material is referred to as *ferruginous saprolite.* Where mottling occurs without loss of the saprolitic fabric it is referred to as *mottled saprolite.* Both are rightfully part of the saprolith rather than the pedolith. Mottled saprolite can be overlain by *collapsed mottled saprolite* (ferruginous breccia). Collapsed mottled saprolite is residual regolith consisting of fragments that display some of the lithic fabric of the underlying saprolite and bedrock. *Collapsed mottled saprolite* as a unit is part of the pedolith rather than the saprolith having lost any preexisting lithic fabric.

The *pedolith* is the upper part of the profile, above the pedoplasmation front, that has been subjected to soil forming processes resulting in the loss of the fabric of the parent rock and the development of new fabrics through non-isovolumetric weathering. The principal horizons of the pedolith are the *plasmic* or *arenose zone, mottled zone* and *lateritic residuum* (lateritic duricrust and lateritic gravel). Particular elements are concentrated in some horizons (Fe and Al in lateritic duricrust and gravel; Si, Ti and Zr in silcretes) and some have secondary structures such as collapsed structures, mottles, nodules and pisoliths.

The *plasmic horizon* is a mesoscopically homogeneous component of a weathering profile developed on quartz-poor rocks. It is dominated by clay or silty clay which has neither the relict fabric of saprolite nor the significant development of secondary segregations such as mottles, nodules or pisoliths. It is a transitional zone of settling and consolidation produced between saprolite and mottled zone by loss of fabric. The loss of lithic fabric is caused by solution and authigenisis of minerals and mechanical processes such as shrinking and swelling of clays and settling of resistant primary and secondary minerals through local instability induced by leaching. Although lithological contacts may be preserved, there is generally some distortion. The equivalent horizon on granitic rocks is the *arenose zone*. This is composed of shardy or very angular quartz sand, with a grain supported fabric. The loss of lithic fabric appears to be caused by solution and removal of kaolinite, and settling of resistant minerals, dominantly quartz. The plasmic and arenose horizons are not always present.

The *mottled zone* is that part of a weathering profile having macroscopic segregations of subdominant colour different from that of the surrounding matrix. The mottles may have sharp, distinct or diffuse boundaries; mostly there is a transition through a few millimeters of a goethite-rich haloe. They typically range in size from 10-100 mm, but may reach several metres in size. Mottles (< 10 mm) have been termed *minimottles* and those >200 mm are *megamottles* (Eggleton, 2001).

The terms *ferruginous duricrust, lateritic residuum* and *ferricrete* may be used to describe the upper part of a weathered ferruginous profile. *Ferruginous duricrust* may be used as a general term to describe regolith materials cemented by Fe, irrespective of the substrate origin. It includes residuum, ferruginised sediment or a mixture of these. The term *ferricrete* is used as a conglomerate of surficial sands and gravels cemented by Fe oxides in sense of Lamplugh (1902). *Lateritic residuum* is used as a collective term for the upper

ferruginous zone of the lateritic profile, composed dominantly of secondary oxides and oxy-hydroxides of Fe (goethite, hematite, maghemite), hydroxides of aluminium (e.g. gibbsite, boehmite) and kaolinite with or without quartz. It consists of *loose lateritic gravels* and/or *lateritic duricrust* that have developed essentially by residual processes and, therefore, have a broad genetic and compositional relationship with the substrate. Where both units are present, the gravels commonly overlie the lateritic duricrust and are formed by the *in situ* fragmentation of duricrust. Lateritic residuum has evolved by partial collapse of mottled or ferruginous saprolite, or the mottled zone involving local vertical and lateral (generally 10 -50 m) movement, following chemical wasting, as well as the introduction and mixing of exotic materials through soil forming and aeolian processes. The processes of Fe oxide precipitation, continued dissolution of clay, dehydration, nodule and pisolith development and collapse of mottled saprolite have probably been repeated several times. Field relationships with appropriate exposure are commonly needed to establish the genesis of particular lateritic gravel units. *Lateritic duricrust* is the indurated component of lateritic residuum. It may be massive or, more commonly, contain various secondary segregations such as nodules, pisoliths and ooliths, and structures such as open and infilled vermiform voids. *Lateritic gravels* are the unconsolidated component of lateritic residuum, consisting of loose ferruginous clasts (nodules, pisoliths and ooliths) and fragments, by convention in the size-range 2-64 mm. The gravels are commonly grain-supported and may have a clay-rich or sandy matrix. *Nodules* are irregular with re-entrant features whereas *pisoliths* are ellipsoidal or spherical. As the sphericity of nodules increases, they merge with *pisoliths*. Both nodules and pisoliths generally have an outer cutan or skin and the distinction between the two is based on shape rather than on absence or presence of cutans.

Few *soils* that had originally overlain the developing lateritic profiles are preserved. Most soils developed from, rather than with the material they overlie. These may include the ferruginous zones of "complete" profiles or the exposed horizons (e.g. mottled zone, saprolite or fresh bedrock) of truncated profiles.

Lag is the residual accumulation of coarse, usually hard, fragments that accumulate at the surface. It has been left as a residue after the physical and chemical dismantling of the upper horizons of the regolith and the removal of finer materials in solution, sheetwash or wind action.

4.0 EVOLUTION OF FERRUGINOUS MATERIALS ON THE YILGARN CRATON

4.1 Introduction

There are four general types of ferruginous materials in the landscapes of the Yilgarn Craton. These are: *ferruginous duricrust and gravel (lateritic residuum and ferricrete), ferruginous mottles, ferruginous saprolite and iron segregations*. They may occur as outcrop, subcrop, as loose surface aggregates contributing to the lag or occur buried beneath sediments. The relationships between these materials and the landscape are illustrated in Figures 4.1-4.3.

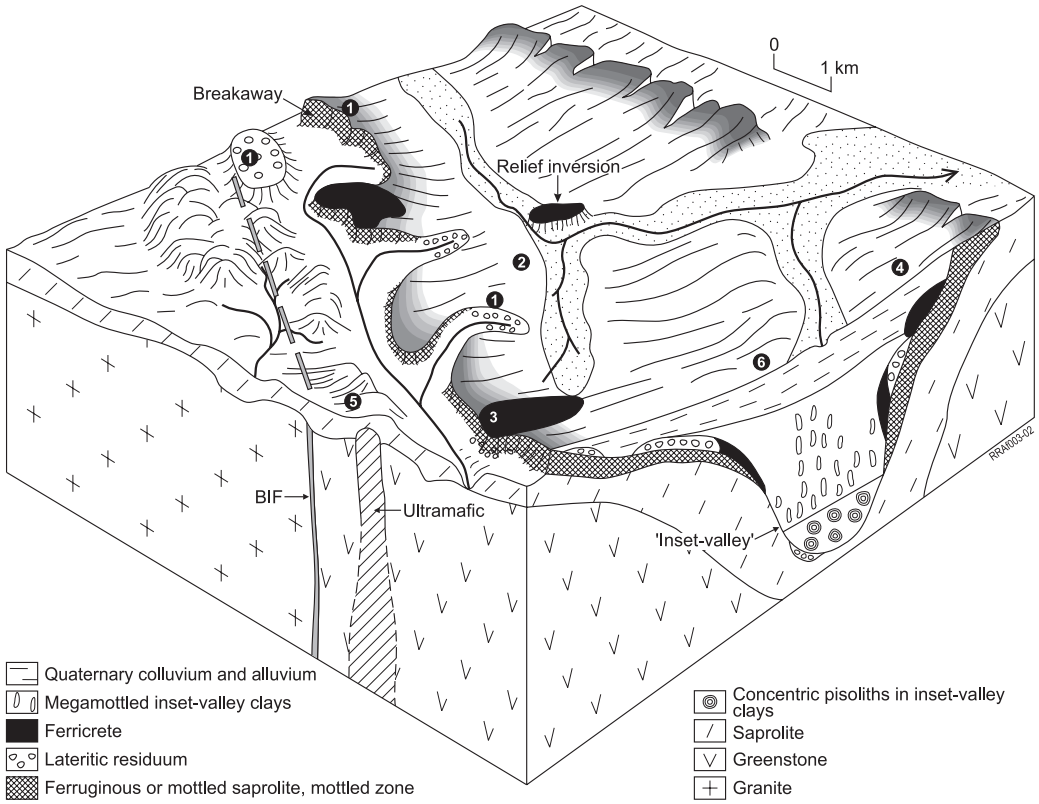

Figure 4.1 Block diagram showing the general relationships between landform and ferruginous regolith materials in the arid parts of the Yilgarn Craton. The numbers 1-6 show locations of the ferruginous profiles shown in Figure 4.2 (modified after Anand 2001).

4.2 Ferruginous duricrust and gravel

Ferruginous duricrust and gravel have developed in a variety of substrates in various topographic positions and geographic locations. They are abundant and bauxitic in the high rainfall zone of the Darling Range, but are not a continuous feature of the deeply weathered arid interior (Anand, 1998). In the Darling Range, the distribution of duricrust coincides with uplands. Inland, the ferruginous duricrust becomes kaolinitic and may form mesas, with Fe oxide-cemented, resistant, sub-horizontal upper surfaces. The softer parts of the profile below comprise the steeper slopes of breakaways. The Fe duricrust occurs on all rock types but is best developed on mafic and ultramafic rocks. Ferruginous duricrust and gravels also occur beneath surficial sediments on the intervening, gently inclined plains, particularly in the northeast, including Lawlers, Mt Gibson (Figure 4.3) and Mt McClure. It appears that transport of the Fe that formed a variety of ferruginous duricrusts in inland areas was related to ancient, wet epochs, and not to recent times which, in the eastern Yilgarn, are now too dry to permit significant mobilisation of Fe. Therefore, most duricrusts are old and

unrelated to the present climate. However, ferruginisation is still operating in humid regions of the Darling Range, especially on the edges of valley floors.

Some Eocene inset-valley sediments[1] contain detrital pisoliths, apparently eroded from ferruginous duricrust, implying that some ferruginous duricrust formed during or before the Eocene. This is consistent with the palaeomagnetic dating of the saprolite from several locations (including Kanowna Belle, North and Turrett Pits at Lawlers), which indicates Tertiary, Cretaceous and even Palaeozoic weathering imprints (B. Pillans, ANU, written communication, 2000). Evidence of continued ferruginisation lies in the weathering profiles in underlying bedrocks and in sediments including the middle to late Eocene inset valley and late Tertiary to Quaternary sediments, which have strongly pisolitic and mottled upper horizons and cemented duricrusts. Recent overprinting of ferruginisation has continued both inland and in the southwest. Inland, silicification, kaolinisation or calcification appears to have deferruginised duricrusts and mottled zones, by replacement and/or displacement. In the southwest, degradation of bauxitic duricrust continues by dissolution of goethite and gibbsite at or near the surface.

As a result of complex weathering and sedimentary processes, ferruginous duricrusts and gravels are developed in residual and transported material. Based on origin, two major types of ferruginous duricrusts are recognised, namely lateritic residuum and ferricrete (Anand, 1998).

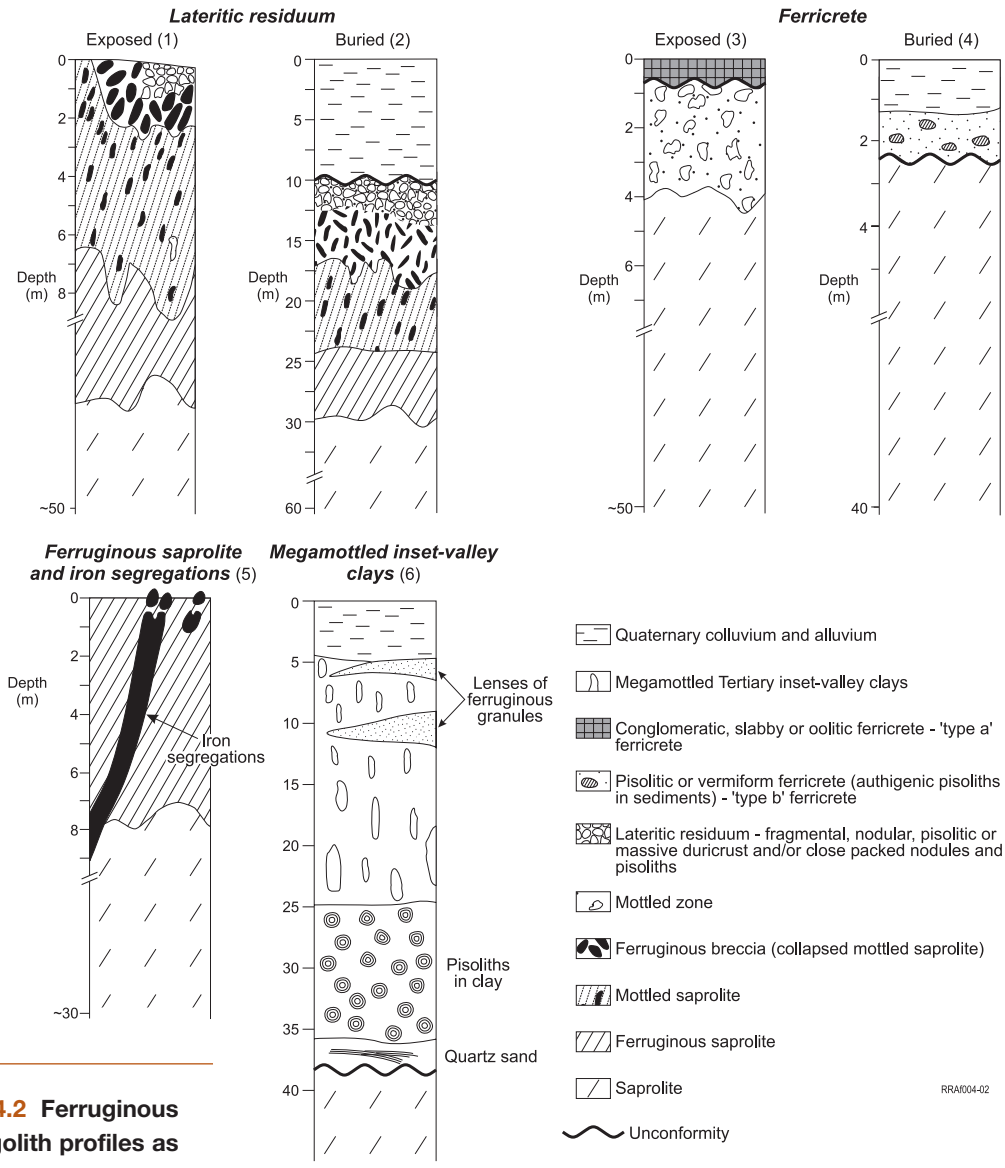

Figure 4.2 Ferruginous regolith profiles as indicated on Figure 4.1

[1] *Previously known as 'palaeochannels' and 'deep leads', they are herein termed 'inset-valleys' to emphasise their subordinate and entrenched position within the bedrock surface of a pre-existing network of much broader 'primary-valleys' (P. de Broekert, CRC LEME, written communication, 2000).*

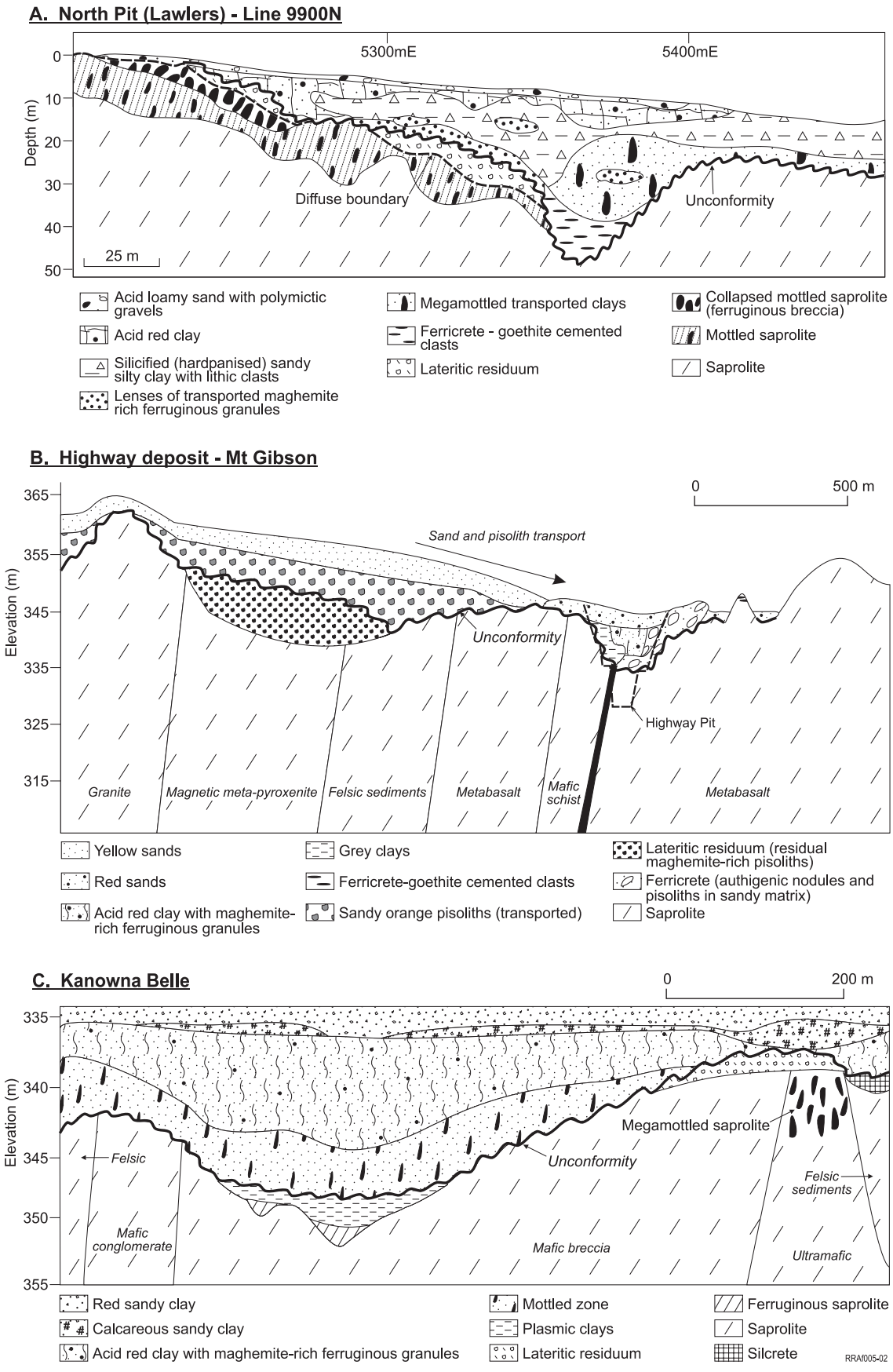

Figure 4.3 **Ferruginous materials distribution in depositional regimes at (A) North Pit, Lawlers (after Anand *et al*., 1991); (B) Highway deposit, Mt Gibson mining area and (C) Kanowna Belle (after Phang, Wildman and Anand, unpublished data).**

Lateritic residuum

Profiles capped with lateritic residuum may include, from top to base, a lag of nodules and pisoliths, pisolitic, nodular, fragmental or massive duricrust or closely packed nodules and pisoliths, ferruginous breccia (collapsed mottled saprolite), mottled saprolite, ferruginous saprolite, saprolite, saprock and bedrock (Figure 4.2). Lateritic residuum may be exposed (Figure 4.4 A-G), or buried beneath sediments (Figure 4.4H). It has evolved by partial collapse of mottled or ferruginous saprolite, involving local vertical and lateral (generally 10-50 m) movement, following chemical wasting, as well as the introduction and mixing of exotic material through soil forming and/or aeolian processes. The processes of Fe oxide precipitation, continued dissolution of clay, dehydration, nodule and pisolith development and collapse of mottled saprolite have probably been repeated several times. The use of the term residuum is not meant to imply that all of the residuum is *in situ*. Rather it has continually formed and been modified during the weathering by introduction of Si, Al, Ca and Fe. Chemically, the residuum is dominated by Si, Al and Fe oxides and consists of hematite, goethite, kaolinite and/or gibbsite and relict quartz in varying proportions, with hematite increasing upwards in the profile. Maghemite, if present, is typically restricted to the upper pisolitic part. Texturally, lateritic residuum can consist of loose or cemented lateritic nodules or pisoliths, or as duricrust commonly 1-3 m thick. The top 1-3 m of lateritic residuum is composed of lateritic nodules and pisoliths of 5-20 mm in diameter. Near the surface, they tend to be dark brown to black but are yellowish brown to brown in ferruginous breccia. The angularity of nodules increases down the profile. Two main types of nodules and pisoliths are recognised, lithic and non-lithic (Anand, 1995). Lithic types preserve the original rock fabric, whereas non-lithic types have one or more generations of Fe oxides disseminated through a clay-or sand-rich matrix. Where there has been extreme ferruginisation, the distinction is lost. The formation of goethite-rich cutans around nodules and pisoliths has been complex. Some cutans are formed at the expense of a hematite-rich core as suggested by Tardy and Nahon (1985) and others are the result of accretionary growth that may have proceeded by either inorganic or biogenic mechanisms (Anand and Paine, 2002).

Ferricrete

Ferricrete is a product of cementation of sediments by introduced Fe oxides. The type of ferricrete formed is controlled by the nature of the clasts and the cement (Anand, 1998). They commonly mark former palaeodrainages, swamps, discharge sites, valley floors, aquifers or groundwater mixing zones. They are either 'type a' formed by the cementation of detrital clasts, sands and clays by Fe oxides or a mixture of Fe oxides, kaolinite or gibbsite (Figure 4.5) or 'type b' authigenic hematite and goethite-rich pisoliths and nodules in sediments (Figure 4.6).

The characteristically narrow, linear to winding distribution of some 'type a' ferricretes fits with dendritic palaeodrainage patterns revealed by shallow, short wavelength signals associated with maghemite in aeromagnetic data (Anand, 2000). These often elevated ferricretes are mostly relics of a former, now inverted, depositional surface. Chan *et al*. (1992) described dendritic ferricretes as of possible Cretaceous age. However, Finkl and Fairbridge (1979) argued that some palaeodrainage relicts from the western part of the Yilgarn date from the Triassic.

'Type b' ferricretes are sandy clay or clay-rich sediments that have been modified by *in situ* formation of hematite and goethite-rich pisoliths or the development of vermiform or cellular fabrics, the internal structure of which is controlled by the original sediments. They are commonly overprinted by a later bleaching (Figure 4.6 D and E). The bleached areas are commonly cylindrical and are cored by tubes that may be filled with secondary kaolinite or silica. Kaolinite precipitation is a later event, superimposed on the ferruginisation (Figure 4.6 F). Widespread preservation of these tubes, presumably fossil root or solution cavity systems, attests to high permeability.

Ferricretes can be difficult to distinguish from lateritic residuum. They can be identified however, by their geomorphic relationships, the presence of an unconformity, preserved sedimentary structures, the presence of rounded quartz grains, transported clasts, broken cutans, abundant low-Al (<10 mole %) substituted colloform goethite and poorly crystalline kaolinite. Some clasts may contain goethite replaced fossil wood fragments (Anand, 1998).

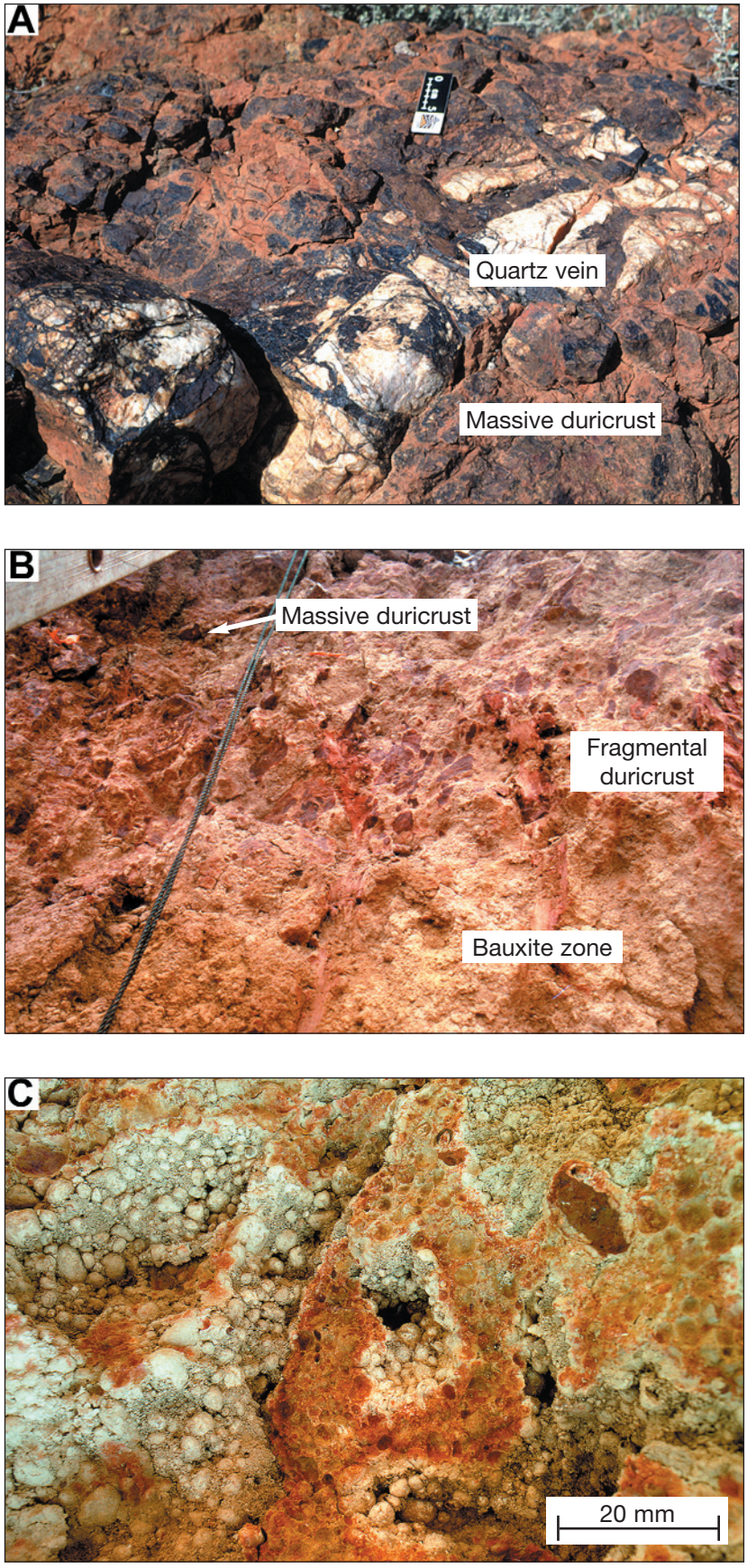

Figure 4.4 **Field photographs of exposed lateritic residuum. (A) A massive ferruginous duricrust on a crest trangressed by a quartz vein indicating that the duricrust has formed *in situ*, Mt Joel; (B) Upper part of a profile at Boddington showing residual massive duricrust overlying fragmental duricrust and bauxite zone; (C) Bauxitic pisolitic duricrust showing areas of dissolution of goethite and gibbsite resulting in packed ferruginous pisoliths, Boddington.**

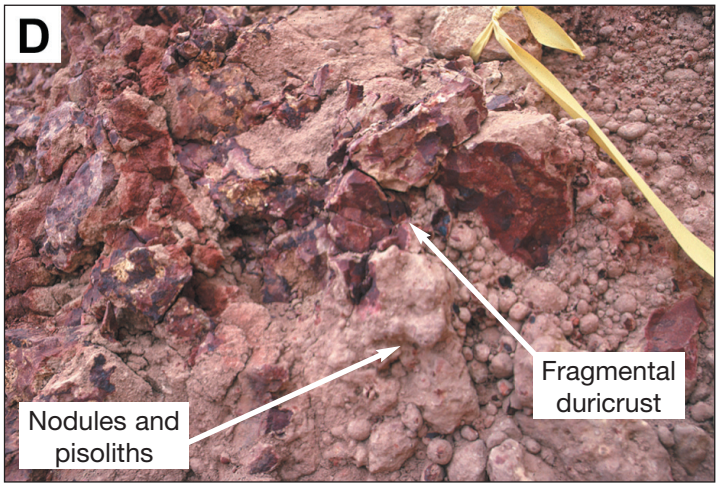

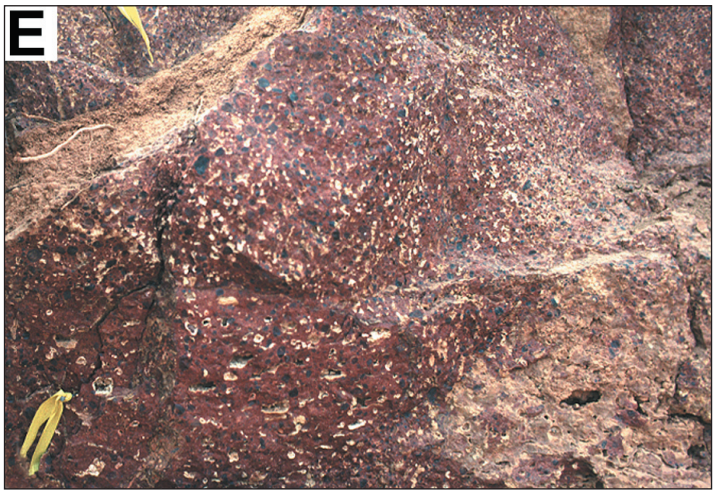

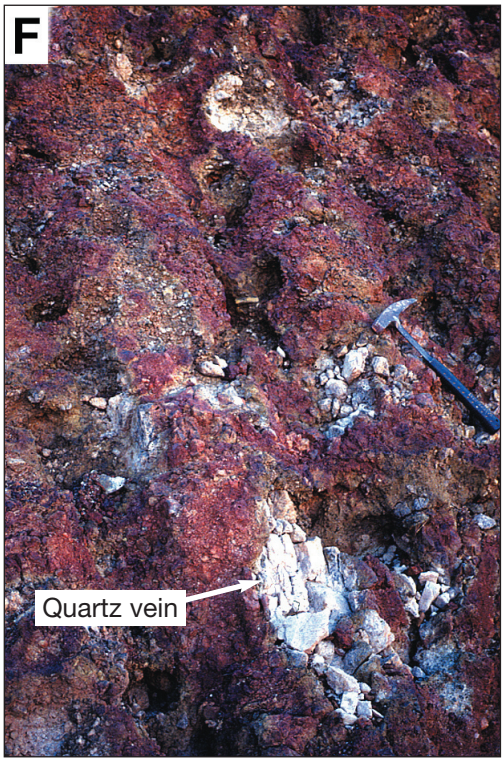

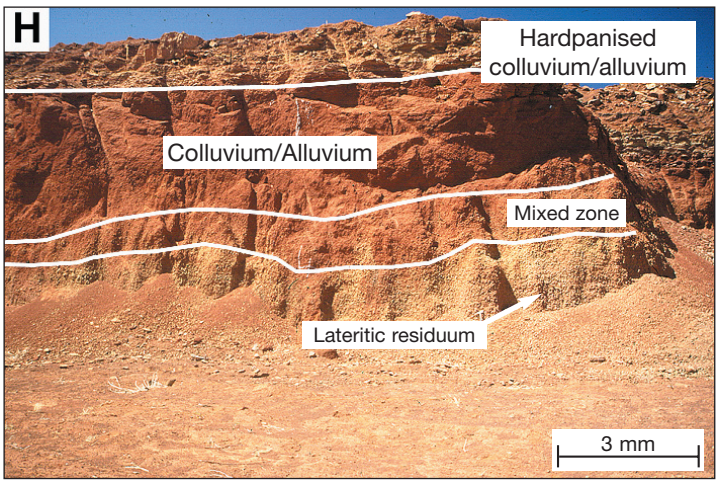

Figure 4.4 cont. **Field photographs of exposed and buried lateritic residuum. (D) Pitwall exposure showing fragmental duricrust surrounded by loose nodules and pisoliths, Boddington; (E) Pitwall exposure showing pisolitic duricrust with small, often lenticular voids filled with yellow, goethitic sandy clays, Boddington; (F) Pitwall exposure showing pisolitic duricrust with a remnant quartz vein, Lancefield; (G) Pitwall exposure showing loose goethitic nodules and pisoliths, Mt Gibson; (H) Pit wall exposure showing colluvium and alluvium overlying lateritic residuum, Empire Pit, Jundee.**

4.3 Ferruginous mottles

Mottling may be developed in saprolite, residual plasmic clays or sediments (4.7 A-D). It results from either the accumulation of Fe-rich material (brown-red mottles) or the loss of Fe (white mottles). Mottles formed in saprolite generally consist of brown, hematite-goethite-rich, tabular fragments aligned with the structure of the bedrock and are generally also visible in the saprock below. Mottled saprolite can be overlain by ferruginous breccia which, in turn, is overlain by lateritic residuum. Ferruginous breccia (breccia of mottled saprolite) is residual regolith consisting of fragments that retain the lithic fabric of the bedrock, although individual fragments may have lost their original orientation due to collapse. At Calista (Mt McClure), a ferruginous vein may be traced in the ferruginous breccia, where it becomes disjointed and terminates in a stone line (Figure 4.8). This vein is evidence of a residual profile. The collapse results from selective volume loss (e.g., by leaching, eluviation) of mottled saprolite and the settling of the resistant portions. The base of ferruginous breccia is very irregular, with pendants penetrating the underlying saprolite.

Ferruginous mottles developed in residual clays generally occur as spots, blotches and streaks that may become segregated into nodules and pisoliths. They result from pedogenic activity and are formed by migration and accumulation of Fe oxides in the kaolinitic matrix or voids.

Megamottles (>200 mm) (Ollier *et al.*, 1988) are typically developed in clay-rich materials (Figure 4.7 A, B and D) and are particularly common in inset-valley sediments. They are probably formed by mobilisation and segregation of Fe along old root systems commonly resulting in pale colored, Fe-poor clay-rich cylinders, with textures implicating root systems that are in some cases ancient and others current. Root systems penetrate mottled sediments and show an intimate relationship with Fe accumulations as these inset-valley sediments would have once supported abundant vegetation.

4.4 Ferruginous saprolite

Where Fe accumulation occurs without the loss of lithic fabric, the material is ferruginous saprolite (Figure 4.9A). Ferruginous saprolite is typically non-magnetic and largely composed of goethite, kaolinite and quartz with small amounts of hematite.

4.5 Iron segregations

Iron segregations form by the replacement and/or modification of iron-rich lithologies including sulphide-rich rocks or as exotic accumulation of Fe oxides along preferred pathways, such as fractures, faults and lithological contacts within saprolite (Figure 4.9 B and C). Erosion exposes iron segregations at the surface, where they disintegrate and contribute significantly to the lag, particularly on low hills. The McCaffery pit, at Lawlers, and its surroundings provide an excellent example of the development of these iron segregations (Figure 4.10) (Anand *et al.*, 1991). Mottled saprolite and the upper parts of the saprolite contain discrete Fe-enriched bodies ranging from a few centimeters to several metres in size. These generally occur along structural surfaces (joints, schistosity, bedding). Their flinty appearance contrasts with the firm, but rather fragile, mottled saprolite surrounding them.

Iron segregations are dense, dark brown to black and commonly are non-magnetic. They may have boxworks and goethite pseudomorphs after pyrite, pyrrhotite and other sulphides and solution cavities filled with chalcedony or goethite.

Detailed chemical and mineralogical analyses of iron segregations are reported in Anand *et al.*, (1991) and Smith *et al.*, (1992). The major and minor element composition of iron segregations differ from that of lateritic residuum in that they are relatively enriched in Fe, Mn, Zn, Co and relatively depleted in Al, Ti, Cr, V and Zr. They typically contain low Al-substituted, highly crystalline goethite.

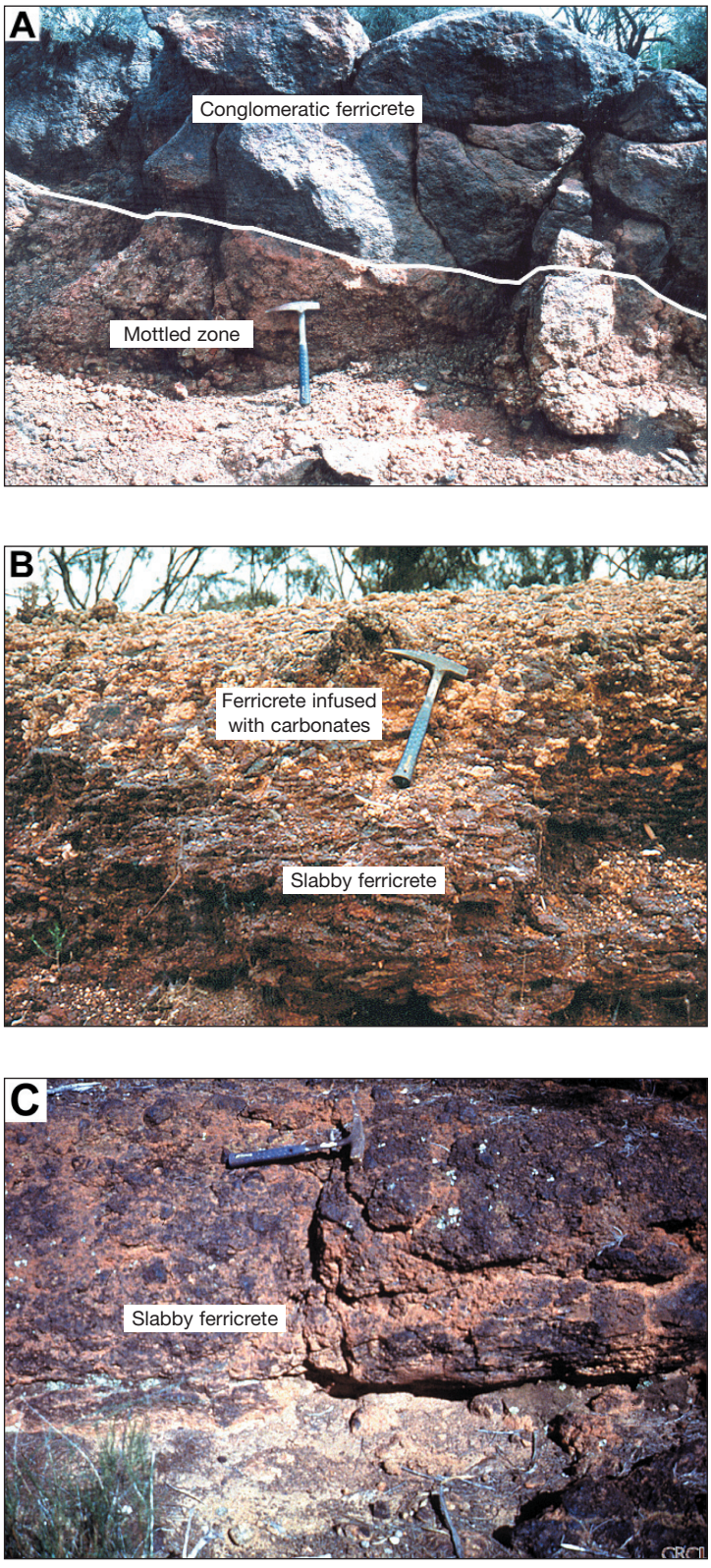

Figure 4.5 **Field photographs of "type a" ferricrete. (A) An outcrop of conglomeratic ferricrete unconformably overlying mottled zone on a crest at Grants Patch. The ferricrete has a marked pebbly/conglomeratic appearance and the hematite-maghemite-rich clasts are cemented by goethite; (B) An outcrop of slabby ferricrete at edges of a lake at Black Flag. The upper part of ferricrete is strongly infused with carbonates; (C) An outcrop of slabby ferricrete on a crest at Ularrie Hill, Bronzewing.**

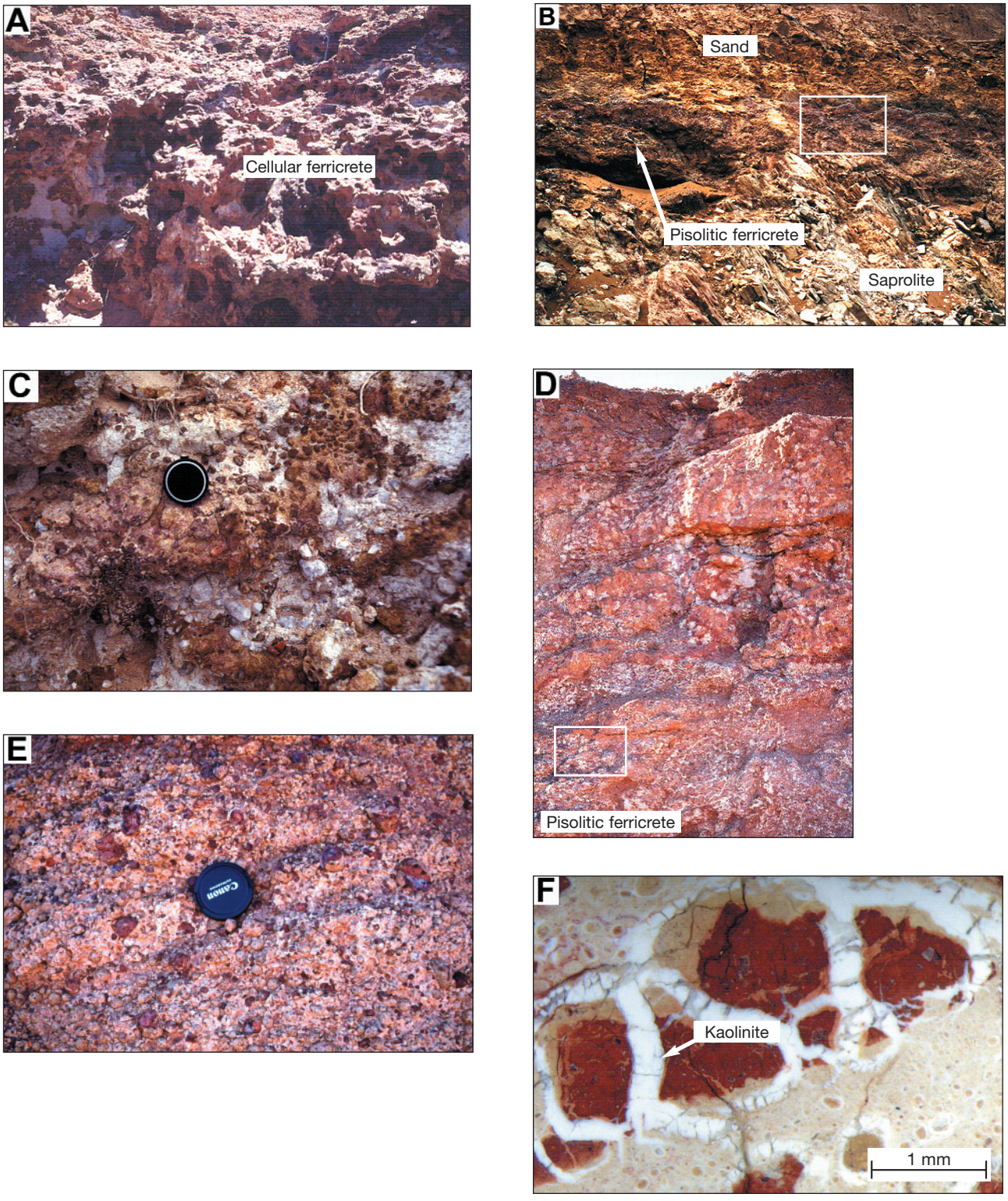

Figure 4.6 **Field photographs of ferricretes. (A) An outcrop of cellular ferricrete overlying mottled zone formed in inset-valley sediments, Wangine Soak, Davyhurst; (B) Mine exposure at the Wombat pit (Mt Gibson) showing pisolitic ferricrete unconformably overlying saprolite. The ferricrete is overlain by sand; (C) The inset photograph from (B) shows subrounded authigenic nodules and pisoliths in a clay matrix. Angular quartz pebbles also occur. (D) Pisolitic ferricrete (authigenic pisoliths in sediments) showing areas of deferruginisation. A subhorizontal fabric is preserved on an outcrop scale, Bulloak Pit, Sandstone; (E) The inset photograph from (D) shows pisoliths and nodules in a variably bleached clay matrix; (F) A photomicrograph of nodular ferricrete showing a ferruginous nodule in a kaolinitic matrix. The nodule exhibits cracks that are filled with secondary kaolinite.**

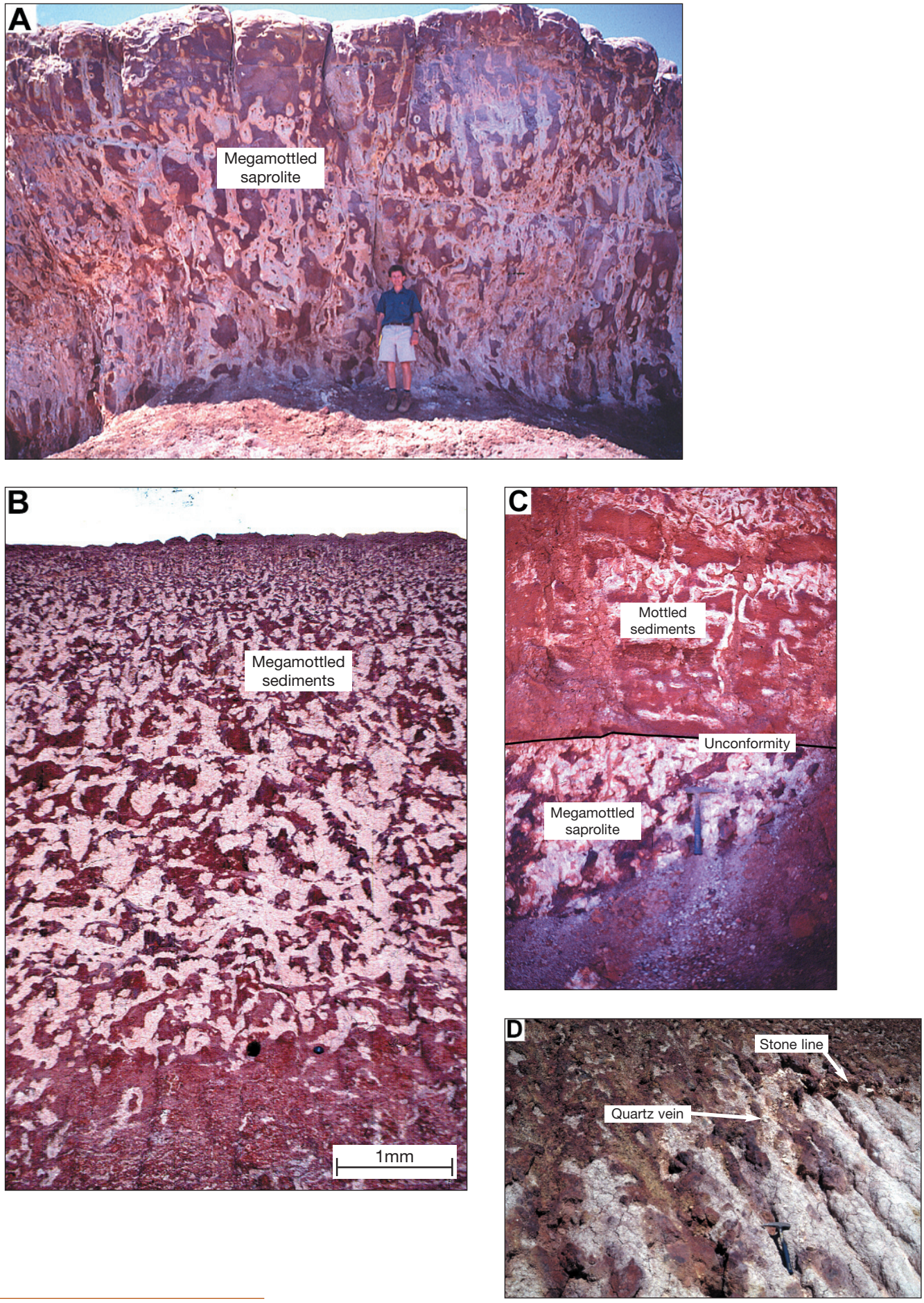

Figure 4.7 **Field photographs of mottled zones (A) Megamottled saprolite, Brown Lake; (B) Megamottled inset-valley sediments, Bronzewing. (C) Megamottled saprolite overlain by mottled sediments, Bulloak Pit, Sandstone; (D) Megamottled clays overlain by megamottled sediments, Mt McClure.**

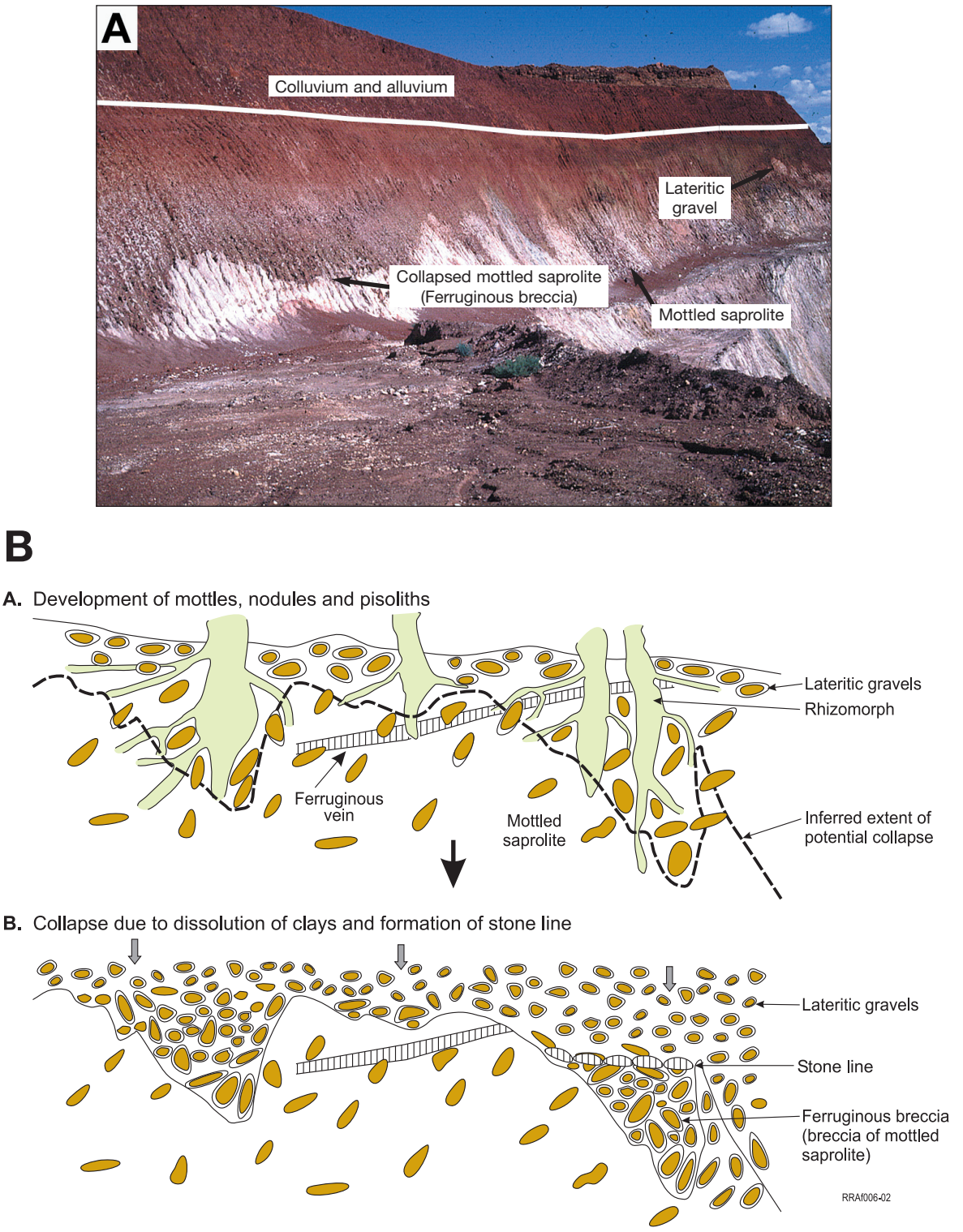

Figure 4.8 (A) Pendant-like features at Calista (Mt McClure) showing collapsed mottled saprolite overlying mottled saprolite. This grades upwards into a residual nodular and pisolitic unit and is overlain by colluvium and alluvium. (B) Interpreted model of the formation of pendant-like structures and associated ferruginous materials. The pendants appear to have resulted from chemical and physical weathering. The shape of the pendants may be governed by the preferential access of tree roots that enhance permeability.

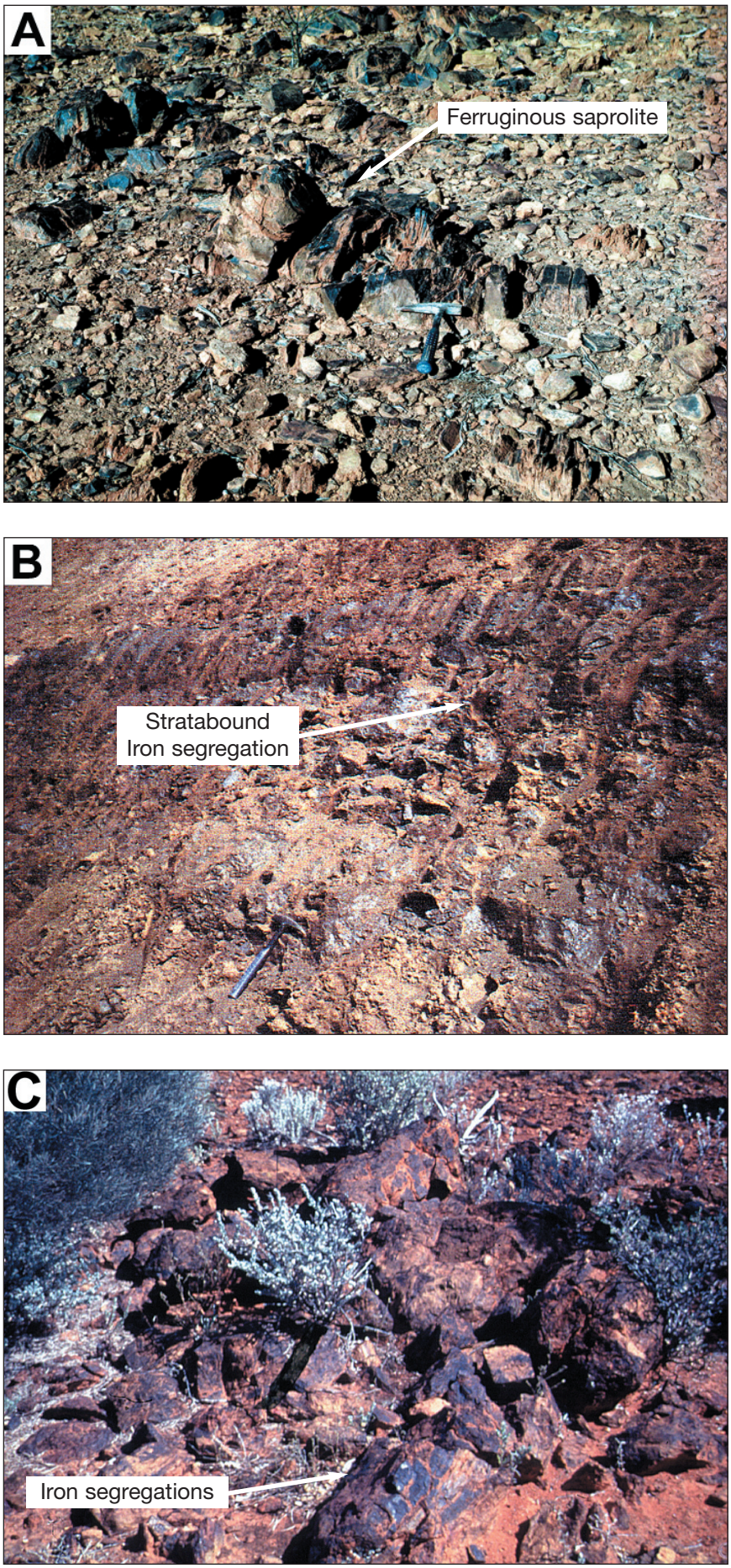

Figure 4.9 **Field photographs of ferruginous saprolite and iron segregations. (A) Ferruginous saprolite, Lawlers; (B) Stratabound hematite-goethite body comprising large, black hematite-goethite segregations within ferruginous saprolite, Lawlers; (C) Outcroping iron segregations, Jundee.**

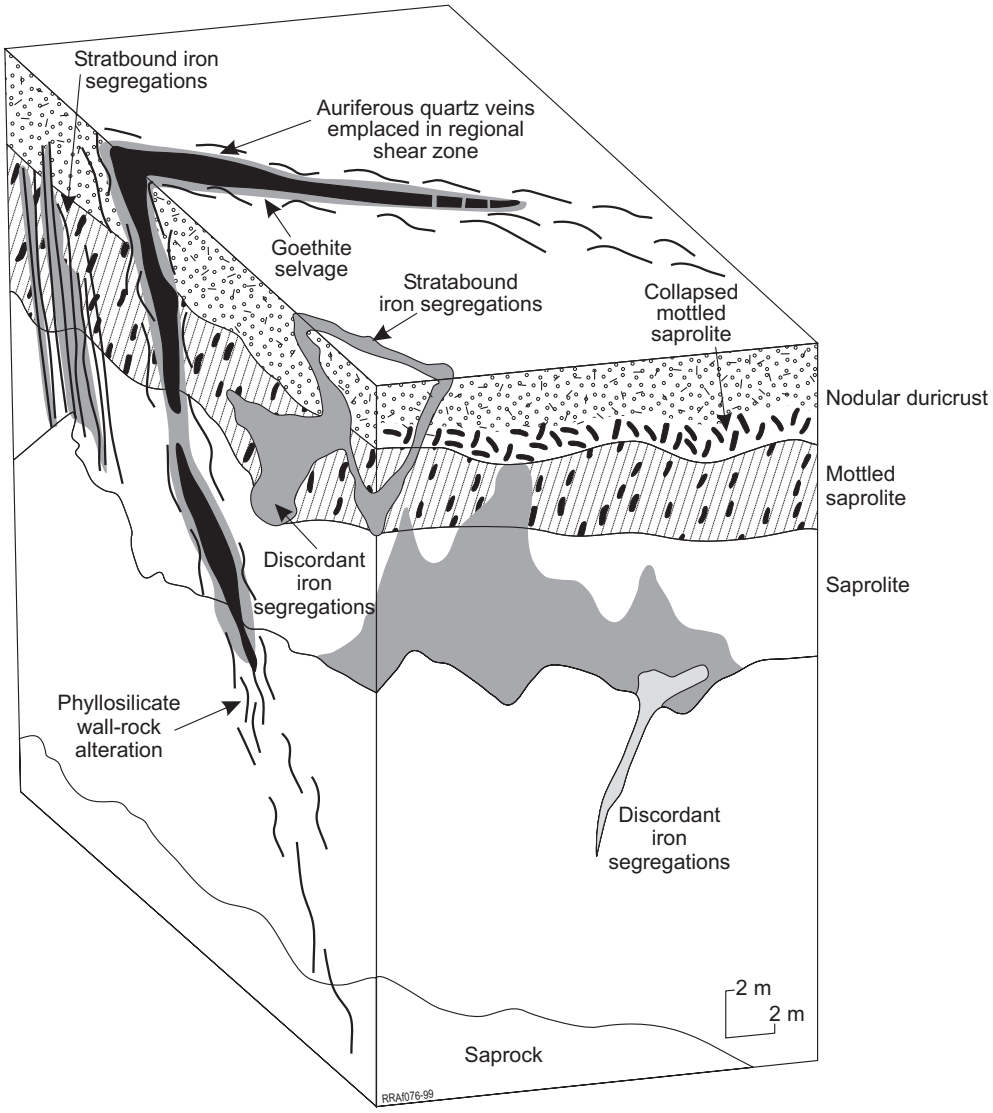

Figure 4.10 **Detailed block diagram showing field relationships for iron segregations, McCaffery Pit, Lawlers (after Anand *et al.,* 1991).**

5.0 SOURCES OF IRON IN FERRUGINOUS DURICRUSTS

Duricrust within a profile generally contains more iron than could be derived from the weathering of the underlying saprolite (Ollier and Galloway, 1990). The presence of an Fe-depleted horizon or 'pallid zone', led to the theory of upward enrichment. Suggestions included seasonal fluctuation of the water-table and/or capillary action that brought about simultaneous depletion of the lower and enrichment of the upper horizons. Some workers have explained the extra amounts of Fe in relation to the underlying saprolite by general landscape lowering (e.g., Trendall, 1962; Tardy and Roquin, 1992; Mann and Ollier, 1985) whereas others (e.g., Bourman, 1993; Ollier and Pain, 1996; Pain, 1998) by lateral and oblique movement of Fe. Trendall (1962), using the Fe content of granite and the 'laterite' over it in Uganda, calculated that 14 m of granite would be required to produce 0.3 m of 'laterite' and proposed an overall process of ground surface lowering to account for a surface covered with 'laterite'. Up to 3 km of surface lowering have been calculated by Tardy and Roquin (1992) for Madagascar. Nahon (1991) gives an average rate for surface lowering of 20 m per million years, but suggests that mafic rocks might be lowered at two to three times this rate. Using the Yilgarn Craton as an example, part of which has been subaerially exposed since the Permian, with a humid tropical climate for at least 200 million years, Ollier and Pain (1996) propose that, by using this model a surface lowering of 4 km on granite, and 8-12 km on the greenstones would result. According to these authors however, two main objections may be raised to total landscape lowering. Firstly, details of weathering profiles and catenas may produce evidence of lateral movement of solution, which would be an effective alternative to vertical movement. Secondly, many landscapes have very old features and deposits that are incompatible with surface lowering of more than a few metres. Examples include Permian glacial pavements, Tertiary lava flows, sediments deposited during marine incursions, and even ferruginous duricrusts dated (by palaeomagnetism) to early Tertiary or Mesozoic times.

Data on ferruginous duricrusts from the Yilgarn Craton suggest that both vertical and lateral accumulation of Fe have contributed to their formation, depending upon the landscape position. Some of these situations (Figure 5.1) illustrate this point. Lowering of the landsurface in the formation of lateritic residuum is suggested through collapse, accompanied by some removal of Fe oxides and clays by physical erosion and chemical dissolution (Anand, 1998). Here, the relationship between the Fe in residuum and the underlying bedrock suggests that Fe is largely derived from weathering of underlying rocks by upward and downward movement with minor lateral input. For example, at Boddington felsic andesite has 6% Fe_2O_3 but the overlying duricrust has about 25% (Anand, 1998). The concentration factor of about 4 is the same for TiO_2 and Zr. It is therefore concluded that the Fe, Ti and Zr represent relatively immobile elements from the weathering of the underlying rock that formally occupied a greater thickness. Similarly, examination of Davy's (1979) data by Eggleton and Taylor (1998) indicates that, assuming Ti, Zr and Nb are relatively immobile, the Fe in the profile is largely locally derived. However, it is not accepted that the duricrust was condensed by as much as suggested by Tardy and Roquin (1992). The extent of lowering is unknown and it is difficult to calculate from mass balance calculations (Ti and Zr are mobile to some extent). Lowering of a few metres is probable and consistent with preservation of Permian and Eocene sediments in old valleys in the eastern Yilgarn.

There has been significant lateral accumulation of Fe in materials developed in sediments (Figure 5.1). Iron is concentrated by both lateral and vertical accumulations in 'type b' ferricretes, where pisoliths have formed *in situ*. This contrasts with 'type a' ferricretes that have developed in a variety of materials in lowlands and palaeodrainages, largely by lateral accumulation of Fe. Some of these now form low hills, due to relief inversion (Figure 5.1).

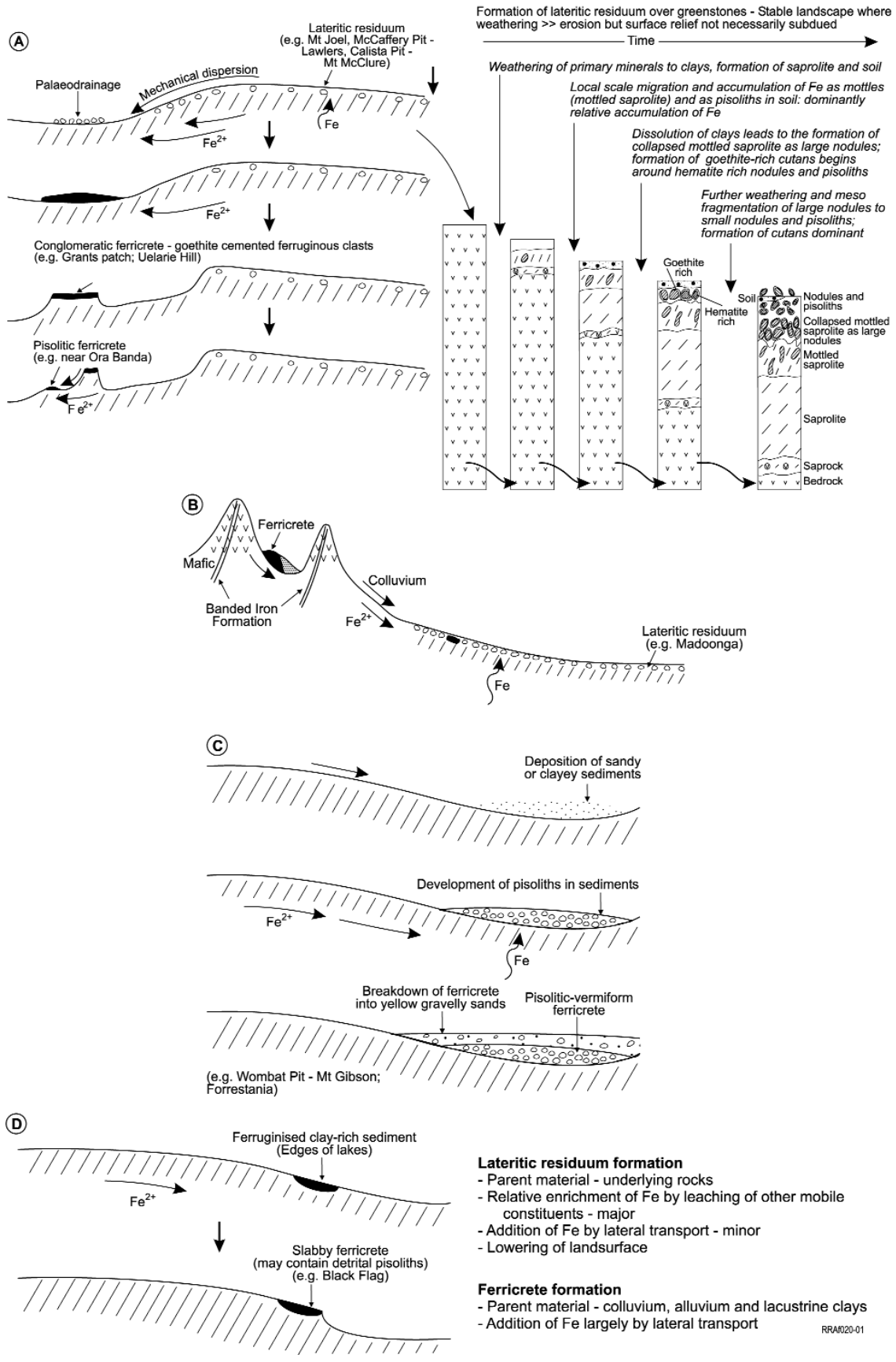

Figure 5.1 **Interpreted models of formation of ferruginous materials in residuum and sediments.**

6.0 ENVIRONMENTS OF FORMATION OF FERRUGINOUS NODULES AND PISOLITHS

Pisoliths and nodules can form in a variety of weathering and sedimentary environments. Their morphology and characteristics suggest three common environments of formation, in soil, saprolite and sub-aqueous environments (Figure 6.1) (Anand, 1995; Clarke and Chenworth, 1995). Pisoliths formed in soil are homogeneous, compound and concentric, whereas those formed in saprolite are commonly lithic (lithorelic and pseudomorphic). Those formed in sub-aqueous environments (inset valleys and lakes) are typically concentric. Nodules formed in saprolite are dominated by goethite, hematite and kaolinite. Maghemite is typically absent. Those formed in soil are hematite and maghemite-rich. Concentric pisoliths from sub-aqueous environments are dominated by goethite with varying proportions of hematite. Possible pathways of formation of nodules and pisoliths in soils, saprolite and inset valley sediments are shown in Figures 6.2 and 6.3.

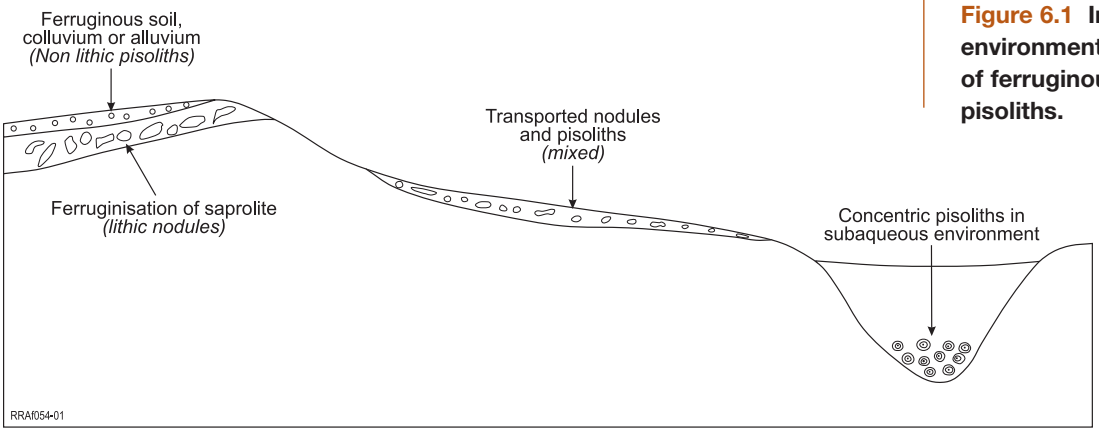

Figure 6.1 Interpreted environments of formation of ferruginous nodules and pisoliths.

6.1 Formation of nodules and pisoliths in surficial environments (soil, colluvium, alluvium)

Pisoliths in surficial environments are formed by replacement or cementation of soil or sediments by Fe oxides. They result from pedogenic activity in the upper part of the profile and are formed by leaching, migration and accumulation of Fe oxides on a microscale in the clay matrix or in voids. This is not a single event, but involves multiple leaching and precipitation of Fe oxides. The process begins with the weathering of bedrock, leaching of more mobile elements and kaolinisation. Much of the ferrous iron, released during weathering of the primary minerals, is oxidised and precipitated near the surface. A red soil horizon develops in the upper part of the profile (Figure 6.2A). Alternatively, colluvium or alluvium is deposited on saprolite. As the weathering front is lowered, upward transport of Fe becomes an important process. The Fe^{2+} ion released at the weathering front is subjected to combined upward diffusion and lateral migration by groundwater flow (Mann, 1983). Iron is subsequently precipitated by oxidation (as Fe^{3+} oxides) and accumulates near the water table. In the early stages, hematite or goethite mottles are formed, largely by local migration and accumulation of Fe. The Fe moves as Fe^{2+} in solution, gradually depleting the surrounding soil, which becomes bleached and kaolinitic. The Fe oxide mineralogy of the soil is controlled by the micro-environment (Tardy and Nahon, 1985). In small pores within kaolinite crystals, water activity is low, so hematite precipitates; whereas between the crystals there is more water activity, precipitating goethite. Organic material has undoubtedly played an important part in mobilising and segregating Fe. Humid tropical regions support abundant vegetation and there are strong relationships between mottling and tree roots. In Kerala, India, for example, roots penetrate to depths of 25 m. A similar relationship can also be seen in the higher rainfall areas of the Darling Range. In these situations, microbial decay of organic matter has produced conditions that reduced, redistribute and segregate Fe within the saprolite, where it oxidises to form ferric iron-rich mottles on contact with oxygen.

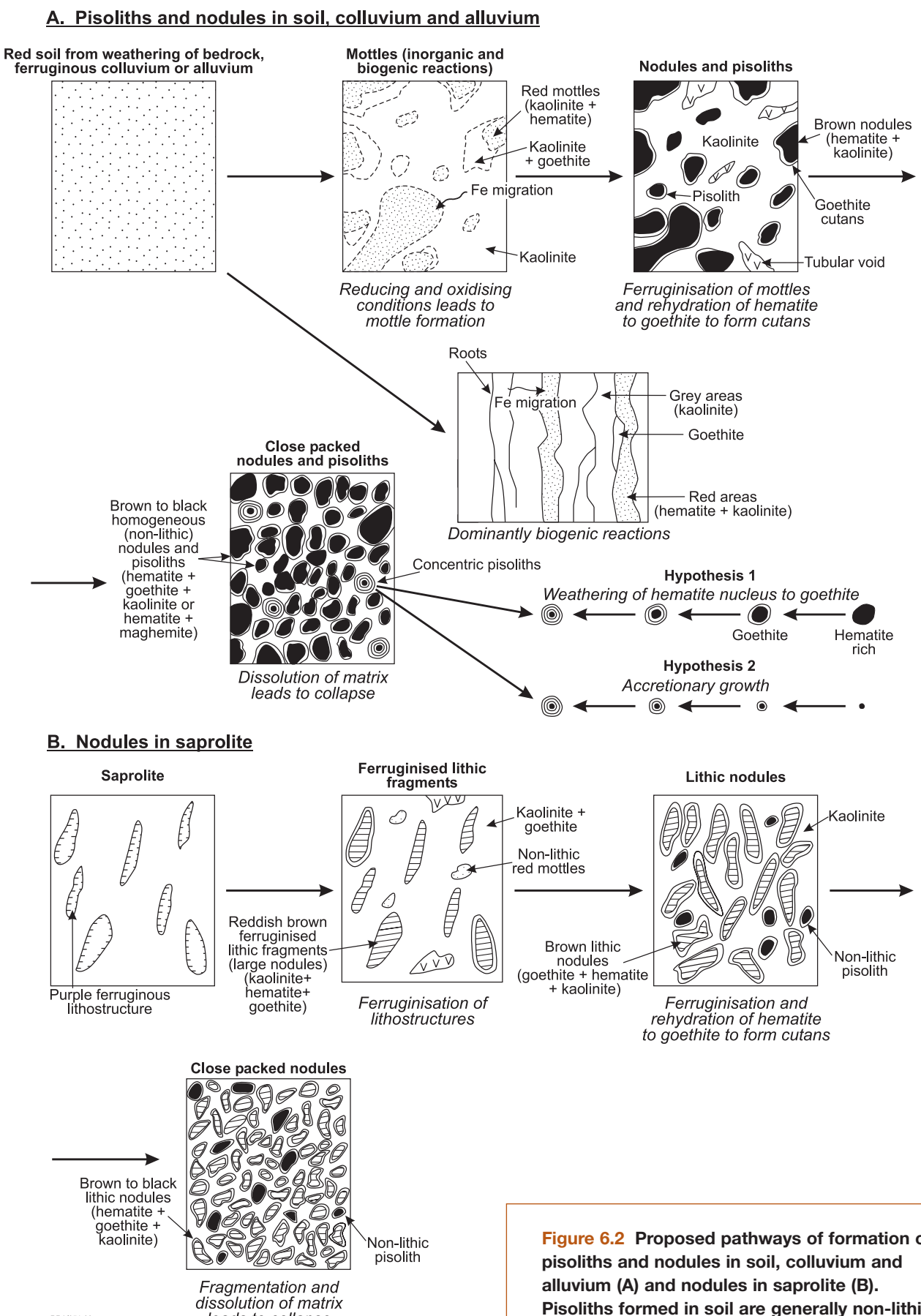

Figure 6.2 **Proposed pathways of formation of pisoliths and nodules in soil, colluvium and alluvium (A) and nodules in saprolite (B). Pisoliths formed in soil are generally non-lithic whereas those formed in saprolite are lithic.**

Accumulation of hematite and replacement of kaolinite and halloysite continues until, hard hematite-rich nodules form. The surrounding yellow-white or white kaolinite-quartz domains are bleached of Fe. With longer weathering, this clay-rich mass becomes modified by solution, destroying original fabrics. Voids develop in the clay surrounding the nodules, which allow water to reach the hematite, to progressively hydrate the edges of the hematite-rich nodules to form thin (0.2-0.5 mm) goethite-rich cutans (Tardy and Nahon, 1985). The process may eventually lead to formation of layered goethite cutans around hematitic cores. Formation of concentric pisoliths by this mechanism is shown by irregular dissolution of edges and scattered remnants of the original nucleus within a pisolith. Further water percolation leads to dissolution of kaolinite, forming macrovoids and cracks. The nodular to pisolitic horizon then collapses to close packed nodules and pisoliths. Alternatively, tubular macrovoids may become infilled with authigenic kaolinite, secondary silica and/or occupied with clay spherites to form a vermiform duricrust. In places, these pisoliths and nodules either coalesce to a massive duricrust as Fe is dissolved and reprecipitated between them (McFarlane, 1976) or cemented by the introduced matrix to form nodular-pisolitic duricrust. The range of duricrust types are variations on a theme.

6.2 Formation of nodules and pisoliths in saprolite

A characteristic of ferruginous materials developed in saprolite is the preservation of rock fabrics within nodules (Anand *et al.*, 1989). These nodules are developed by ferruginisation and fragmentation of saprolite. Initially, the saprolite was impregnated by Fe, deposited as tiny particles of goethite and hematite (Figure 6.2B). In places, ferruginisation is controlled by the foliation of the bedrock. Further weathering results in a marked porosity at the mesoscopic scale similar to that described above, causing coarse voids. Where such voids are intensively developed, the mass is generally referred to as vesicular duricrust. Amalgamation of these coarse voids leads to collapse of the duricrust. However, much of the void space may become occupied by eluvium from upper parts of the regolith. Cutans are deposited on the surface of the fragments (large nodules) and the whole mass may be cemented, forming a complex, fragmental duricrust.

6.3 Formation of pisoliths in sub-aqueous environments (inset-valley sediments)

Pisoliths occur in some inset valley clays. These pisoliths are well to sub-rounded and most are 1-15 mm in diameter (Figure 6.3). Some have a single thin cutan (<1 mm), but most have multiple cutans and a variety of cores including hematite-maghemite fragments, ferruginous clay, organic debris, quartz or a mixture of these. Some nuclei are simple (a single particle) or complex (composite particles). The likely pathways of formation of pisoliths in inset valley sediments are shown in Figure 6.4 and have a complex history. Calcareous, pisolitic and oolitic structures are common in the sedimentary record, having been described from a variety of marine and non-marine sequences. Theories of formation of pisoliths and ooliths are numerous (review by Pettijohn, 1975) and include: (1) accretionary growth by precipitation of new material on the grain surface in a free-rolling environment as in many modern-day marine oolite shoals, (2) concretionary growth by replacement of nucleus materials, and (3) *in situ* precipitation of new material in a relatively static environment such as soils. Pisoliths in inset valley sediments appear to have formed in a static environment as described below.

1. In the inset valley environments, pisoliths, originally developed within the upper part of the relict profile, have been eroded and deposited within the grey clay facies of the inset valley sediments. This is indicated by incomplete or broken cutans, compound pisoliths, the presence of maghemite-rich fragments within cores, and a different quartz grain distribution between these nodules and pisoliths and that of the grey clay.
2. Some of these pisoliths may have been partly dissolved in an originally reducing environment.
3. Subsequently, however, a second generation of pisoliths has formed *in situ* either without a nucleus or around a detrital nucleus of fine quartz, organic debris, hematite-maghemite-rich fragments or clay. Accretionary growth may have proceeded by either inorganic or biogenic mechanisms. Ostwald (1990) attributed fine layering to organically mediated growth in a fluid medium. Pisoliths containing fossil wood exhibit a stromatolitic pattern of blue green algae and, thus, it is possible that some concentric pisoliths in inset valley clays formed in this way. However, in places it is difficult to determine which process (organic or inorganic) is dominant.

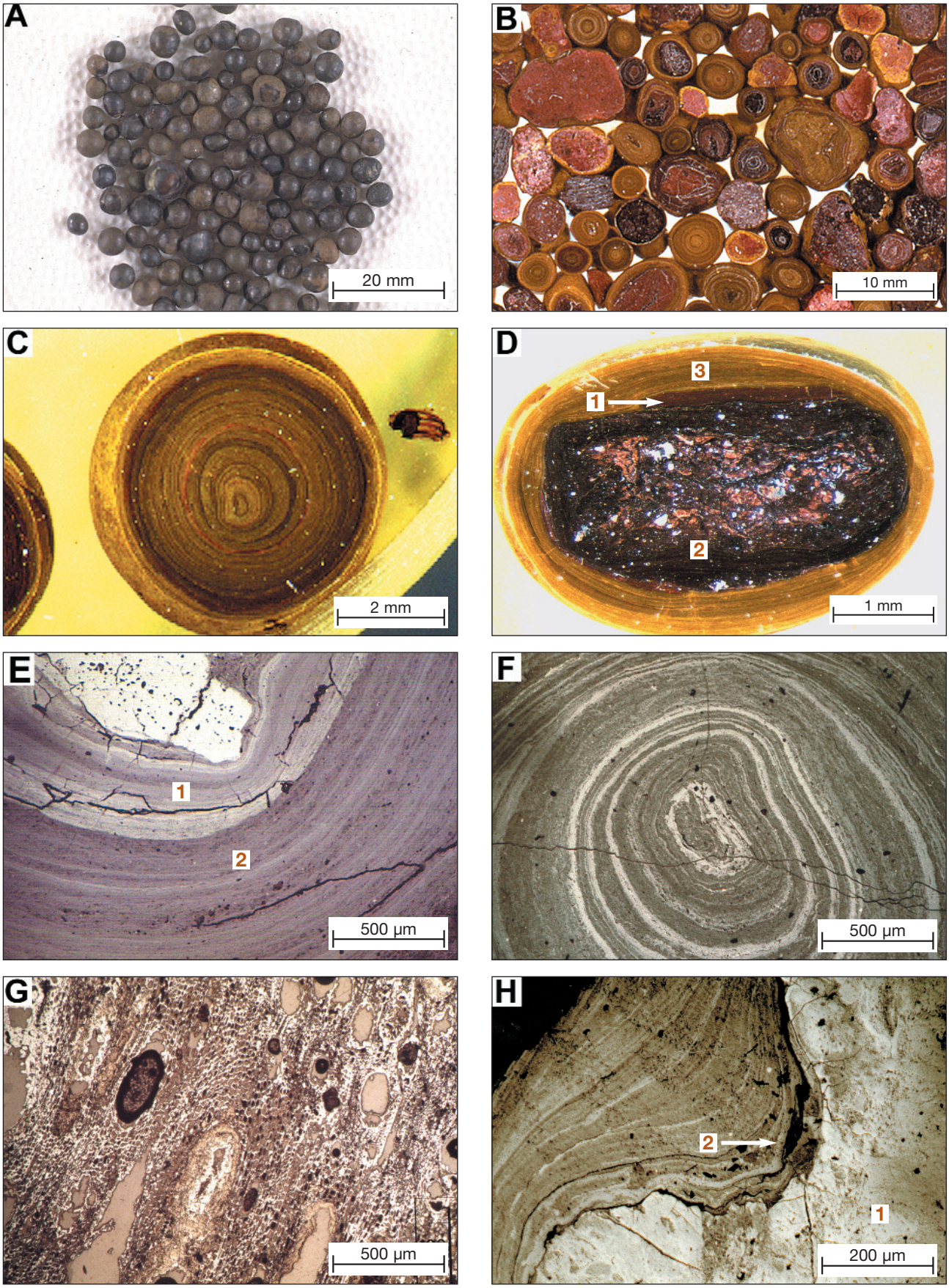

Figure 6.3 Photographs of pisoliths from inset valley sediments. (A) Handpicked black pisoliths typical of inset valley sediments (B) Concentric pisoliths with thick, finely laminated cutans around a variety of nuclei, Paddington; (C) Details of pisolith in A showing finely laminated cutans; (D) Concentric pisolith showing fragmented and truncated inner cutans (1) around ferruginised lithic nucleus (2) which have been subject to abrasion, encased by goethite-rich concentric cutan accretion (3), indicating a polyphase development; (E) Photomicrograph of a polished block taken in nrl showing a hematitic core surrounded by hematite-rich (1) and goethite-rich (2) cutans, Sundowner; (F) Photomicrograph of a polished block taken in nrl showing a concentric pisolith with well-developed finely laminated, accretionary cutans, Paddington. This type of layering is common in pisoliths developed in inset valley sediments; (G) Photomicrograph of a polished block taken in nrl showing a concentric pisolith with a core comprising a hematitic wood fragment, Paddington; (H) Photomicrograph of a polished block taken in nrl showing a concentric pisolith with an irregular core (1) surrounded by concentric goethitic cutans (2), Paddington. The first few cutans closely follow the small external irregularities of the core, the cutans become more and more regular and circular outwards.
nrl = normally reflected light.

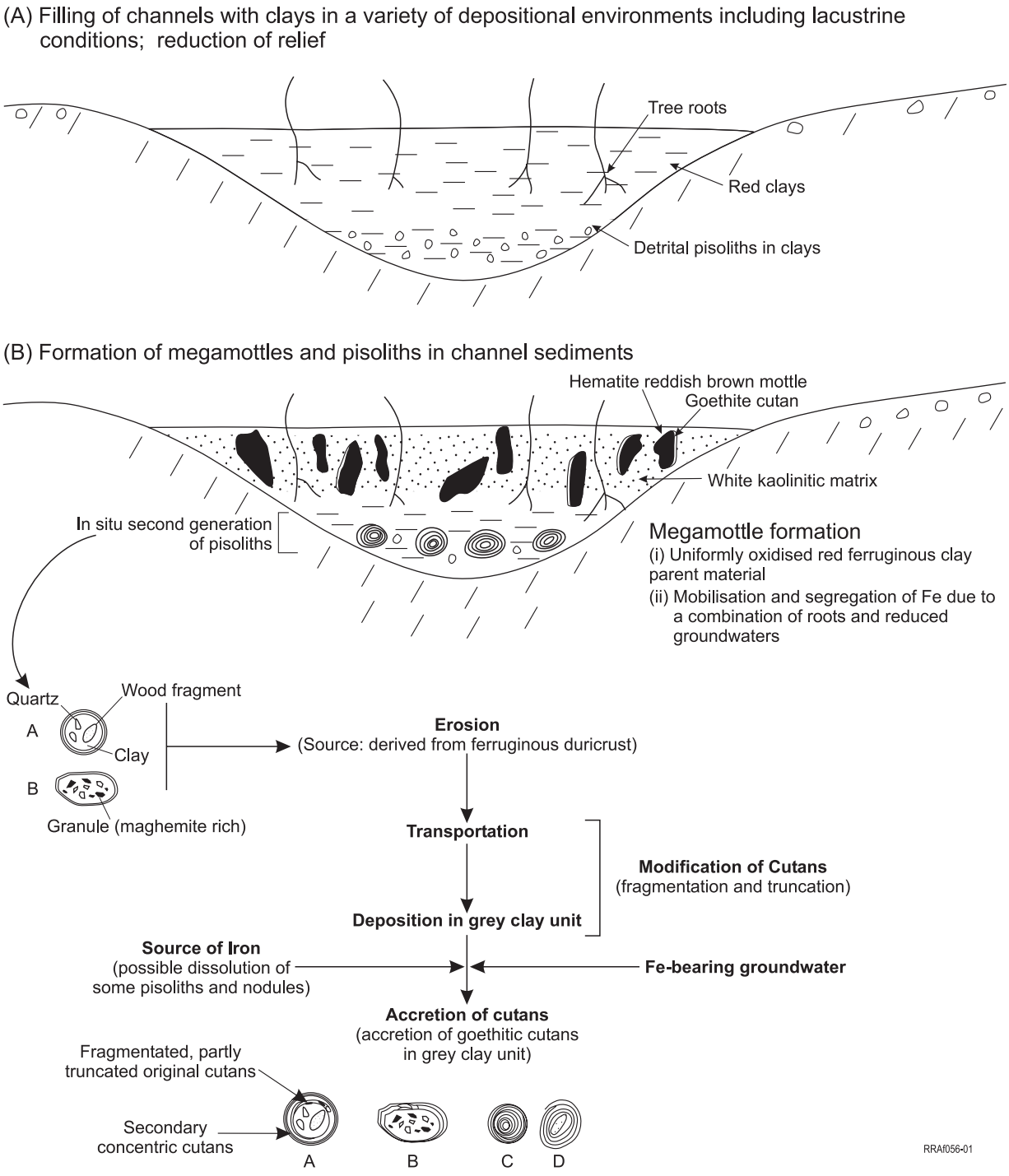

Figure 6.4 Interpreted pathways of formation of megamottles and pisoliths in inset valley sediments. Pisoliths formed in inset valley environments are formed by accretionary process and are typically concentric with multiple cutans (after Anand *et al*., 1993; Dusci, 1994).

7.0 PISOLITH CLASSIFICATION

Based on fabric, Anand *et al*. (1989) subdivided pisoliths and nodules into four basic types (Figure 7.1). These are *homogeneous* (no internal fabric), lithorelics (grains with relict rock fabrics and at least partial preservation of primary mineralogy), *pseudomorphic* (purely secondary minerals, but some preservation of primary fabrics), and *concentric* (with multiple cutans indicating concretion or accretion). Each of the four types could be modified by any of three additional terms. These were *cutanic* (thin outer layer or layers present, but not enough to impart a true concentric fabric), *compound* (several originally separate grains that have been cemented together), and *syneresis* (vuggy and fissured internal fabrics indicating dewatering of clay and oxyhydroxides). Clarke and Chenworth (1995), also based on fabric, have proposed a four-level classification of lags, expanding on the scheme of Anand *et al*. (1989). The first is based on initial observation necessary to recognise the class of regolith materials to which ferruginous surface granules (FSG) belong, namely lags. The second separates FSGs from other lag components, such as rock fragments and resistant mineral grains, and hence requires more detailed observation of the sampled material. The third level of classification requires petrographic and mineragraphic examination; the main textural types are homogeneous, lithorelic, pseudomorphic, vesicular, sandy and oolitic. The fourth level of classification identifies modifying microfabrics, namely concentric, cutanic, compound, mottled and syneresis fabrics.

Homogeneous pisoliths may have thin, goethite-rich cutans. Pseudomorphic and lithorelic nodules can have a variety of internal fabrics depending upon the nature of the host material. In pseudomorphic nodules, the internal fabric is very closely related to the fabric of the primary minerals that have been pseudomorphed. Pseudomorphic fabric relationships are seen best in the cores: examples are gibbsite pseudomorphs after feldspars in fragmental duricrust, kaolinite and goethite after mica, goethite after talc and fine, kaolinite booklets after amphiboles. Pseudomorphs are not readily seen in hand specimen, though a few larger grains may be visible under a hand lens; they are best recognised by microscopy. Lithorelic pisoliths are characterised by preservation of rock fabrics in their cores. Thus, at Madoonga, pisoliths of former BIF have a layered internal fabric, with layers still composed largely of Fe oxides and quartz (Von Perger, 1992). Relics of former schist retain a schistose fabric.

Concentric pisoliths may have a variety of cores. In places, pisoliths are entirely banded without any obvious core. Where alternate darker and lighter cutans are seen under the microscope, the lighter cutans gave relatively higher Al and lower Fe contents and are kaolinite-gibbsite-rich. Concentric cutans may include micro-lenses of detrital quartz grains suggesting a complex history of their formation.

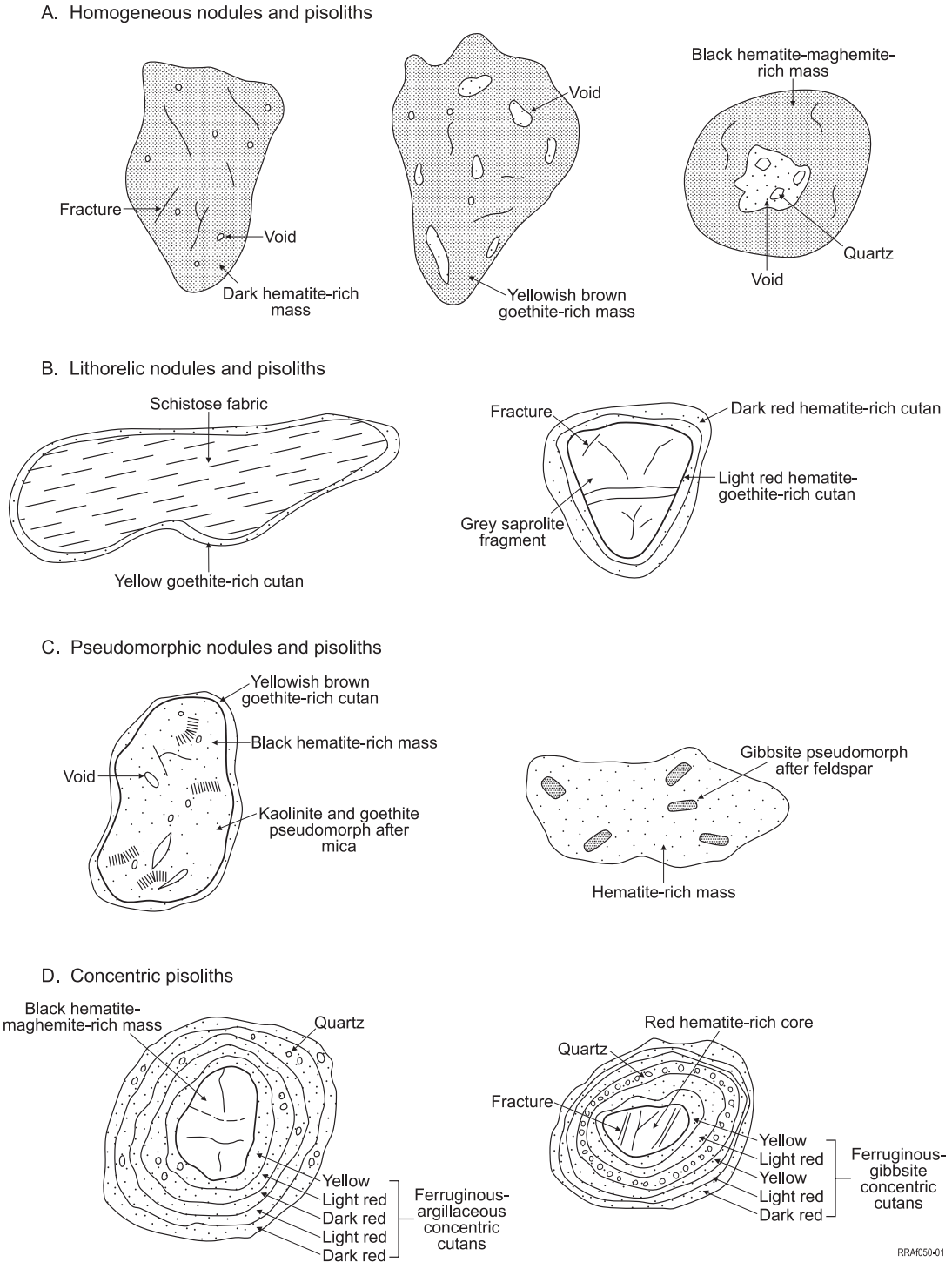

Figure 7.1 Classification of ferruginous nodules and pisoliths (modified after Anand *et al.*, 1989). (A) Homogeneous nodules and pisoliths, commonly 5-20 mm in diameter; (B) Nodules and pisoliths having lithorelics as their cores, typically 10-40 mm in diameter; (C) Pseudomorphic nodules and pisoliths, 5-15 mm in diameter and (D) concentric pisoliths, 2-10 mm in diameter.

8.0 REVIEW OF SOME CLASSIFICATION SCHEMES OF FERRUGINOUS DURICRUSTS

8.1 Introduction

Bourman (1993) pointed out that attempts to classify ferruginous materials have been confusing because the ill-defined term 'laterite' has tended to be used alone, without describing the detailed characteristics of these ferruginous materials. Various morphological and genetic classification schemes of 'laterite' are summarised in Table 8.1.

8.2 Chemical classification

Chemical classification schemes of 'laterite' (e.g., Martin and Doyne, 1932; Dury, 1969; Schellman, 1981) have been reviewed by Bourman (1993). Martin and Doyne (1932) were among the first to advocate a chemical classification of 'laterite'. They proposed silica-alumina ratios to measure varying degrees of lateritisation, but the values of this ratio were disputed by several workers. Schellman (1981) classified laterite by the degree of lateritisation as indicated by positions on a Si-Al-Fe diagram (Figure 8.1). He considered samples with high iron and/or aluminium to be strongly lateritised. Bourman (1993) questions the indiscriminate use of the term 'laterite' to describe a diverse range of materials. Furthermore, ferruginous duricrust may have formed in various ways (Anand *et al.*, 1989; Bourman, 1993; Anand, 1998); and may not be genetically related to the underlying bedrock and, therefore, will not simply reflect the intensity of weathering. Confusion may arise if the sample contains transported material. A chemical classfication is not readily applicable to field identification of weathered materials (Bourman, 1993).

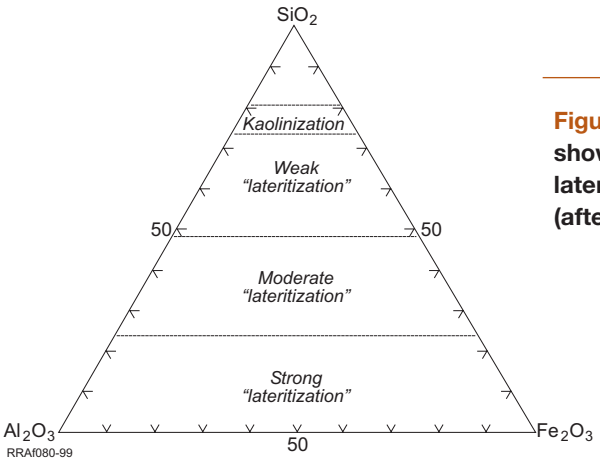

Figure 8.1 Triangular diagram showing different degrees of lateritisation on granitic bedrock (after Schellmann, 1981).

8.3 Morphological classification

Anand *et al.* (1989) identified several types of ferruginous duricrusts in the landscapes of the Yilgarn Craton (Table 8.1). They proposed a descriptive classification based on hand specimen morphology. They sub-divided duricrusts according to their dominant secondary structures i.e. massive, mottled, fragmental, nodular, pisolitic, oolitic, vermiform, vesicular and cellular. These terms are similar to those used by other workers (Pullan, 1967; McFarlane, 1976; Bourman *et al.*, 1987; Bourman, 1993).

Bourman (1993), from work in South Australia, has provided a useful classification scheme of 'ferricrete', also based on hand specimen description (Table 8.1). He believes that an individual 'ferricrete' reflects both the character of the original material that has been ferruginised and the accumulated effects of subaerial processes. Bourman classified ferricrete into simple (ferruginised bedrock, ferruginised clastic, organic and Fe-rich sediments) and complex (pisolitic, nodular, slabby and vermiform) ferricrete. He suggested that there is generally no genetic relationship between ferricrete and the underlying saprolite. This model does not entirely fit materials found on the Yilgarn Craton, where ferruginous duricrusts have formed both in residual and transported materials. A distinction between residual and transported categories is essential, particularly from the explorationists perspective.

8.4 Genetic classification

Several authors have proposed genetic classifications of 'laterite' based on its mode and mechanisms of formation. The morphological classification scheme of Pullan (1967), developed in Nigeria, recognised vermicular, vesicular, cellular, cellular-nodular, nodular, oolitic and pisolitic (primary forms), recemented nodular, recemented conglomeratic, recemented breccia and platy (secondary forms) lateritic ironstones as well as ferruginised rock and sediment. Primary ironstones are those developed *in situ* from different parent materials, without the introduction of externally derived Fe, whereas secondary ironstones are developed from the partial destruction of primary lateritic ironstones, transportation of fragments of the original ironstone, their subsequent deposition and recementation with Fe oxides. On the basis of their morphological characteristics and mode of occurrence, Anand (1995, 1998) classified ferruginous duricrusts into two broad groups i.e. lateritic residuum and ferricrete.

McFarlane (1976) distinguished two types of 'laterites' in Uganda: pedogenic and groundwater laterites. Pedogenic laterites are considered to be formed in the unsaturated zone of the soil whereas groundwater laterites are formed in the zone of fluctuation of the groundwater table, in both the soil (as a closely packed layer directly overlying the saprolite) and in the underlying saprolite (as more or less widely spaced pisoliths). A more comprehensive and complex classification of lateritic materials has been presented by Aleva (1986), which involves the mechanism of accumulation and mineralogical and chemical compositions. However, the first subdivision between autochthonous (relative accumulation) and allochthonous (absolute accumulation) is questionable, because it is sometimes difficult to identify the source of iron (Bourman, 1993).

9.0 PROPOSED CLASSIFICATION SCHEME

9.1 Introduction

The following classification scheme is based on an initial scheme developed by Anand *et al.* (1989). These authors set out to provide a scheme that could be used in exploration, research and education. This revised classification system, draws upon an additional twelve years of research in a variety of geographic locations.

A classification scheme for ferruginous materials that is to be useful to geoscientists, especially those in mineral exploration, should reflect the type and origin of ferruginous materials. The following scheme uses both descriptive and genetic characteristics. Where the genetic framework of a particular sample cannot be determined, a descriptive classification can still be made. For example, mottles and ferruginous duricrust and gravels have formed in both residual and transported materials. A distinction between residual and transported materials is highly desirable, but is not always able to be determined. Thus, a third term is introduced where ferruginous materials can be described where the nature of the substrate is unknown.

9.2 Scheme

The proposed classification scheme shown in Figure 9.1 utilises a multi-level, alpha-numeric classification scheme. The five major subdivisions are *ferruginous saprolite, ferruginous clays, ferruginous mottles, ferruginous duricrust and gravel* and *iron segregations*. The next stage of classification places the sample being classified into a genetic framework. In the case of ferruginous mottles, the substrate may be specified as unknown, saprolite, residual clays or sediments. Ferruginous clays and ferruginous duricrust and gravels may form in an unknown substrate, in residuum or in sediments. Ferruginous saprolite and iron segregations after suphide-rich rocks do not require this genetic component to their classification.

The final level of classification relies on the description of the morphological characteristics of the specimen. Thus, duricrusts are divided according to there dominant secondary structures i.e. massive, mottled, fragmental, nodular, pisolitic, oolitic, vermiform, vesicular and cellular. These structures are not mutually exclusive and varying proportions of structures may occur within a single hand specimen resulting in categories such as "nodular-pisolitic". Voids of various shapes are common in all the lateritic duricrusts but they also vary in abundance. Thus, a sub-division was made on the basis of the dominance of either solid or void phase. The terms used seek to describe the dominant features of the specimen without providing a plethora of terms to confuse the user. Subsequent modification by silicification, calcification and hardpanisation are represented using a specified suffix.

Table 8.1 Classification systems of ferruginous duricrust and gravel ('laterite'/'ferricrete')

Morphological Classification		Morphological-genetic classification		Genetic classification	
Anand *et al* (1989)	**Bourman (1993)**	**Pullan (1967)**	**Anand (1995, 1998)**	**Mc Farlane (1976)**	**Aleva (1986)**
1. Lateritic gravel (Loose) • Loose pisoliths • Loose nodules • Loose nodules and pisoliths • Loose ooliths	**1. Simple ferricrete** • Ferricreted bedrock • Ferricreted sediment Ferricreted clastic sediment Ferruginised organic sediment Ferricreted iron-rich sediment	**1.Primary lateritic ironstone** • Vermicular • Vesicular • Cellular • Cellular-nodular • Nodular • Oolitic • Pisolitic	**1. Lateritic residuum** • Loose nodules and pisoliths • Nodular duricrust • Fragmental duricrust • Mottled duricrust • Massive duricrust	1. **Groundwater laterite** • Spaced pisolitic • Packed pisolitic • Massive (vermiform)	**1. Autochthonous**
2. Lateritic duricrust (cemented) • Massive • Mottled • Fragmental • Nodular • Pisolitic • Pisolitic-nodular • Oolitic • Vermiform • Vesicular • Cellular	**2. Complex and Composite ferricrete** • Pisolitic • Nodular • Slabby • Vermiform	**2. Secondary lateritic ironstone** • Recemented nodular • Recemented conglomeratic • Recemented beccia • Platy	**2. Ferricretes** • Conglomeratic • Pisolitic • Vesicular • Ferruginised palaeochannel sediments	**2. Pedogenetic laterite** • Spaced pisolitic • Packed pisolitic • Massive (cellular)	**2. Allochthonous**

CLASSIFICATION OF FERRUGINOUS MATERIALS

Ferruginous saprolite (FS)

Ferruginous clays (FC)

- Ferruginous clays in an unknown substrate (FC 100)
- Ferruginous residual clays (FC 300)
- Ferruginous sedimentary clays (FC 400)

Ferruginous mottles (MZ)

- Ferruginous mottles in an unknown substrate (MZ 100)
  - Pisolitic mottles (MZ101)
  - Platy mottles (MZ102)
  - Columnar mottles (MZ103)
  - Lenticular mottles (MZ104)
  - Vermiform mottles (MZ105)
  - Irregular mottles (MZ106)
  - (MZ 107)
  - (MZ 108)
  - (MZ 109)
  - (MZ 110)
  - (MZ 111)
- Ferruginous mottles in saprolite (MZ 200)
  - Pisolitic mottles (MZ201)
  - Platy mottles (MZ202)
  - Columnar mottles (MZ203)
  - Lenticular mottles (MZ204)
  - Vermiform mottles (MZ205)
  - Irregular mottles (MZ206)
  - (MZ 207)
  - (MZ 208)
  - (MZ 209)
  - (MZ 210)
  - (MZ 211)
- Ferruginous mottles in residual clays (MZ300)
  - Pisolitic mottles (MZ301)
  - Platy mottles (MZ302)
  - Columnar mottles (MZ303)
  - Lenticular mottles (MZ304)
  - Vermiform mottles (MZ305)
  - Irregular mottles (MZ306)
  - (MZ 307)
  - (MZ 308)
  - (MZ 309)
  - (MZ 310)
  - (MZ 311)
- Ferruginous mottles in sediments (MZ 400)
  - Pisolitic mottles (MZ401)
  - Platy mottles (MZ402)
  - Columnar mottles (MZ403)
  - Lenticular mottles (MZ404)
  - Vermiform mottles (MZ405)
  - Irregular mottles (MZ406)
  - (MZ 407)
  - (MZ 408)
  - (MZ 409)
  - (MZ 410)
  - (MZ 411)

NB Mottles may be further classified using the following suffix:

M = Megamottles: Mottles > 200 mm in mean diameter.
S = Minimottles: Mottles < 10 mm in mean diameter.

e.g. Irregular mini mottles in an unknown substrate = MZ 106 S

Ferruginous duricrust and gravels (L)

- Unknown substrate (LQ)
  - ***Ferruginous gravel (LQ100) (Unconsolidated)***
    - Loose ooliths (LQ101)
    - Loose pisoliths (LQ102)
    - Loose pisoliths and nodules (LQ103)
    - Loose nodules (LQ104)
  - ***Ferruginous duricrust (LQ200) (Consolidated)***
    - Oolitic duricrust (LQ201)
    - Pisolitic duricrust (LQ202)
    - Pisolitic-nodular duricrust (LQ203)
    - Nodular duricrust (LQ204)
    - Fragmental duricrust (LQ205)
    - Packed oolitic duricrust (LQ211)
    - Packed pisolitic duricrust (LQ212)
    - Packed pisolitic-nodular duricrust (LQ213)
    - Packed nodular duricrust (LQ214)
    - Vermiform duricrust (LQ231)
    - Cellular duricrust (LQ232)
    - Vesicular duricrust (LQ233)
    - Mottled duricrust (LQ241)
    - Massive duricrust (LQ242)
    - Slabby duricrust (LQ 243)
- Lateritic residuum (LT)

  Relative accumulation of Fe ⟷ *Absolute accumulation of Fe*
  - ***Lateritic gravel (LT100) (Unconsolidated)***
    - Loose ooliths (LT101)
    - Loose pisoliths (LT102)
    - Loose pisoliths and nodules (LT103)
    - Loose nodules (LT104)
  - ***Lateritic duricrust (LT200) (Consolidated)***
    - Oolitic duricrust (LT201)
    - Pisolitic duricrust (LT202)
    - Pisolitic-nodular duricrust (LT203)
    - Nodular duricrust (LT204)
    - Fragmental duricrust (LT205)
    - Packed oolitic duricrust (LT211)
    - Packed pisolitic duricrust (LT212)
    - Packed pisolitic-nodular duricrust (LT213)
    - Packed nodular duricrust (LT214)
    - Vermiform duricrust (LT231)
    - Cellular duricrust (LT232)
    - Vesicular duricrust (LT233)
    - Mottled duricrust (LT241)
    - Massive duricrust (LT242)
- Ferricrete (LF) (Ferruginised sediments)
  - ***Fericrete clasts (LF100) (Unconsolidated)***
    - Loose ooliths (LF101)
    - Loose pisoliths (LF102)
    - Loose pisoliths and nodules (LF103)
    - Loose nodules (LF104)
  - ***Ferricrete (LF200) (Consolidated)***
    - Oolitic ferricrete (LF201)
    - Pisolitic ferricrete (LF202)
    - Pisolitic-nodular ferricrete (LF203)
    - Nodular ferricrete(LF204)
    - Conglomeratic ferricrete (LF206)
    - Vermiform ferricrete (LF231)
    - Vesicular ferricrete (LF233)
    - Mottled ferricrete (LF241)
    - Slabby ferricrete (LF243)

Iron segregations (IS)

- ***Goethite-hematite segregations (IS 100)***
  - Vesicular goethite pod (IS101)
  - Discordant hematite-goethite body (IS102)
  - Stratabound hematite-goethite body (IS103
  - Goethite selvage to quartz veins (IS111)
- ***Hematite segregations (IS 200)***
  - Strata bound hematite layer (IS201)

Lag (LG)

- ***Lateritic lag (LG100)***
  - Ooliths (LG101)
  - Pisoliths (LG102)
  - Nodules and pisoliths (LG103)
  - Nodules (LG104)
  - Hardened mottles (LG105)
  - Nodules and hardened mottles (LG106)
  - Nodules, hardened mottles and pisoliths (LG 107)
- ***Lag, other (LG 200)***
  - Ferruginous saprolite (LG 231)
  - Iron segregation fragments LG 241)
  - Gossan fragments (LG261)

NB Calcification, Hardpanisation and silicification are further classified using the following suffixes:

Calcification *is an authigenic process which can effect a variety of materials. Please refer to codes for each material that is being classified and add CF as a suffix. Example: LT202CF is a calcified pisolitic duricrust.*

Hardpanisation *is an authigenic process which can act upon a variety of materials. Please refer to codes for each material that is being classified and add HP as a suffix. Example: LT202HP is a hardpanised pisolitic duricrust.*

Silicification *is an authigenic process which can act upon a variety of materials. Please refer to codes for each material that is being classified and add SF as a suffix. Example: LT202SF is a silicified pisolitic duricrust. The term hardpanisation takes precedence where silicification has resulted in the formation of a hardpan, or a marked tendancy towards a hardpan, namely, where hardpan fabric (silicification along sub-horizontal partings) is developed.*

Figure 9.1 Classification scheme for ferruginous materials

10.0 ATLAS OF FERRUGINOUS REGOLITH MATERIALS

10.1 Introduction

The atlas has been subdivided according to the four major types of ferruginous materials (Figure 9.1) namely:

A. Ferruginous saprolite

B. Ferruginous mottles

C. Ferruginous clays

D. Ferruginous duricrust and gravels (lateritic residuum and ferricrete)

E. Iron segregations

Samples from each major type have been classified according to the alpha-numeric scheme given in Figure 9.1. The relevant portion of this scheme is included at the base of the corresponding descriptive page for ease of reference.

Examples are shown from a number of sites. Where possible, landscape and profile positions are provided. Subsequent modification by calcification, silicification and hardpanisation are reflected in the code suffix and examples of these modifications are given in the Modifications section of the atlas. The dominant lag types are also included. These represent the residual accumulation of coarse, usually hard, fragments that accumulate at the surface.

Close up photographs (similar to what may be seen through a hand lens) and field photographs are included in the atlas. Photomicrographs of thin sections, polished thin sections and polished blocks are used to illustrate the various micromorphological features that may be used to describe and identify ferruginous materials.

The chemical compositions (determined by XRF analyses) of the samples are graphed where available. The elements graphed are: SiO_2, Al_2O_3, Fe_2O_3, TiO_2 (%) and Mn, Cr, V, Ni and Zr (ppm). The bars on the graph are linked by colour to the sample label in the top left hand corner of the photograph and photomicrograph of the matching sample. Complete analytical data is available for most samples from CRC LEME upon request.

10.2 FERRUGINOUS SAPROLITE

Ferruginous saprolite (FS)

A

Ferruginous saprolite (FS). This unit occurs beneath 10 m thick colluvial-alluvial sediments on a depositional plain. It forms a continuous 2-5 m thick horizon and is overlain by collapsed mottled saprolite (ferruginised breccia; see E) and lateritic residuum. This ferruginous saprolite comprises red-brown, uniformly ferruginised clay formed from basalt. A preserved schistosity and it's orientation are shown (1).

Sample 07-4606. Central Pit, Bronzewing. *Photograph of the polished surface of a hand specimen taken in oblique reflected light.*

B

Preserved rock schistosity (1) in a matrix of kaolinite variably impregnated with hematite and goethite.

Sample 07-4606. *Photomicrograph of a polished thin section taken in transmitted plain polarised light and oblique reflected light.*

C

Ferruginous saprolite (FS). Extreme ferruginisation of saprolite at a depth of 20 m in the regolith profile overlying a zone of bleached saprolite developed over mafic bedrock. Yellow liesegang banding (1) in a matrix of fine-grained hematite and kaolinite (2) is evident. In outcrop, the banding is developed on a scale of tens of meters and is discordant to lithological layering.

Sample 07-1175. *McCaffery Pit, Lawlers. Photograph of the polished surface of a hand specimen taken in oblique reflected light.*

D

Liesegang colour banding characterised by thin, alternating bands of fine-grained yellow-brown goethite and kaolinite (1) and rouge hematite and kaolinite (2).

Sample 07-1175. *Photomicrograph of a polished thin section taken in transmitted plain polarised light and oblique reflected light.*

E

Ferruginous breccia (FS). This sample of ferruginous breccia occurs beneath 8 m of colluvial-alluvial sediments on a depositional plain. It was taken from a thin layer of collapsed mottled saprolite developed on ferruginous saprolite. The collapsed mottled saprolite grades upwards into lateritic residuum. The sample exhibits relict bedrock fabrics as indicated (1) and is composed of hematite and kaolinite.

Sample 07-4604. Central Pit, Bronzewing. *Photograph of the polished surface of a hand specimen taken in oblique reflected light.*

F

Sheets of dark grey mica (1) lie enclosed in light grey goethite (2) that has split some of the mica sheets. The mica still contains potassium but has been partly hydrated.

Sample 07-2717. Central Pit, Bronzewing. *Photomicrograph of a polished block taken in normally reflected light.*

Ferruginous saprolite (FS) | Ferruginous clays (FC) | Ferruginous mottles (MZ) | Ferruginous duricrust and gravels (L) | Iron segregations (IS)

Ferruginous saprolite (FS)

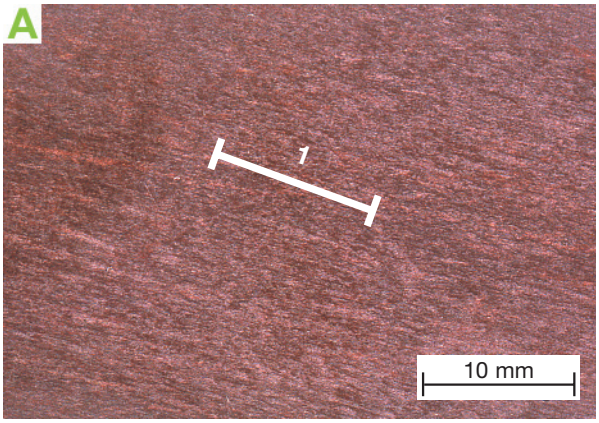

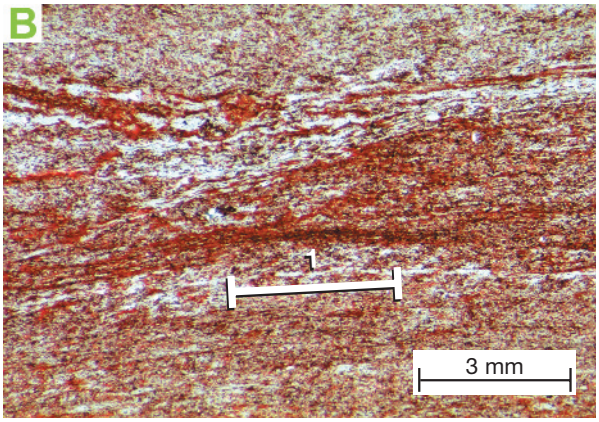

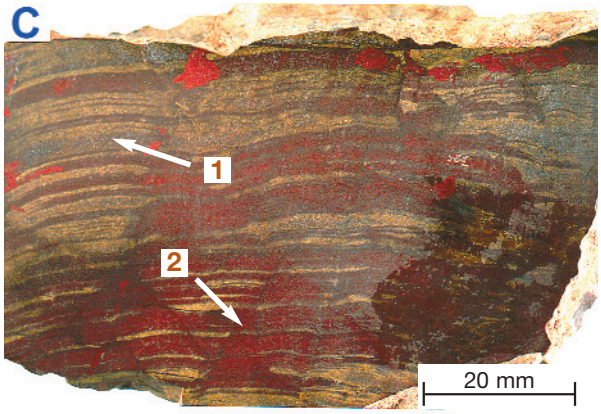

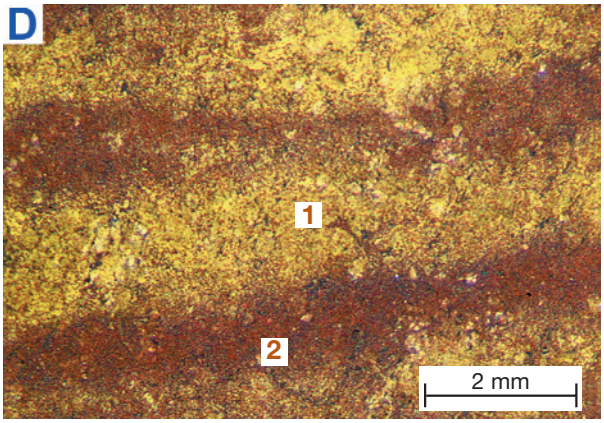

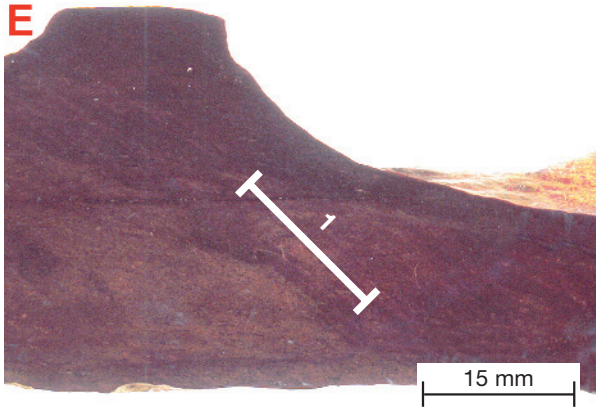

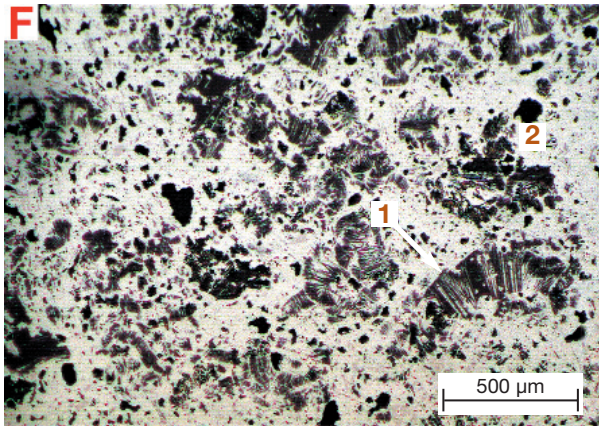

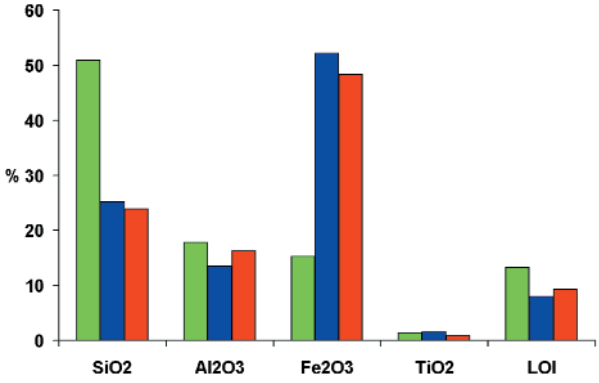

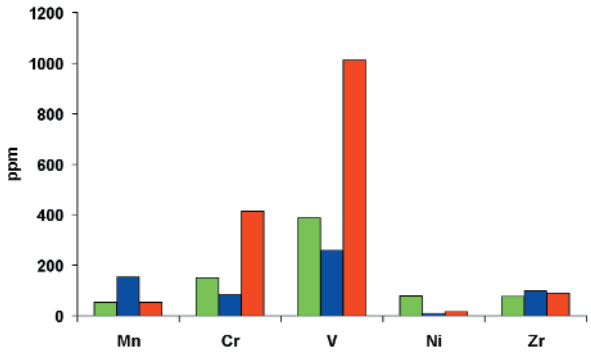

10.3 FERRUGINOUS CLAYS

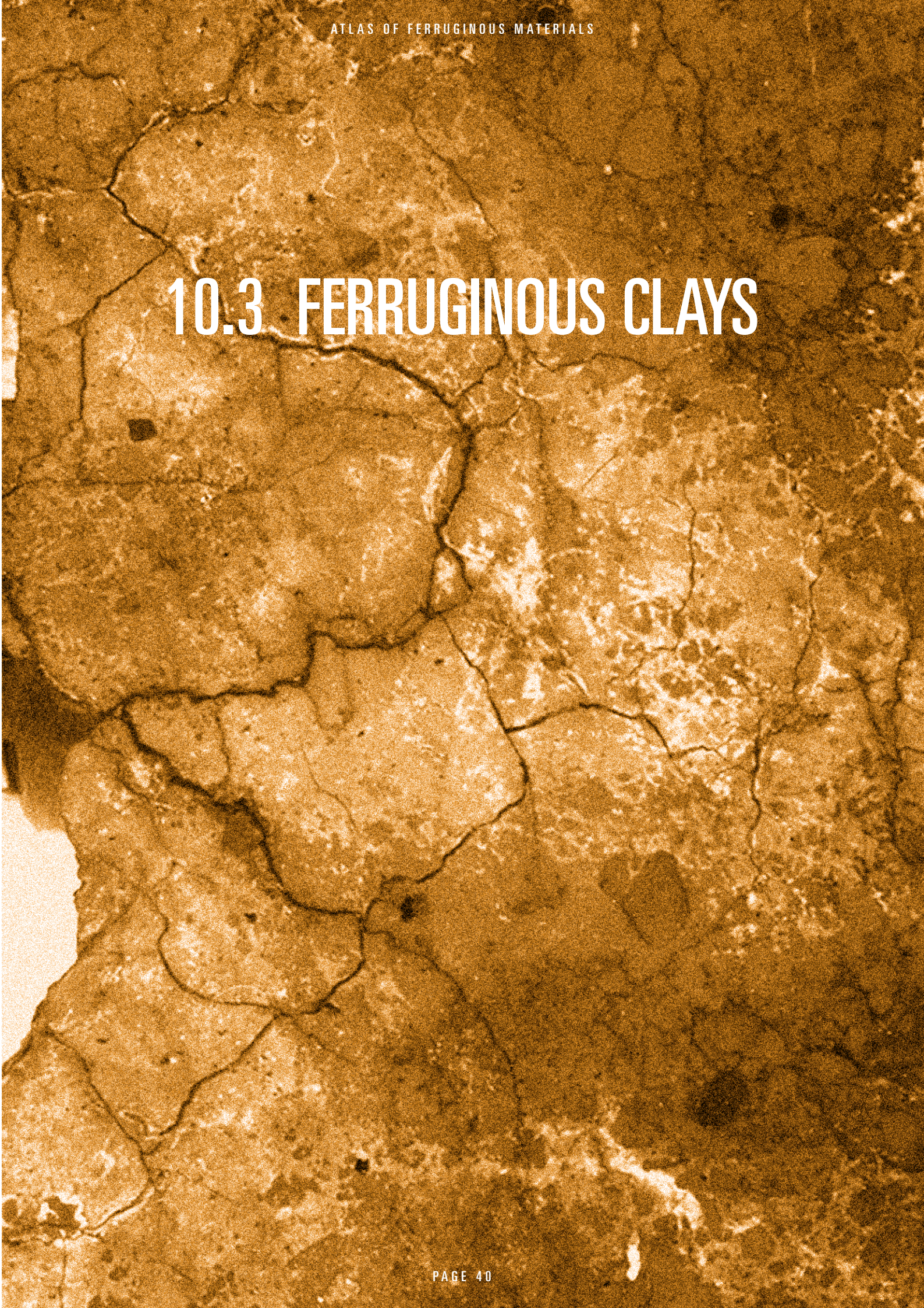

Ferruginous clays (FC)

A

Ferruginous residual clays (FC300).
This ferruginous clay (1) is developed over dolerite. Corestones of dolerite (2) display typical "onion skin" weathering.

Pit A, Boddington

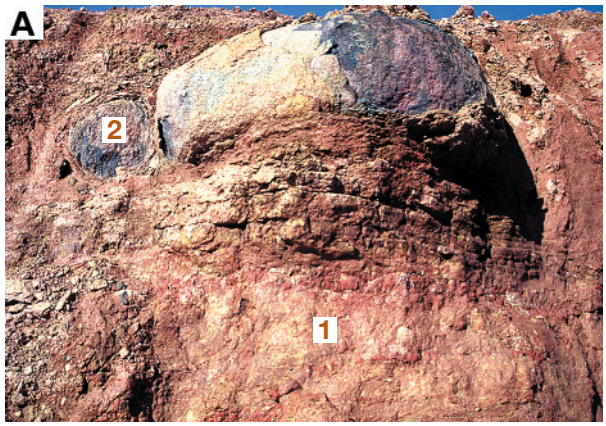

B

Ferruginous sedimentary clays (FC400).
This ferruginous clay shows incipient pisolith development (1) in a variably hematite impregnated kaolinitic clay. Fine cracks also occur (2).

Sample 07-3573. Kanowna Belle. *Photograph of the polished surface of a hand specimen taken in oblique reflected light.*

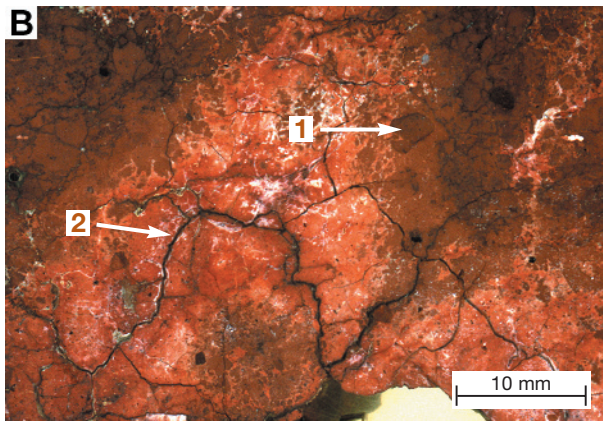

C

Ferruginous sedimentary clays (FC400).
Angular, poorly sorted quartz grains (1) set in variably impregnated kaolinitic clay. Fine cracks (2) are associated with bleaching in places.

Sample 07-3573. *Photomicrograph of a thin section taken in transmitted light with crossed polarisers and oblique reflected light.*

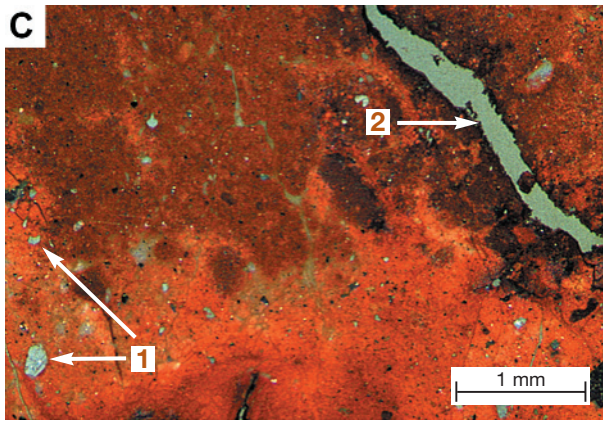

10.4 FERRUGINOUS MOTTLES

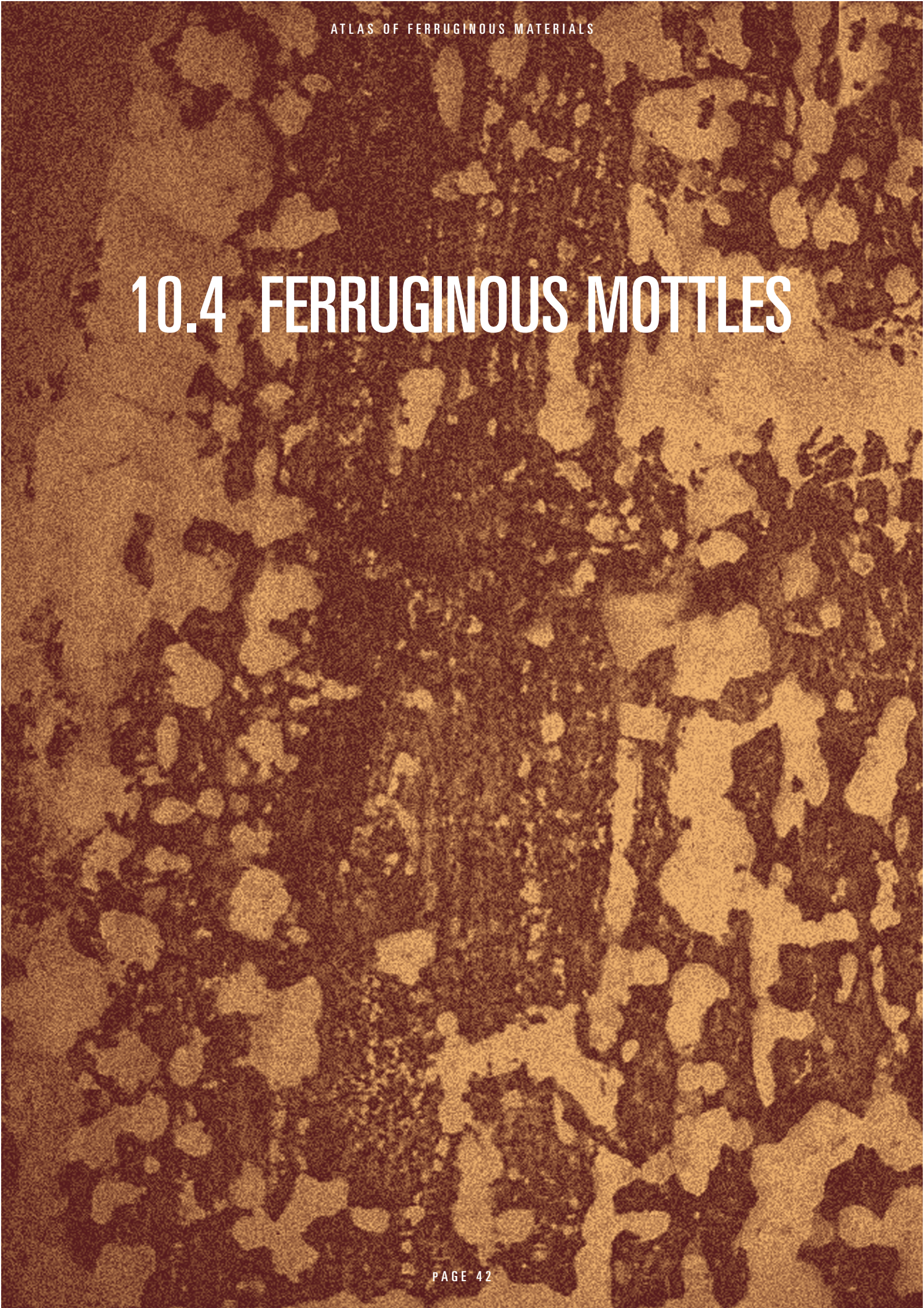

Ferruginous mottles - Field photographs (MZ)

A

Columnar mottles in saprolite (MZ203). This columnar mottled saprolite forms a rise and is overlain by a 1 m thick massive duricrust. Yellow to reddish brown blocky, columnar mottles that contain hematite, goethite and kaolinite have formed from basalt. The orientation of these mottles is controlled by jointing within the bedrock.

Lady Evlyn, Ora Banda.

B

Irregular mottles in residual clays (MZ306). This mottled zone forms a low hill. A close-up photograph of a megamottle shows the transition from a hematite- kaolinite-rich mottle (1) to surrounding kaolinitic clay (2) through a few millimeters of goethite-rich cutan (3). The removal of Fe oxide is inferred to have occurred along palaeo-root holes (4).

Brown Lake, Kalgoorlie.

C

Pisolitic mottles in residual clays (MZ301). This mottled zone occurs beneath 5 m of colluvium-alluvium on a depositional plain. Pisolitic hematite-rich mottles (1) are set in a structureless, variably Fe stained, white, kaolinitic clay (2). Mottles are formed by migration and accumulation of hematite in the kaolinitic matrix or voids. A pale yellow-brown kaolinite-rich cavity fill (3) may be associated with bioturbation.

Midway North Pit, Mt Gibson.

D

Vermiform mottles in inset-valley sediments (MZ405).
This mottled zone in Tertiary inset-valley clays occurs beneath 4 m of Quaternary sediments on a depositional plain. Mottled clays with "worm-like", white mottles (1) are set in a hematitic matrix (2). White mottles are probably the result of bleaching along old root channels. It is envisaged that the whole unit was once oxidised and red; bleaching is a later event.

Bottle Creek.

E

Irregular mottles in residual clays (MZ306). This mottled zone is underlain by ferruginous saprolite developed from basalt and is overlain by a ferruginous breccia of collapsed mottled saprolite. The large, irregular goethite-kaolinite mottle is set in a white kaolinitic matrix.

Gourdis 81400 Pit, Jundee.

F

Platy mottles in inset-valley sediments (MZ402). This mottled zone forms a ridge crest. It comprises platy or tabular red hematite-rich mottles (1), the orientation of which reflects the bedding preserved in the weathered sedimentary substrate. Some mottles transgress the primary bedding. The irregularly shaped bleached areas may be the product of leaching around palaeoroot systems. It is envisaged that the whole unit was once oxidised and red; bleaching is a later event.

Wangine Soak, Davyhurst.

Ferruginous mottles (MZ)

Ferruginous mottles in an unidentified matrix (MZ 100)	Ferruginous mottles in saprolite (MZ 200)	Ferruginous mottles in residual clays (MZ 300)	Ferruginous mottles in sediments (MZ 400)
Pisolitic mottles (MZ101)	Pisolitic mottles (MZ201)	Pisolitic mottles (MZ301)	Pisolitic mottles (MZ401)
Platy mottles (MZ102)	Platy mottles (MZ202)	Platy mottles (MZ302)	Platy mottles (MZ402)
Columnar mottles (MZ103)	Columnar mottles (MZ203)	Columnar mottles (MZ303)	Columnar mottles (MZ403)
Lenticular mottles (MZ104)	Lenticular mottles (MZ204)	Lenticular mottles (MZ304)	Lenticular mottles (MZ404)
Vermiform mottles (MZ105)	Vermiform mottles (MZ205)	Vermiform mottles (MZ305)	Vermiform mottles (MZ405)
Irregular mottles (MZ106)	Irregular mottles (MZ206)	Irregular mottles (MZ306)	Irregular mottles (MZ406)

Ferruginous mottles - Field photographs (MZ)

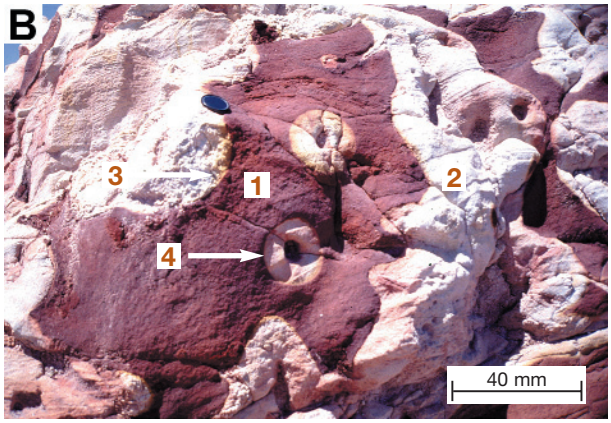

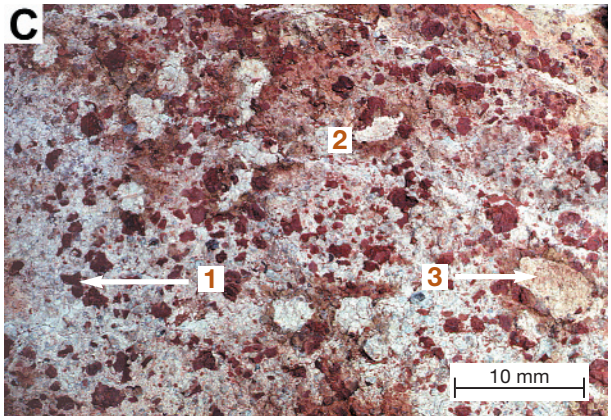

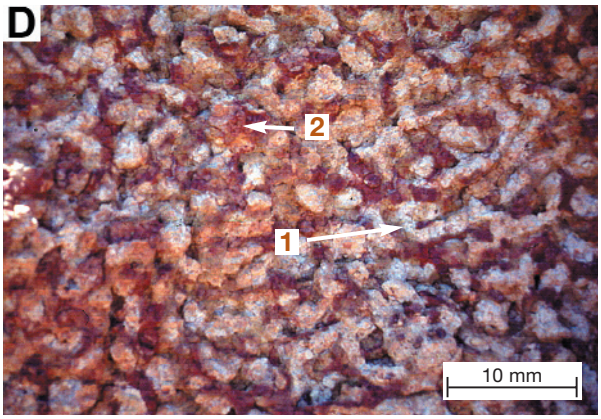

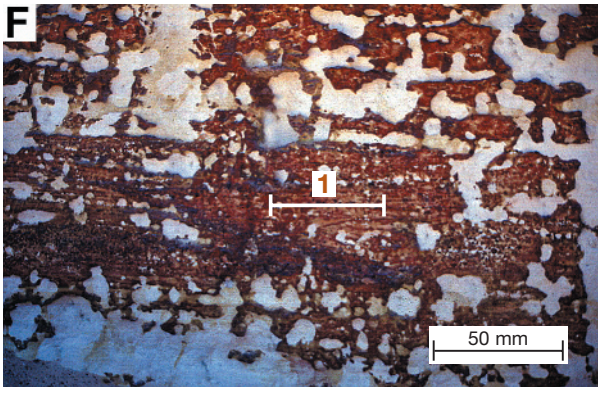

Ferruginous mottles - Hand specimens (MZ)

A

Irregular mottles in residual clays (MZ306). This kaolinitic clay derived from mafic schist is mottled by goethite and hematite and occurs beneath a 1 m thick pisolitic duricrust on a ridge crest. Mottles (1) are poorly defined, yellow to red and are goethite- and hematite-rich. A few incipient nodules (2), comprising goethite and hematite, have diffuse outer rims and are only slightly indurated. The quartz-kaolinite matrix is porous (pores mostly <1mm), relatively soft and kaolinitic.

Sample 07-0291. C Pit, Mt Gibson. *Photograph of the polished surface of a hand specimen taken in oblique reflected light.*

B

Hematite and goethite staining of a quartz-kaolinite matrix (1). Angular to sub-angular quartz grains (2) occur throughout as do fine, vein-like fractures (3).

Sample 07-0291. *Photomicrograph of a thin section taken in transmitted light with crossed polarisers and oblique reflected light.*

C

Irregular mottles in residual clays (MZ306). Mottled granitic clay occurs beneath 2 m of bauxite zone and pisolitic duricrust on the upper slopes at Jarrahdale. Sub angular quartz grains (1) are suspended in both the hematitic mottle and the kaolinitic matrix. A moderately sharp boundary separates the mottle (2) from the pale kaolinitic matrix. (3)

Sample 07-4309. Railway cutting, Jarrahdale. *Photograph of the polished surface of a hand specimen taken in oblique reflected light.*

D

Goethite forms a diffuse rim (1) that separates the hematite stained kaolinite (2) from the unstained kaolinite (3) and around some small cracks (4). Disaggregated angular to sub rounded quartz grains (5) occur in both the mottled and leached clays formed on granite.

Sample 07-4309. *Photomicrograph of a thin section taken in transmitted light with crossed polarisers and oblique reflected light.*

E

Irregular mottles separated from inset-valley sediments (MZ406). This mottle formed in inset-valley sediments occurs beneath 5 m of colluvium-alluvium. The mottle consists of kaolinite, hematite and goethite and contains hematitic pisoliths (1) formed in situ.

Sample 07-3308. Kanowna Deep Leads. *Photograph of the polished surface of a hand specimen taken in oblique reflected light.*

F

Hematite and goethite impregnated kaolinite. Small incipient hematitic pisoliths (1) are formed in situ. Small, angular quartz (2) occurs throughout the matrix. Fine fractures are associated with bleaching (3).

Sample 07-3308. *Photomicrograph of a thin section taken in transmitted light with crossed polarisers and oblique reflected light.*

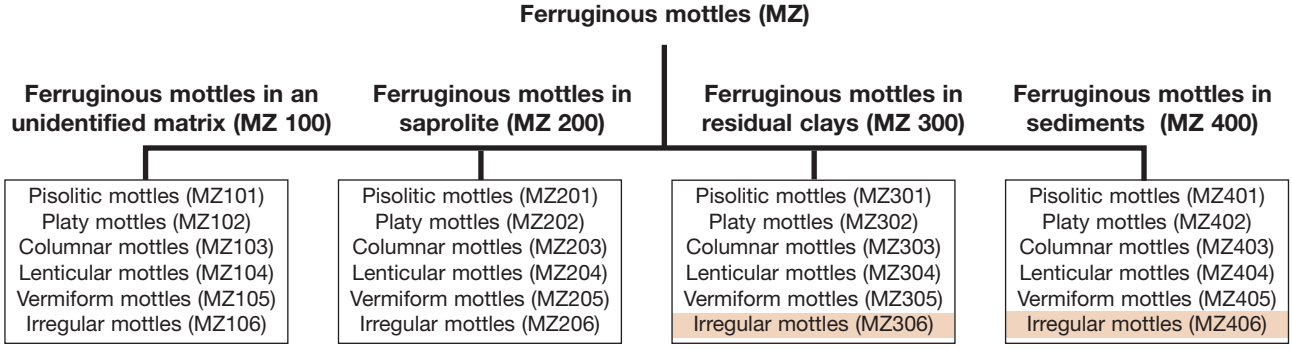

Ferruginous mottles - Hand specimens (MZ)

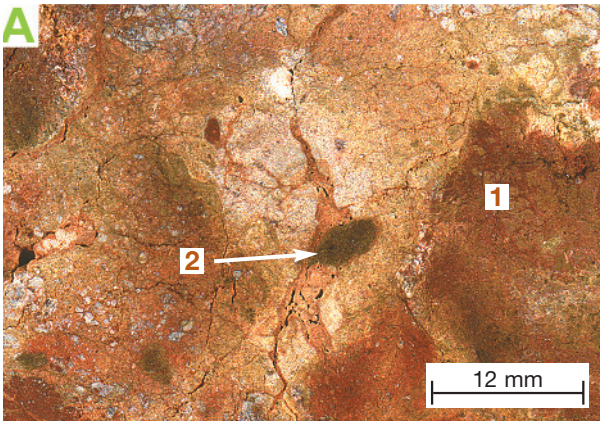

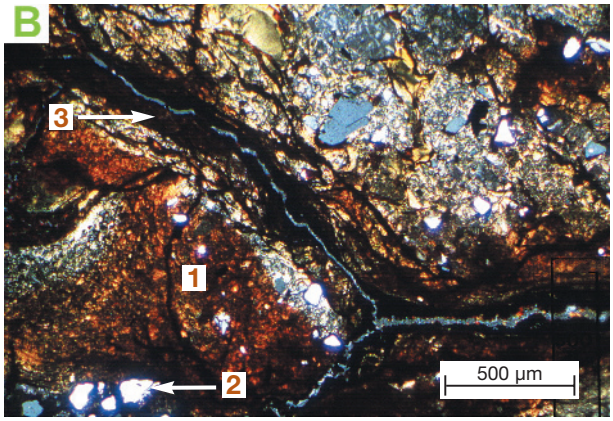

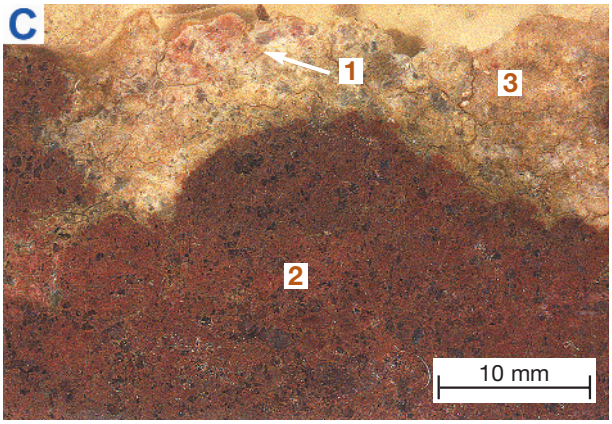

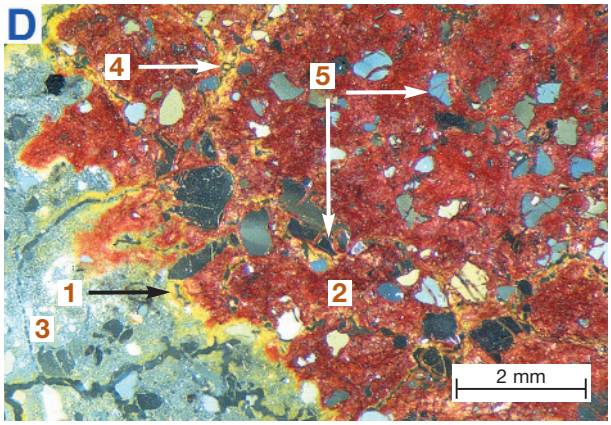

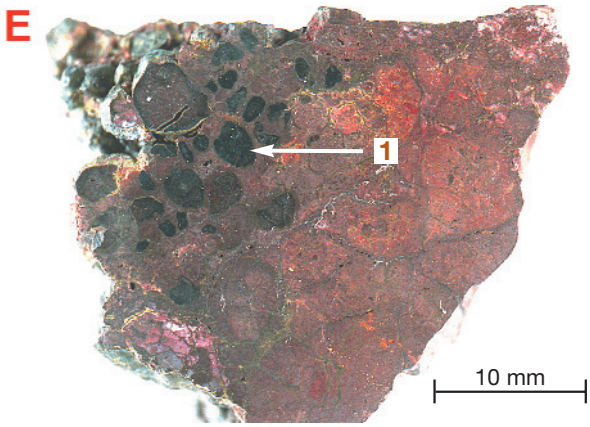

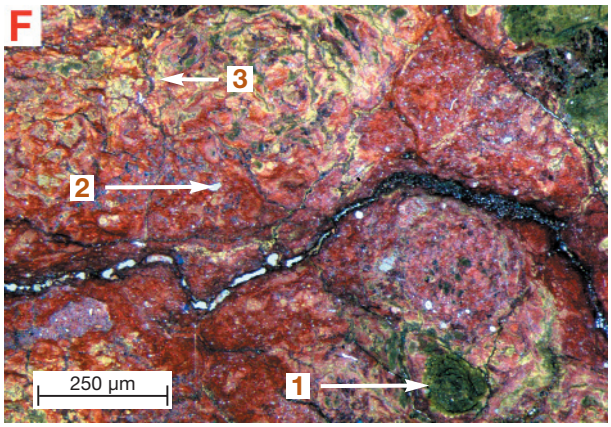

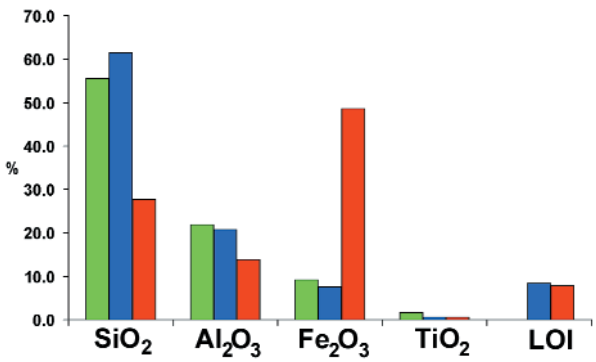

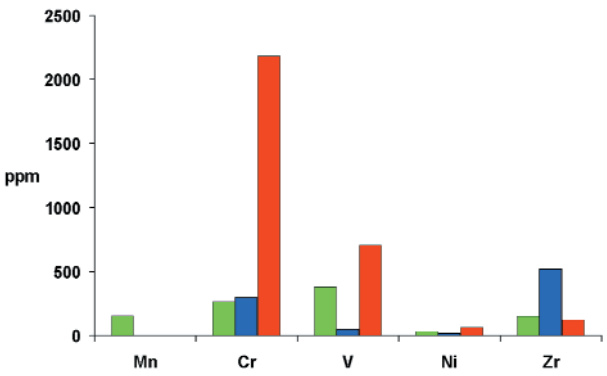

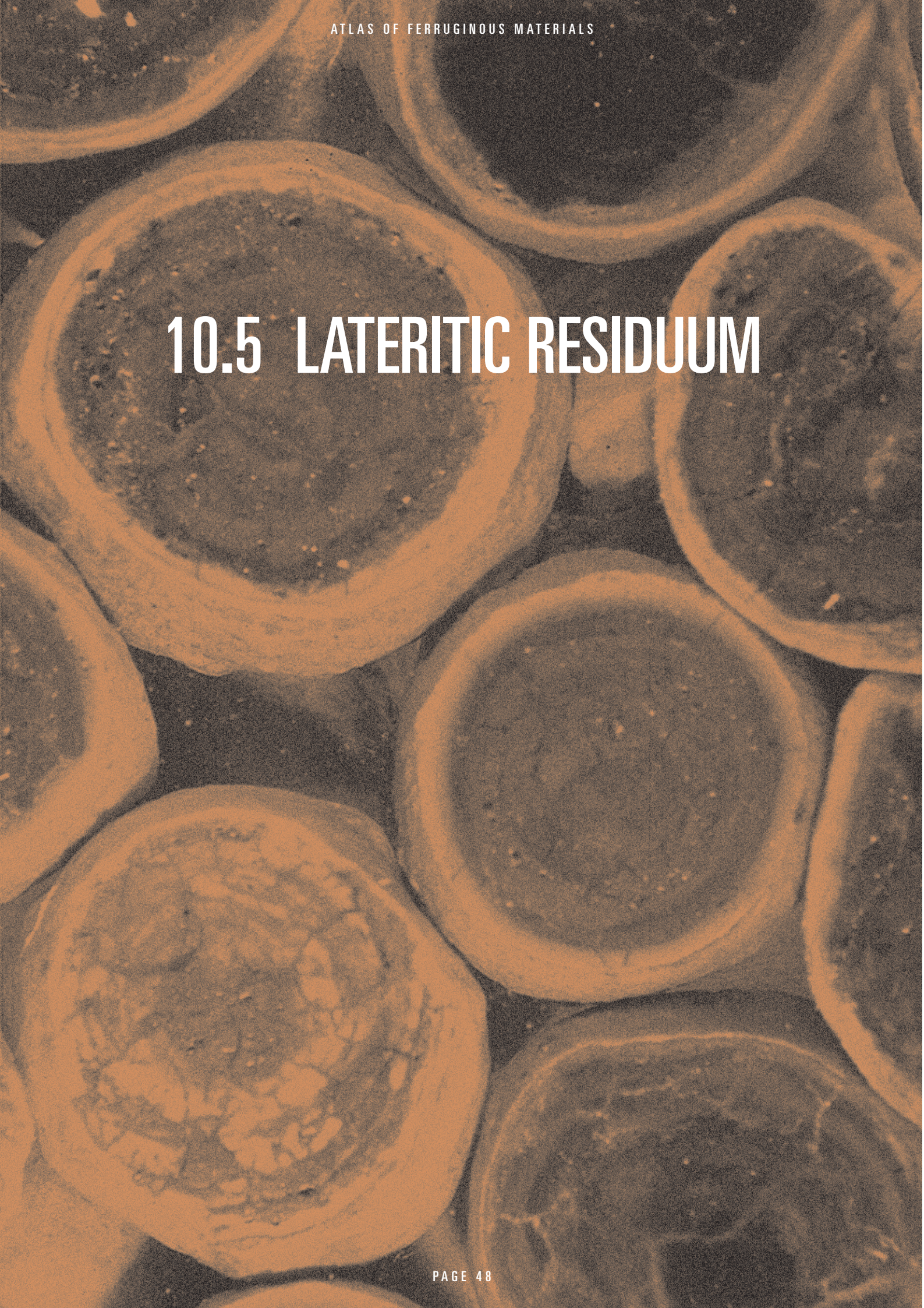

10.5 LATERITIC RESIDUUM

Lateritic gravel (LT100)

The pisoliths shown in photographs A, C and E are characterised by cores and cutans of varying thicknesses. They have formed in surficial environments by the replacement or cementation of soil or colluvium by Fe oxides. They result from pedogenic activity and are formed by leaching, migration and accumulation of Fe oxides in a kaolinitic and/or gibbsitic matrix or in voids. This is not a single event, but involves multiple leaching and precipitation of Fe oxides. The different bands of the cutans indicate a varying pedogenic environment during their formation.

A

Loose pisoliths (LT102). These loose pisoliths occur on upper slopes and are underlain by bauxite developed on granite. The pisoliths have well-developed yellow gibbsite and goethite-rich accretionary cutans (1). Internally, some pisoliths have brown to black hematite-rich cores (2), others are paler and gibbsitic (3).

Sample 07-4332. Toodyay Gravel Pit, Darling Ranges. *Photograph of a polished block taken in oblique reflected light.*

B

A hematite-rich core (1) containing angular quartz grains (2) surrounded by very porous accretionary goethite-rich cutans (3). Accordian-like goethite pseudomorphs after mica (4) also occur.

Sample 07-4332. *Photomicrograph of a polished block taken in normally reflected light.*

C

Loose pisoliths (LT102). Pisoliths from the near-surface formed over granite. There are two types of pisolith: a homogeneous hematite-goethite-quartz pisolith (1) with a thin, yellowish brown goethite-gibbsite-rich cutan (2) and a concentric pisolith with multiple goethite-gibbsite-rich cutans (3).

Sample 07-4312. Railway cutting, Jarrahdale. *Photograph of a polished block taken in oblique reflected light.*

D

A pisolith showing a partially replaced hematite-gibbsite core (1) with finely laminated goethite-gibbsite cutans (2) to form islands of hematite-rich core (3). The process may eventually lead to the formation of multiple goethitic cutans around a hematitic core.

Sample 07-4312. *Photograph of a polished block taken in oblique reflected light.*

E

Loose pisolith (LT102). The pisolith shown contains a red hematite-kaolinite core with gibbsite within small fractures. The 10-15 mm thick light and dark cutans of goethite and gibbsite surrounding the core are concentrically banded.

Sample 07-0508. S Pit, Mt Gibson. *Photograph of the polished surface of a hand specimen taken in oblique reflected light.*

F

A hematitic core (1) encompassed by a series of goethite-kaolinite-rich cutans (2). Small quartz grains (3) occur throughout the sample, both in the core and in the cutans.

Sample 07-0508. *Photomicrograph of a polished block taken in normally reflected light.*

Lateritic gravel (LT100)
(Unconsolidated)
Loose ooliths (LT101)
Loose pisoliths (LT102)
Loose pisoliths and nodules (LT103)
Loose nodules (LT104)

Lateritic gravel (LT100)

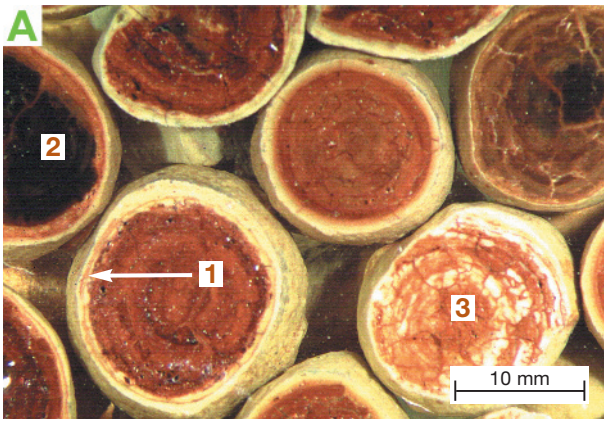

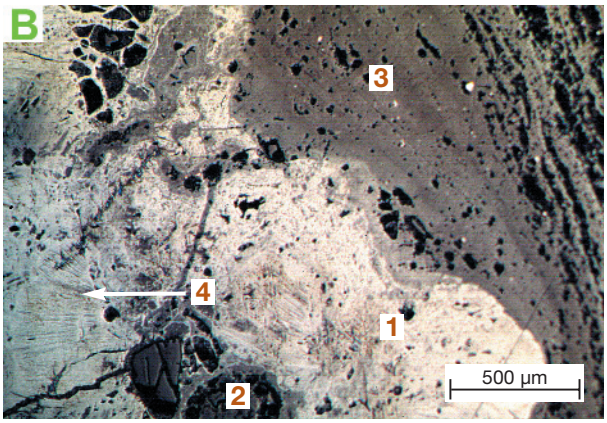

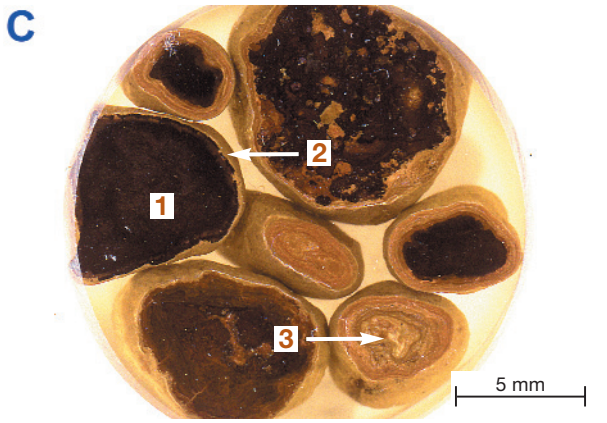

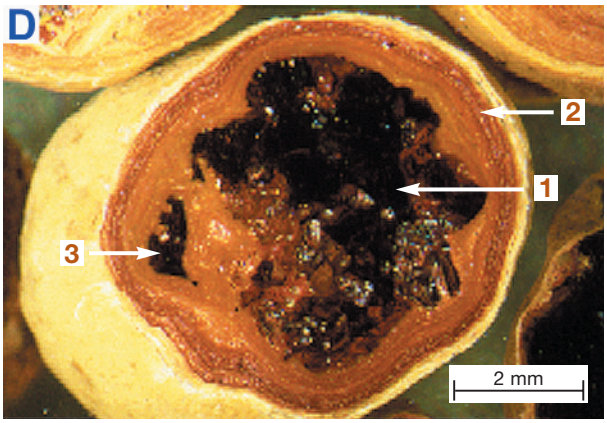

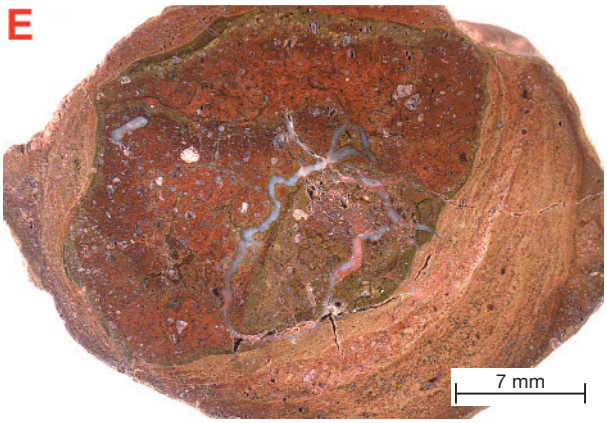

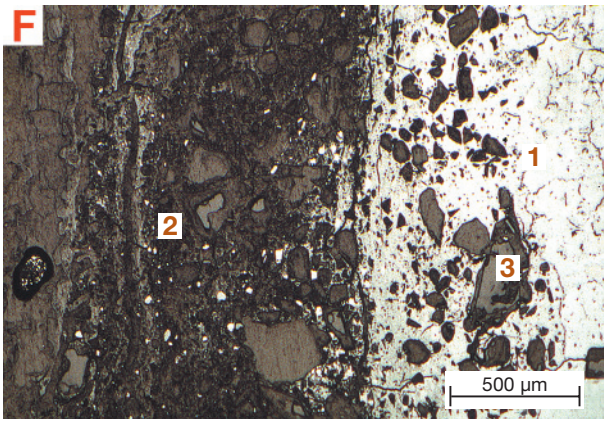

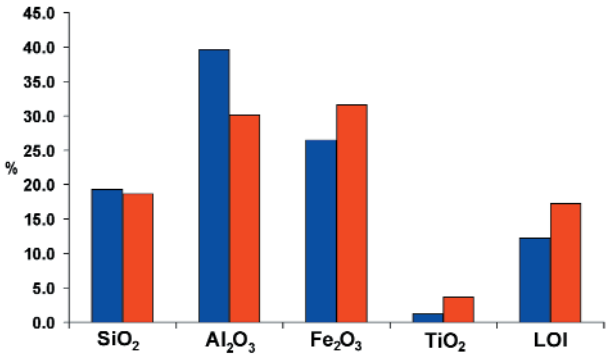

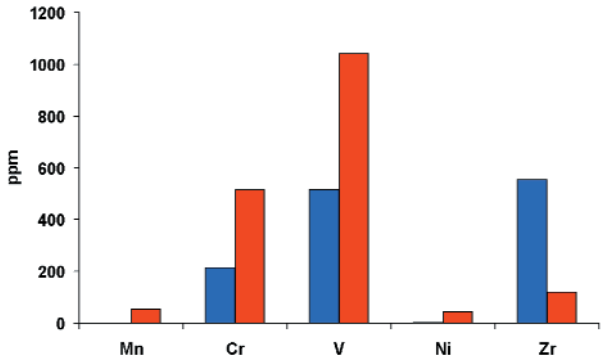

Lateritic gravel (LT100)

The nodules in micrographs A, C and E were formed by ferruginisation of saprolite. They show a simple history relative to the pisoliths shown in the previous page.

A

Loose pisoliths and nodules (LT103). Pisoliths and nodules formed on basalt are dark brown to black, irregular with rounded edges and are hematite-rich. Lithic nodules preserve an original fabric (1). Many of the pisoliths and nodules have syneresis cracks (2) and all are surrounded by thin yellow-brown cutans (3). Some of the cores contain maghemite.

Sample 07-2729. Central Pit, Bronzewing. *Photograph of a polished block taken in oblique reflected light.*

B

A highly reflective hematitic core (1) surrounded by clays variably impregnated with hematite and goethite often as small, concentric ooliths (2). The core has a radial network of cracks due to dessication. The density of this network is greater in the periphery than in the centre.

Sample 07-2729. *Photomicrograph of a polished block taken in normally reflected light.*

C

Loose nodules (LT104). These lithic goethite-rich nodules formed on basalt occur beneath 19 m of sediments on a depositional plain. These are interpreted to be less mineralogically mature than the nodules and pisoliths shown in A. The nodules are angular, comprising ferruginous saprolite fragments, many of which have thin yellow cutans. The schistose fabric (1) of the bedrock is preserved in some fragments.

Sample 07-2528. Central Pit, Bronzewing. *Photograph of a polished block taken in oblique reflected light.*

D

The internal structure of a lateritic nodule showing a preserved schistose fabric (1) comprising a mixture of goethite and kaolinite. Darker areas contain more kaolinite than lighter areas.

Sample 07-2528. *Photomicrograph of a polished thin section taken in normally reflected light.*

E

Loose nodules (LT104). Sections of loose lithic nodules with diffuse hematite-kaolinite mottles (1), incipient goethitic pisoliths (2) and vermiform voids filled with kaolinite and goethite (3)

Sample 07-1310. Meatoa Prospect, Lawlers. *Photograph of the polished surface of hand specimens taken in oblique reflected light.*

F

A void linned with colloform goethite and hematite (1) set in fine grained goethite (2).

Sample 07-1310. *Photomicrograph of a polished block taken in normally reflected light.*

Lateritic gravel (LT100)
(Unconsolidated)
Loose ooliths (LT101)
Loose pisoliths (LT102)
Loose pisoliths and nodules (LT103)
Loose nodules (LT104)

Lateritic gravel (LT100)

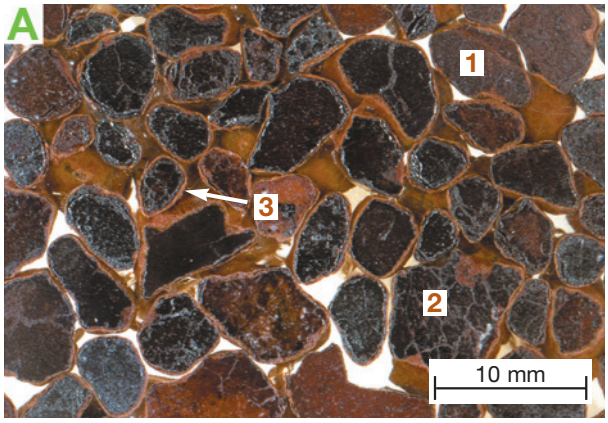

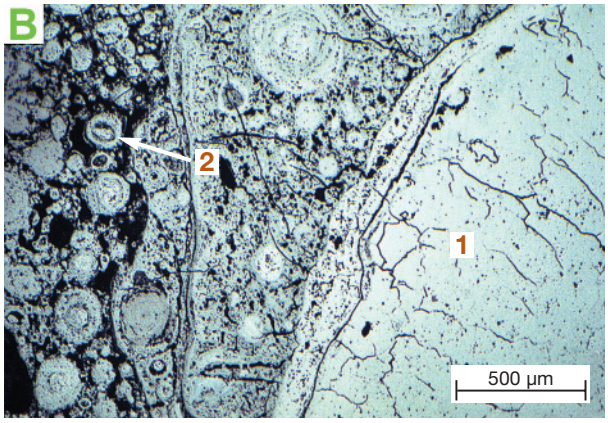

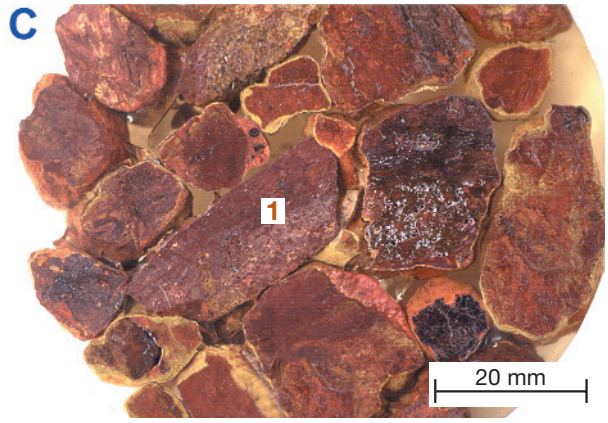

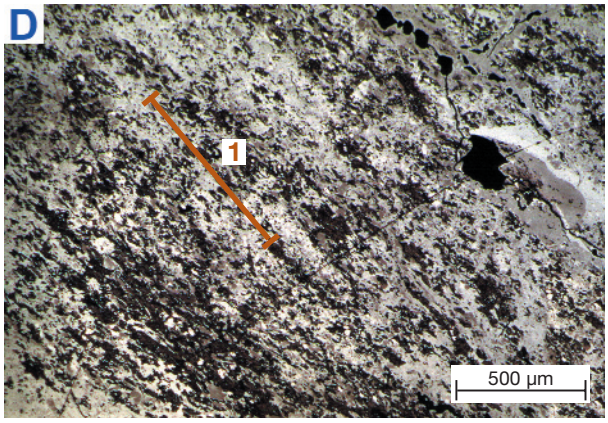

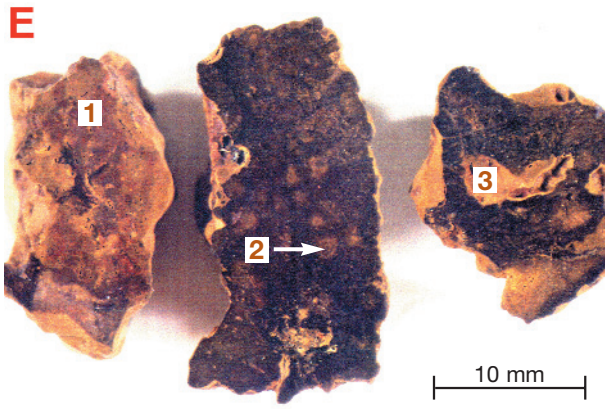

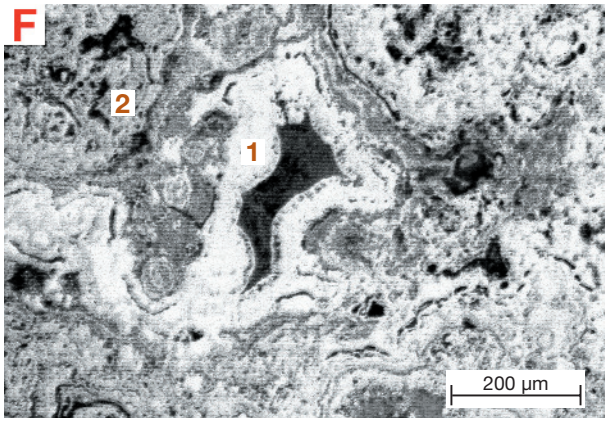

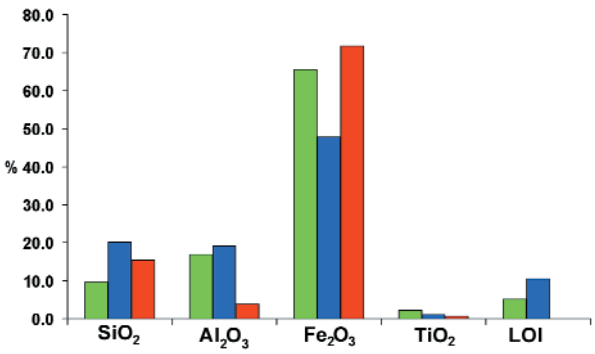

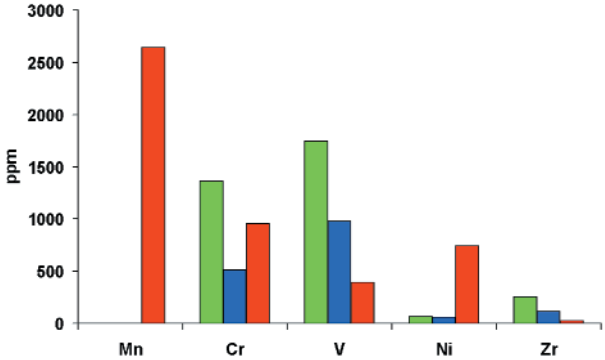

Lateritic duricrust (LT200)

A

Pisolitic duricrust (LT202) This pisolitic duricrust, derived from mafic bedrock, occurs on a ridge crest and is underlain by a mottled zone. It consists of earthy yellow-brown (1) and dark brown (2) pisoliths set in a small amount of kaolinite-rich matrix. Numerous pale areas (3) that are possibly the result of deferruginisation. The duricrust is slightly indurated and its cohesion is due only to the numerous bridges between adjacent cutanic pisoliths (4). The cutans appears to have formed at the expense of the matrix.

Sample 07-0769. TV tower, 4 km NW of Kalgoorlie Hospital. *Photograph of the polished surface of a hand specimen taken in oblique reflected light.*

B

The section shown illustrates the contact between a hematite-rich pisolith (1) and the surrounding goethite-kaolinite-rich matrix (2). Fine cracks (3) transgress the contact between the two and are lined with hematite and goethite.

Sample 07-0769. *Photomicrograph of a polished block taken in normally reflected light.*

C

Pisolitic duricrust (LT202). This pisolitic duricrust, formed in colluvium, occurs on mid slopes and is underlain by bauxite. The polished surface shows concentric pisoliths with thick alternating light (goethite-rich) (1) and dark (hematite-rich) (2) cutans set in a homogeneous, goethite-stained, gibbsite-rich matrix. Some pisoliths have a hematite-maghemite-rich core (3); others are entirely concentrically banded (4). Differing cutans suggest a varying pedogenic environment during their formation. Vermiform voids are lined with yellow gibbsite and kaolinite (5).

Sample 07-1304. Cobiac Pit, Jarrahdale. *Photograph of the polished surface of a hand specimen taken in oblique reflected light.*

D

An opaque hematite-rich core (1) with sub-angular to sub-rounded quartz grains (2). Multiple yellow (3) and brown cutans (4) divide the core of the pisolith from the surrounding orange to brown sandy clay gibbsitic matrix (5). An oval shaped pisolith also occurs (partly shown) which has a lithic fragment as its core (6).

Sample 07-1304. *Photomicrograph of a polished thin section taken in transmitted plain polarised light.*

E

Pisolitic duricrust (LT202) This pisolitic duricrust occurs on mid to lower slopes. The variety of pisoliths suggest that they have formed upslope before being transported (and mixed) to a position further down slope. Pisoliths have cores ranging from earthy red, hematite-stained gibbsite (1) to dark brown to black hematite and maghemite (2) surrounded by red to brown cutans that have formed *in situ* at the expense of the matrix. Some compound pisoliths occur (3) having pre-existing or earlier generations of pisoliths within them (4). The matrix is yellow to light brown gibbsitic sandy clay (5) and has numerous small voids (6).

Sample 07-1094. Boddington. *Photograph of the polished surface of a hand specimen taken in oblique reflected light.*

F

A reflective hematite-rich core (1) set in a matrix of aggregates of goethite stained kaolinite (2). The subrounded aggregates of clay are coated and cemented with colloform goethite (3). Numerous voids also occur (4).

Sample 07-1094. *Photomicrograph of a polished block taken in normally reflected light.*

Lateritic duricrust (LT200)
(Consolidated)
Oolitic duricrust (LT201)
Pisolitic duricrust (LT202)
Pisolitic-nodular duricrust (LT203)
Nodular duricrust (LT204)
Fragmental duricrust (LT205)

Lateritic duricrust (LT200)

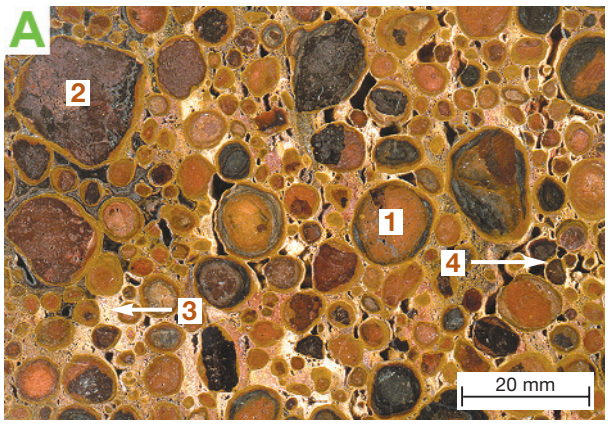

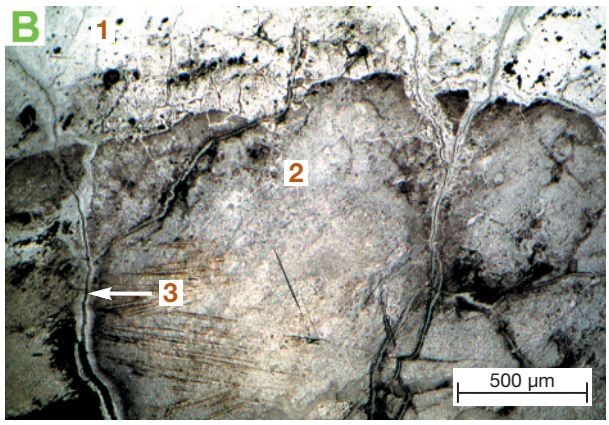

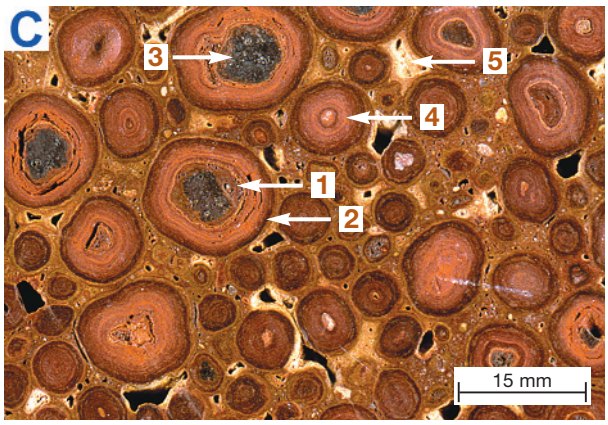

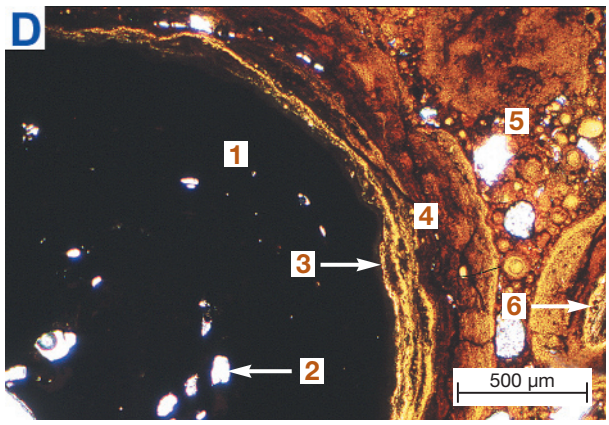

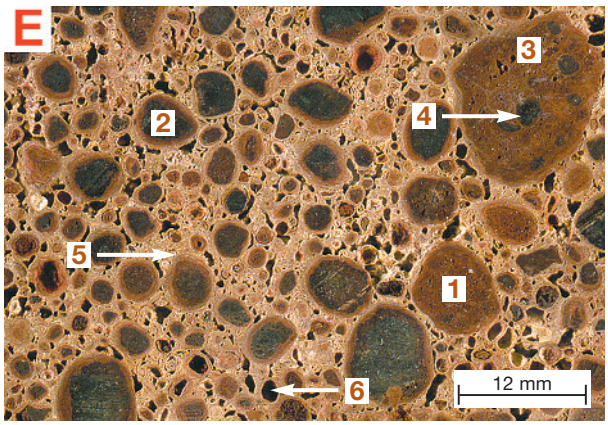

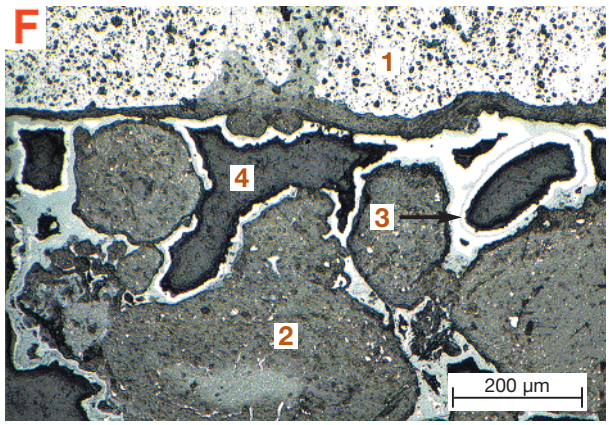

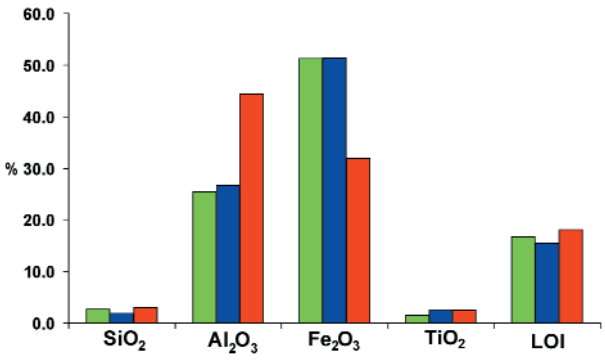

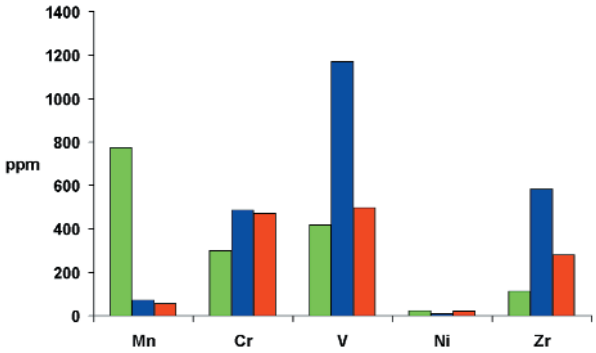

Lateritic duricrust (LT200)

A

Pisolitic nodular duricrust (LT203). This duricrust has formed in colluvium and occurs beneath 3 m of sediments on a depositional plain. A variety of poorly sorted angular to subangular, hematite- and goethite-rich nodules range from earthy red-brown (1) to black hematite fragments (2). They are set in a porous, brown sandy clay matrix (3). Most nodules, derived from the weathering of the underlying bedrock, are encapsulated in a thin, yellow goethitic cutan. Much of the matrix is derived from the overlying sediments.

Sample 07-1468. Midway North Pit, Mt Gibson. *Photograph of the polished surface of a hand specimen taken in oblique reflected light.*

B

Angular to subangular, lithic, earthy red-brown hematite and kaolinite nodules (1) and massive, black, hematite-rich nodules (2) and pisoliths with yellow, goethite-rich clay cutans (3) are set in a brown sandy clay matrix that contains white clay spherites (4). The heterogeneous nature of the nodules, pisoliths and matrix suggests that they were locally transported prior to deposition in an unconsolidated matrix that was later indurated.

Sample 07-0769. *Photomicrograph of a polished thin section taken in transmitted plain polarised light and oblique reflected light.*

C

Pisolitic-nodular duricrust (LT203) This duricrust, developed from granite, consists of large, irregular nodules (1) containing hematite, quartz and gibbsite in a matrix of gibbsite and goethite that contains pisoliths and ooliths (2). The nodules are surrounded by red hematitic (3) and goethitic (4) cutans and become paler towards the centre. They are formed by the ferruginisation of saprolite whereas the pisoliths and ooliths (See D) are formed at the expense of the matrix near the surface.

Sample 07-4311. Railway cutting, Jarrahdale. *Photograph of the polished surface of a hand specimen taken in oblique reflected light.*

D

Ooliths of different sizes with cores of goethite impregnated gibbsite (1) and sub angular to sub rounded quartz (2) surrounded by goethitic cutans (3) set in a matrix of smaller ooliths cemented by goethite (4).

Sample 07-4311. *Photomicrograph of a polished thin section taken in transmitted light with crossed polarisers.*

E

Nodular duricrust (LT204) This duricrust occurs in a midslope position and is underlain by fragmental duricrust. Nodules formed upslope were deposited on midslope and were cemented by locally derived gibbsite and hematite. Reddish brown to black, hematite and maghemite nodules (1) are set in a red hematite and gibbsite matrix (2). The presence of maghemite in nodules suggests they have been in a bush fire in a near surface environment in which much goethite changes to maghemite. The nodules have subsequently been buried or incorporated into a soil. Thus magnetic pisoliths are a clastic component and are different from the matrix in which they occur. Dissolution cavities (3) are common in the matrix.

Sample 07-0361. Pit A, Boddington. *Photograph of the polished surface of a hand specimen taken in oblique reflected light.*

F

Massive, black, hematite-maghemite-rich nodules (1) that are typically surrounded by red, hematitic cutans (2) that follow the irregularities of the outer surface of the core. The matrix comprises variably goethite and hematite impregnated gibbsite (3).

Sample 07-0361. *Photomicrograph of a polished thin section taken in transmitted plain polarised light and oblique reflected light.*

Lateritic duricrust (LT200)
(Consolidated)
Oolitic duricrust (LT201)
Pisolitic duricrust (LT202)
Pisolitic-nodular duricrust (LT203)
Nodular duricrust (LT204)
Fragmental duricrust (LT205)

Lateritic duricrust (LT200)

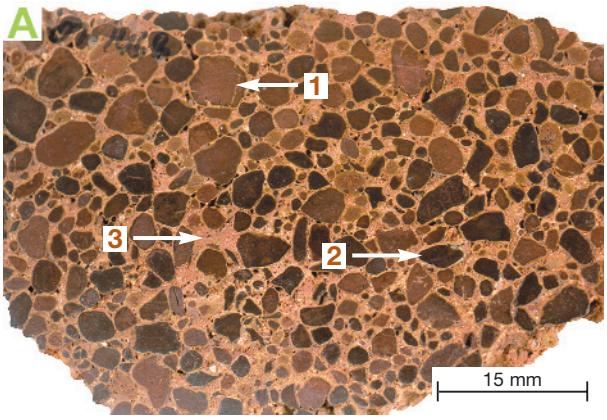

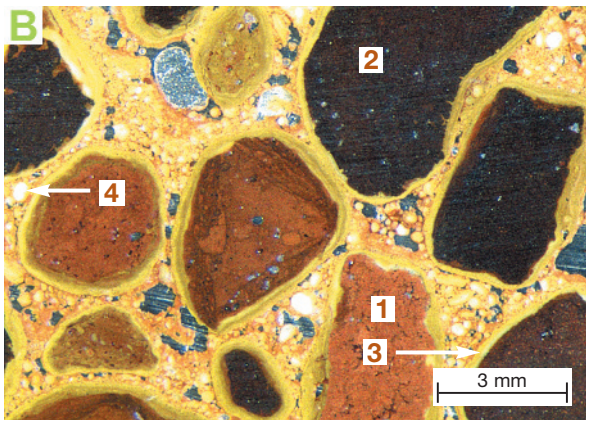

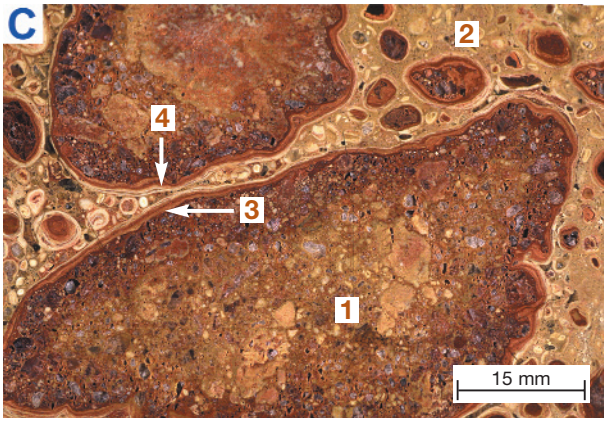

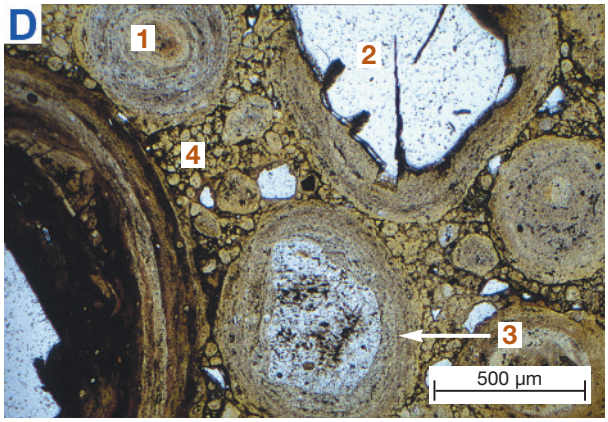

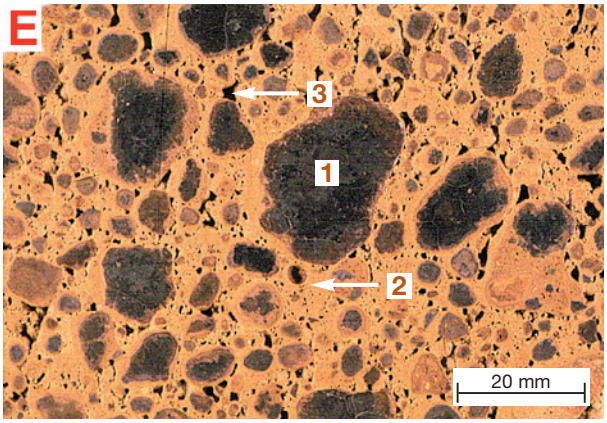

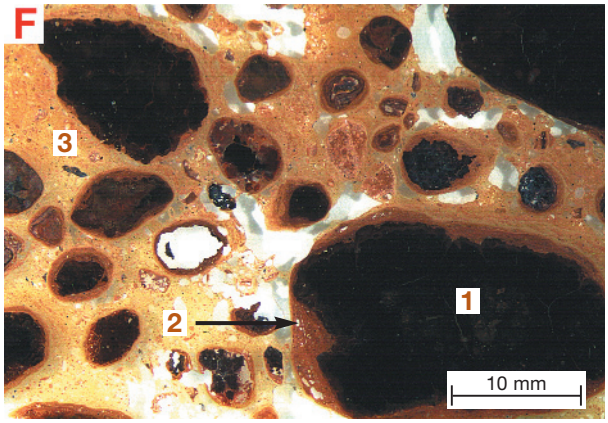

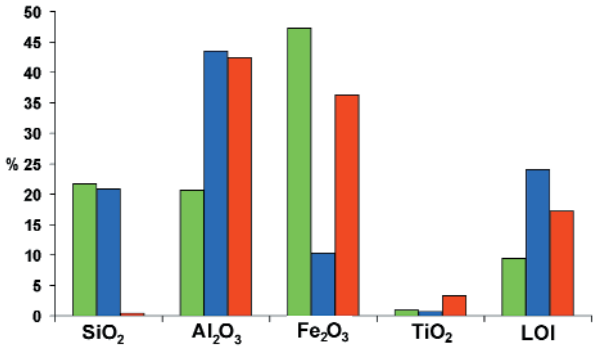

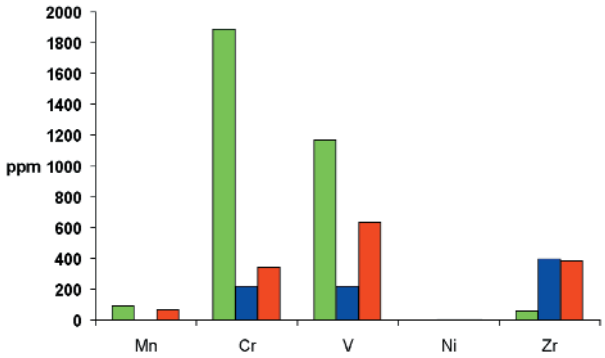

Lateritic duricrust (LT200)

Fragmental duricrusts are ferruginous mottles or fragments of ferruginous saprolite in a matrix of kaolinite or gibbsite derived from saprolite or locally derived colluvium which have been later cemented by goethite.

A

Fragmental duricrust (LT205). This fragmental duricrust formed from basalt occurs beneath 1 m thick hardpanised sediments in a midslope position. Large, brown, hematite-rich lithic fragments with thin yellow cutans (1), some of which contain a primary fabric, are set in a partly silicified, slightly porous matrix of detrital quartz and sand-sized ferruginous detritus (2). The matrix is largely derived from the overlying colluvial sediments. A variety of smaller fragments comprise yellow to red, silicified, hematite and goethite (3).

Sample 07-0523. S Pit, Mt Gibson. *Photograph of the polished surface of a hand specimen taken in oblique reflected light.*

B

Part of a lithic fragment showing relic talc set in a goethite and hematite matrix.

Sample 07-0523. *Photomicrograph of a polished block taken in normally reflected light.*

C

Fragmental duricrust (LT205). This duricrust, developed on felsic andesite, occurs in an upslope position and is overlain by pisolitic duricrust. Angular to sub angular, dark red, hematite-gibbsite fragments (1) many of which contain pseudomorphs after feldspars, are set in a pale gibbsite-rich matrix (2). Voids have been infilled with kaolinite and gibbsite.

Sample 07-1106. Pit D, Boddington. *Photograph of the polished surface of a hand specimen taken in oblique reflected light.*

D

The matrix of plate C showing gibbsite pseudomorphs after feldspar (1).

Sample 07-1106. *Photomicrograph of a polished thin section taken in transmitted plain polarised light.*

E

Fragmental duricrust (LT205). Subangular hematite-rich fragments (1), some of which retain a lithic fabric (2) and pisoliths (3) in a matrix of goethite- and quartz-rich gibbsitic clay (4). Some voids also occur (5). This duricrust has formed on an iron-rich sediment of the Horseshoe Formation.
(Sample and description after Robertson et al, 1996).

Sample 09-1199. Baxter. *Photograph of the polished surface of a hand specimen taken in oblique reflected light.*

F

Hematite-rich fragments and pisoliths. Grains of magnetite are now pseudomorphed by hematite (1) with a characteristic trellis fabric (martite). The cementing matrix is goethite- and quartz- rich gibbsitic clay (2) with numerous voids (3).
(Sample and description after Robertson *et al*, 1996).

Sample 09-1199. *Photomicrograph of a polished block taken in normally reflected light.*

Lateritic duricrust (LT200)
(Consolidated)
Oolitic duricrust (LT201)
Pisolitic duricrust (LT202)
Pisolitic-nodular duricrust (LT203)
Nodular duricrust (LT204)
Fragmental duricrust (LT205)

Lateritic duricrust (LT200)

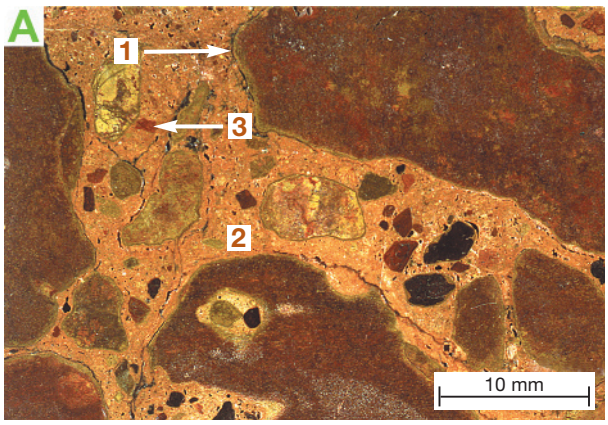

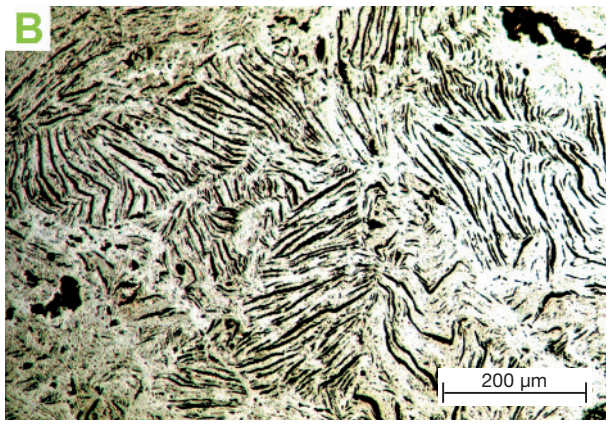

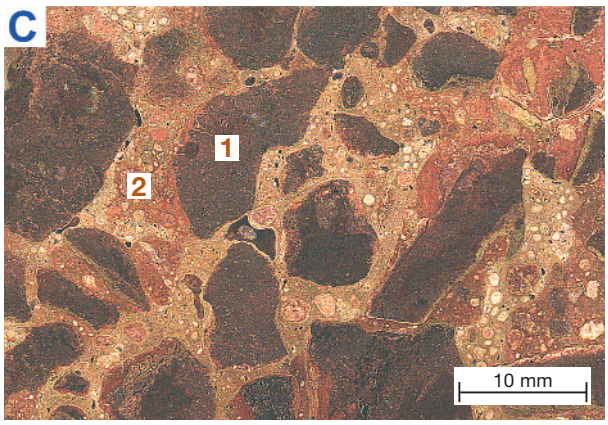

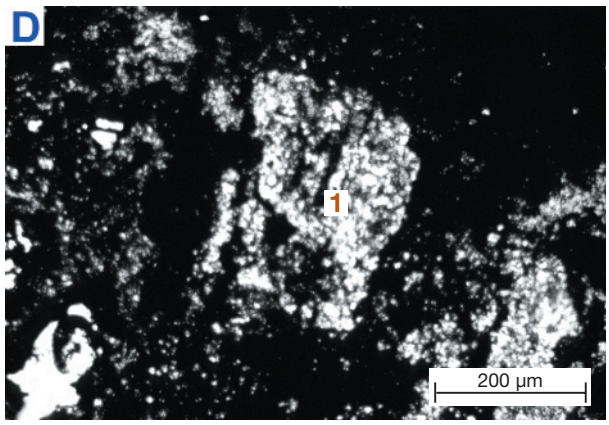

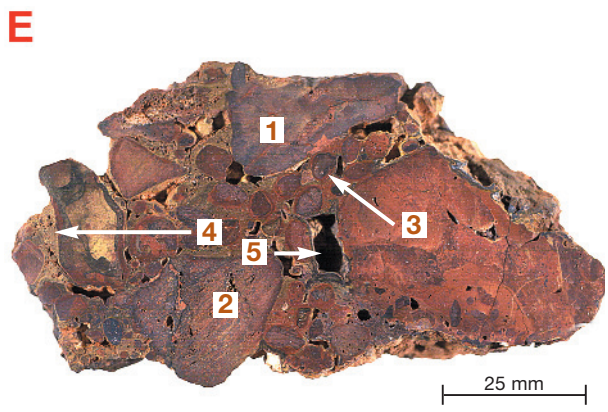

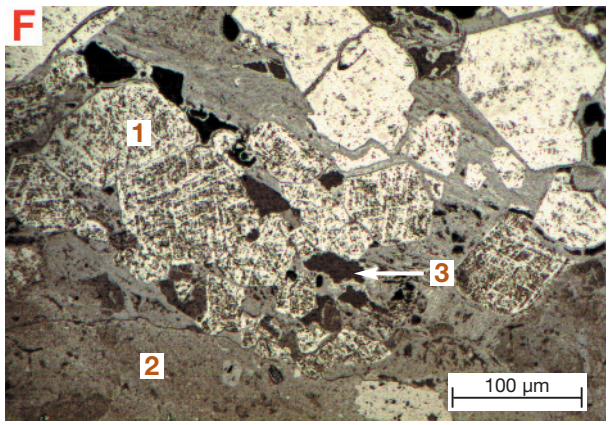

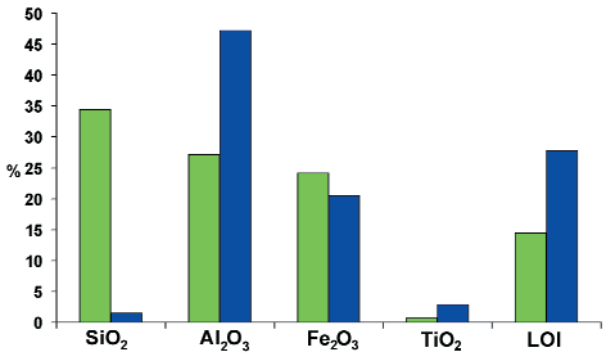

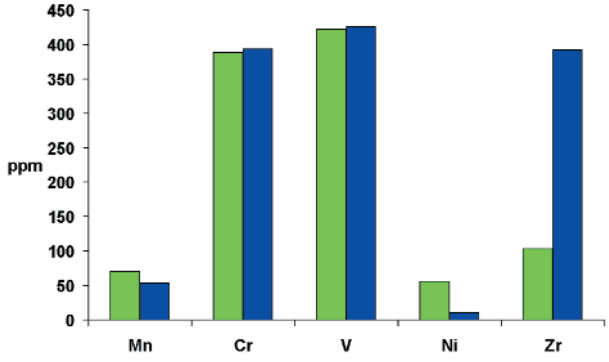

Lateritic duricrust (LT200)

A

Packed pisolitic duricrust (LT212). This packed pisolitic duricrust occurs on lower slopes and overlies a bauxite zone. It comprises reworked hematite and gibbsite pisoliths cemented by their goethite-quartz outer cutans.

Sample 07-1306. Cobiac Pit, Jarrahdale. *Photograph of a hand specimen taken in oblique reflected light.*

B

Pisoliths (1) the cores of which are red to black, hematite-rich fragments, some of which are magnetic. Most pisoliths have yellow-brown, goethite-gibbsite-rich cutans (2) with fine, sand-sized quartz grains. Intersticial cavities between pisoliths (3) occur with sporadic patches of iron-cemented quartz-rich sand (4) and larger quartz grains (5).

Sample 07-1306. *Photomicrograph of a polished thin section taken in transmitted light with crossed polarisers and oblique reflected light.*

C

Packed pisolitic-nodular duricrust (LT213). This duricrust occurs on a lower slope. Poorly sorted, irregular, hematite-rich nodules with yellow cutans are weakly re-cemented by outer cutans or in places by small amounts of matrix. Isolated, round frosted quartz grains, reaching 5 mm in size, occur as part of the detrital framework. Interstices have resulted in a very porous and permeable duricrust with some sandy yellow clay infilling.

Sample 07-1307. Huntly Mine, Darling Range. *Photograph of a hand specimen taken in oblique reflected light.*

D

A hematitic reflective core (1) surrounded by a series of goethite-clay-rich cutans (2). The inner cutan is less reflective and contains small, angular quartz grains (3). The outer, more reflective cutan has lesser angular quartz grains (4). Angular to sub angular quartz grains are set in the sandy clay matrix (5) and in the core (6).

Sample 07-1307. *Photomicrograph of a polished block taken in normally reflected light.*

E

Packed pisolitic-nodular duricrust (LT213). This duricrust comprises black, poorly sorted, irregular hematite-maghemite-rich nodules and pisoliths cemented by hematite. Detrital angular quartz grains occur within the matrix.

Kalgoorlie. *Photograph of a hand specimen taken in oblique reflected light.*

Lateritic duricrust (LT200)
(Consolidated)
Oolitic duricrust (LT201)
Pisolitic duricrust (LT202)
Pisolitic-nodular duricrust (LT203)
Nodular duricrust (LT204)
Fragmental duricrust (LT205)

Packed oolitic duricrust (LT211)
Packed pisolitic duricrust (LT212)
Packed pisolitic-nodular duricrust (LT213)
Packed nodular duricrust (LT214)

Vermiform duricrust (LT231)
Cellular duricrust (LT232)
Vesicular duricrust (LT233)

Mottled duricrust (LT241)
Massive duricrust (LT242)

Lateritic duricrust (LT200)

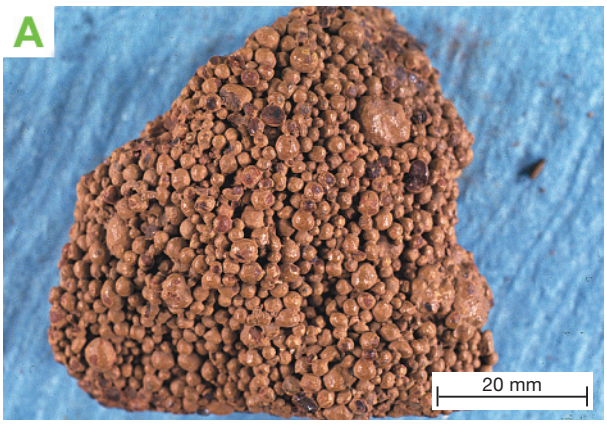

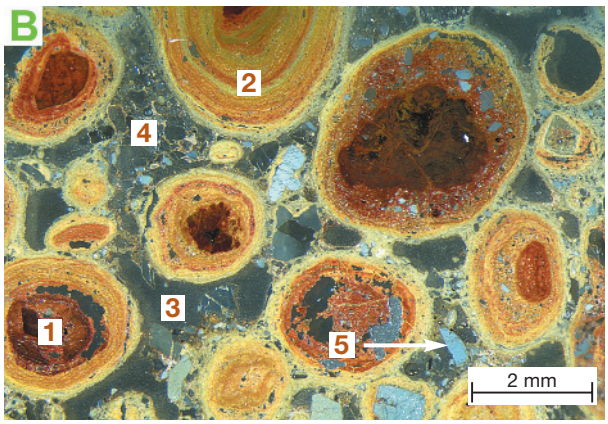

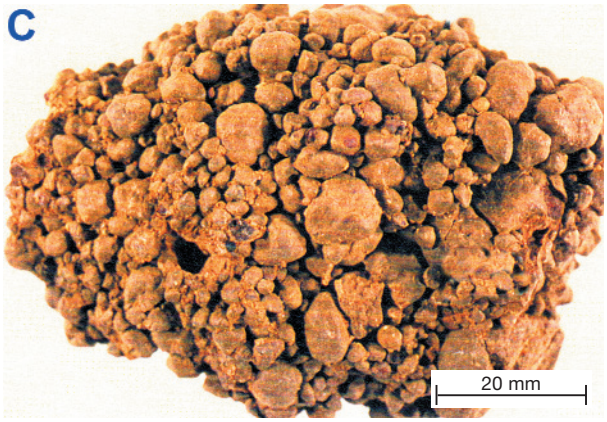

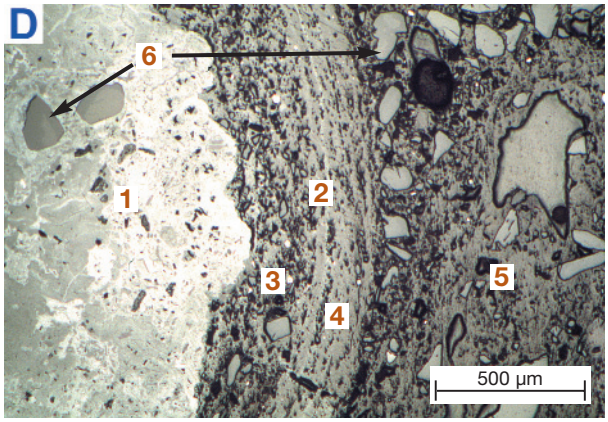

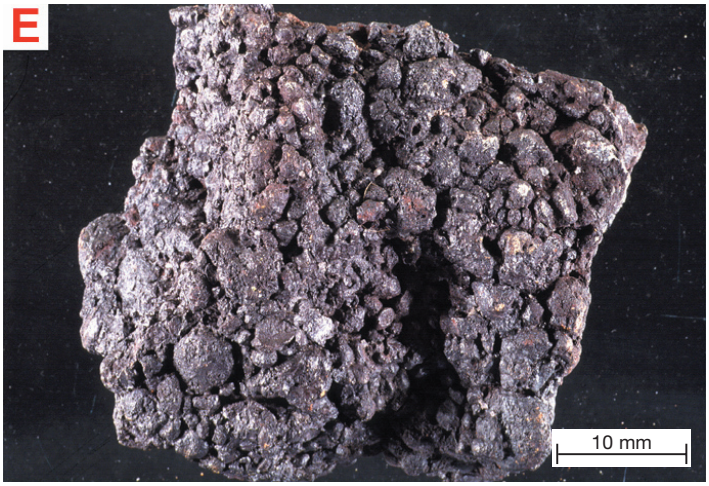

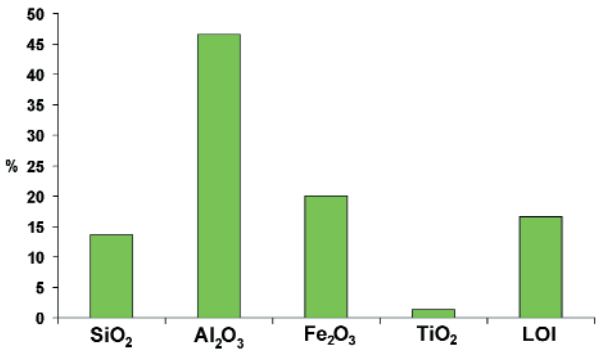

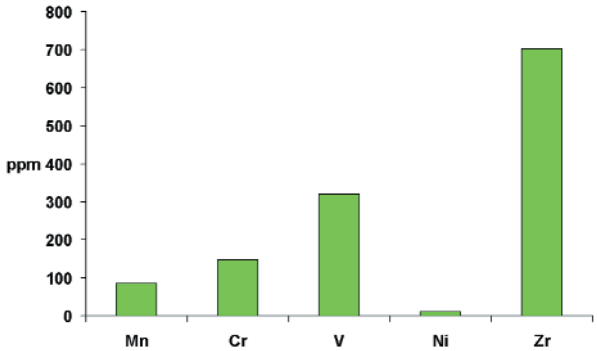

Lateritic duricrust (LT200)

A

Vermiform duricrust (LT231) This duricrust comprises a red-brown hematite-kaolinite-rich matrix (1) in which vermiform voids (2) occur. The voids are filled with a weakly cemented saccaroidal framework of glassy quartz grains and kaolinite.

Sample 07-0569. S Pit, Mt Gibson. *Photograph of the surface of a hand specimen taken in oblique reflected light.*

B

A section showing both the matrix (1) and the void fill (2) of hematitic clay spheres (3) that are cemented by goethite. In places the goethite-rich areas have been partly dissolved leaving interlinked vesicles (4).

Sample 07-0569. *Photomicrograph of a polished block taken in normally reflected light.*

C

Vermiform duricrust (LT231) This duricrust, developed on mafic bedrock, occurs on a ridge crest and is overlain by pisolitic duricrust. It is characterised by an orange to brown hematitic-gibbsitic matrix (1) with red, hematite-rich nodules (2) that have formed in situ. Crystalline, laminated goethite fills the vermiform cavities (3) and other areas of yellow to brown goethite infilling also occur (4).

Sample 07-0770. TV tower, Kalgoorlie. *Photograph of the polished surface of a hand specimen taken in oblique reflected light.*

D

Goethite lamellae growing radially from the walls of a vermiform cavity.

Sample 07-0770. *Photomicrograph of a polished thin section taken in transmitted light with crossed polarisers.*

E

Cellular duricrust (LT232) This duricrust occurs in a mid slope and is underlain by mottled zone. It is characterised by bubble-shaped voids, some of which are thinly lined by goethite and kaolinite. The voids appear to be the result of dissolution of the matrix. There is no infilling in the voids.

Sample 07-1307. Mt Gibson. *Photograph of a hand specimen taken in oblique reflected light.*

Lateritic duricrust (LT200)
(Consolidated)
Oolitic duricrust (LT201)
Pisolitic duricrust (LT202)
Pisolitic-nodular duricrust (LT203)
Nodular duricrust (LT204)
Fragmental duricrust (LT205)

Packed oolitic duricrust (LT211)
Packed pisolitic duricrust (LT212)
Packed pisolitic-nodular duricrust (LT213)
Packed nodular duricrust (LT214)

Vermiform duricrust (LT231)
Cellular duricrust (LT232)
Vesicular duricrust (LT233)

Mottled duricrust (LT241)
Massive duricrust (LT242)

Lateritic duricrust (LT200)

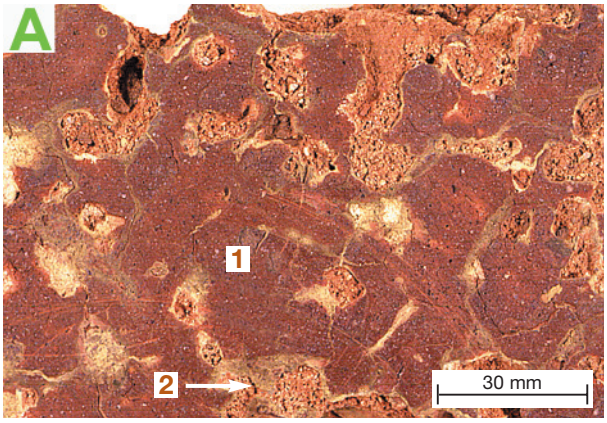

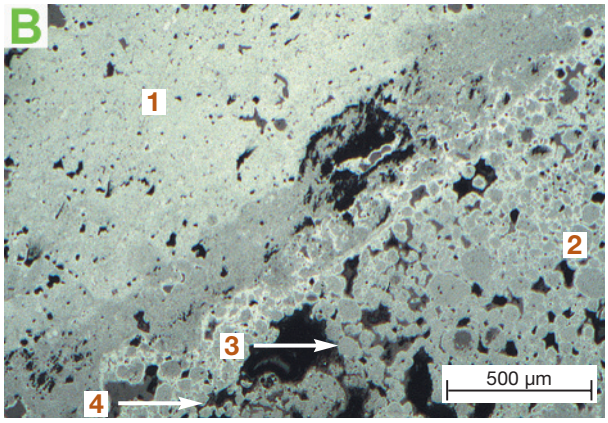

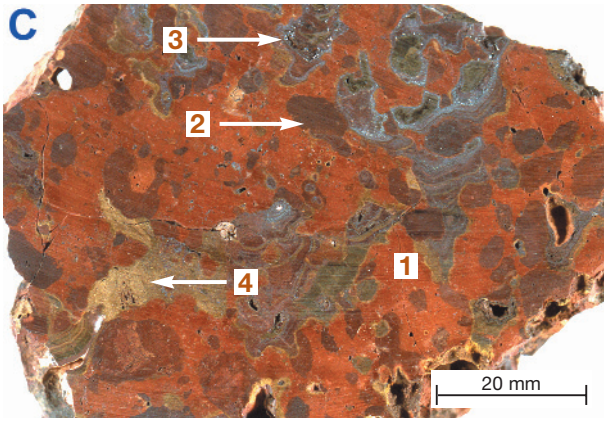

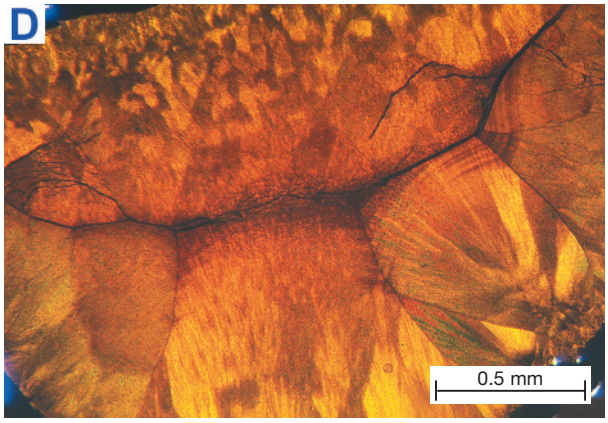

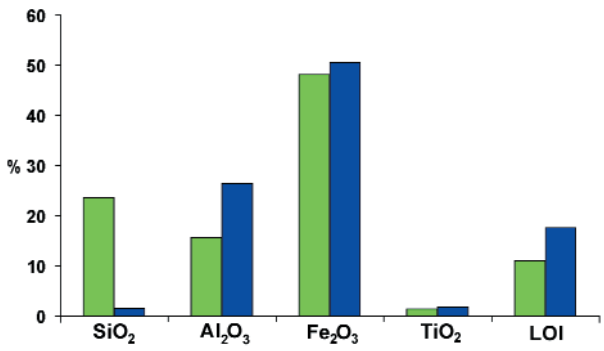

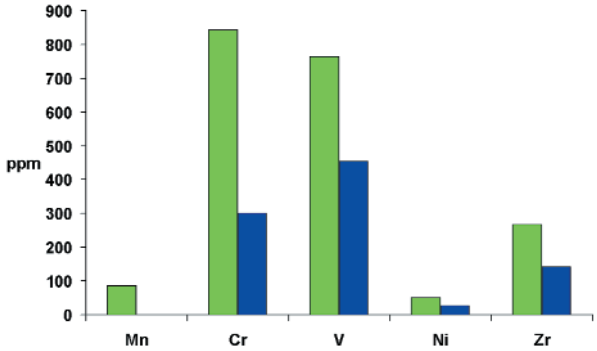

Lateritic duricrust (LT200)

A

Vermiform duricrust (LT231) This vermiform duricrust occurs in an upper slope position. It has a red to brown Fe indurated matrix (1) comprising hematite, goethite and gibbsite that is penetrated by numerous vermiform voids (2). The sandy infill sediment in some voids is weakly cemented quartz grains and white-orange soft kaolinitic spherules (3).

Sample 07-4620. Cobiac Pit, Darling Range. *Photograph of the polished surface of a hand specimen taken in oblique reflected light.*

B

Vesicular duricrust (LT233) This duricrust, derived from gabbro, forms a ridge crest. It has a red-brown-black hematite-rich matrix (1) with small vesicles (2), some of which are filled with goethite stained clays (3). The matrix contains some quartz grains (4) and the sample is non-magnetic.

Sample 07-0716. Clifford, Leonora. *Photograph of the polished surface of a hand specimen taken in oblique reflected light.*

C

Leaching of massive hematite-rich material along various voids and fractures has resulted in Fe-rich (1) and Fe-poor (2) areas. Some leaching haloes mirror the shape of the void they encompass.

Sample 07-0716. *Photomicrograph of a polished block taken in normally reflected light.*

D

Massive duricrust (LT242) The section shows massive hematite with some fine irregular cracks (1). Some pitting occurs on the surface which represents areas of lesser induration and hence greater friability.

Sample 07-1314. Meatoa Prospect, Lawlers. *Photograph of the polished surface of a hand specimen taken in oblique reflected light.*

Lateritic duricrust (LT200)
(Consolidated)
Oolitic duricrust (LT201)
Pisolitic duricrust (LT202)
Pisolitic-nodular duricrust (LT203)
Nodular duricrust (LT204)
Fragmental duricrust (LT205)

Packed oolitic duricrust (LT211)
Packed pisolitic duricrust (LT212)
Packed pisolitic-nodular duricrust (LT213)
Packed nodular duricrust (LT214)

Vermiform duricrust (LT231)
Cellular duricrust (LT232)
Vesicular duricrust (LT233)

Mottled duricrust (LT241)
Massive duricrust (LT242)

Lateritic duricrust (LT200)

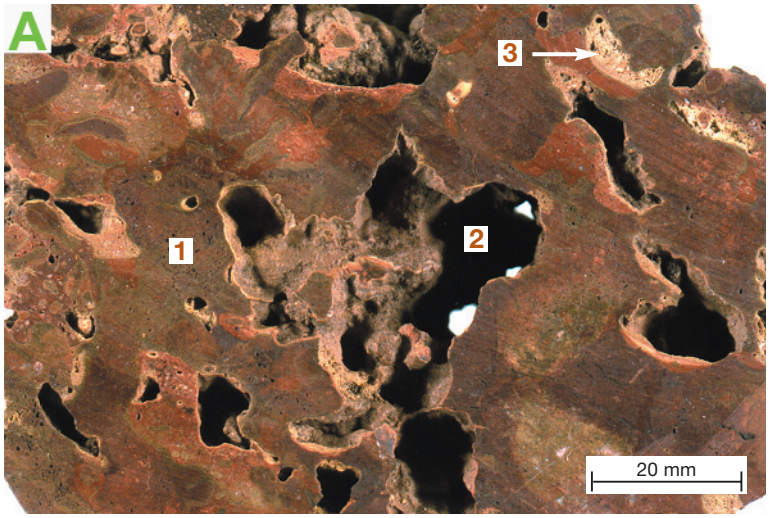

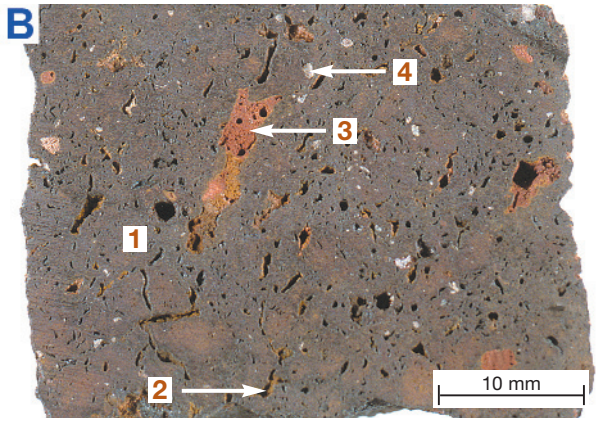

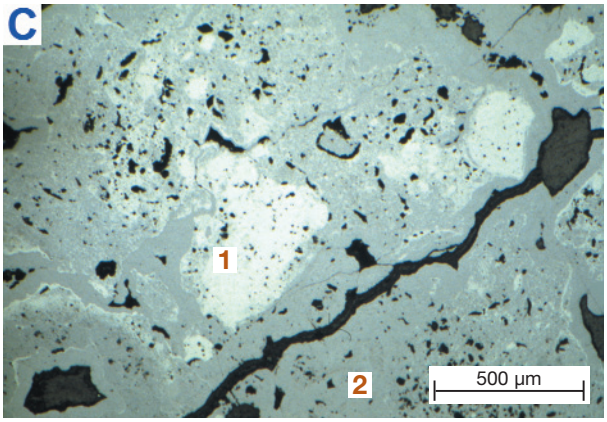

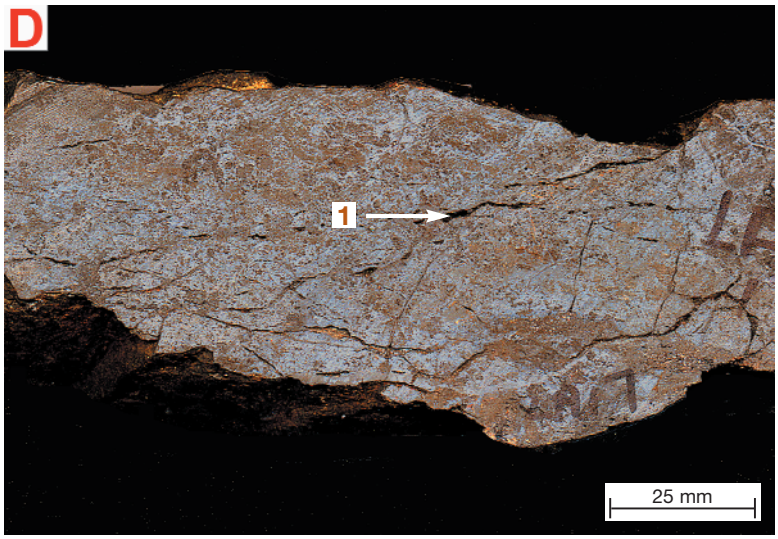

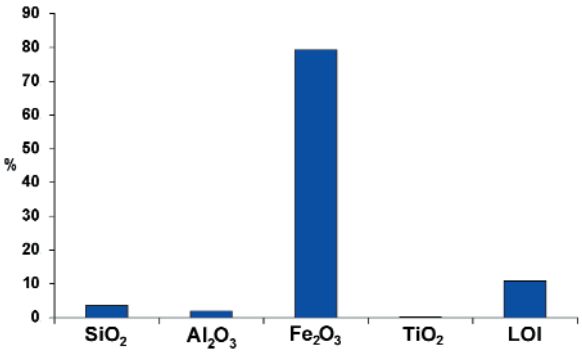

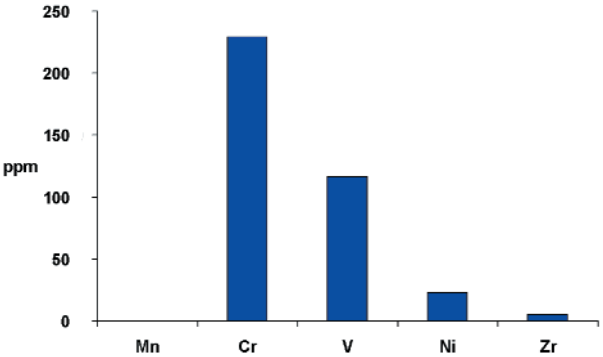

10.6 FERRICRETE

Ferricrete (LF200)

Ferricrete is an Fe oxide cemented sediment. The type of ferricrete is controlled by the nature of the sediment and the cement. The ferricretes shown are either (a) formed by the cementation of coarse clasts, sands and clays by Fe oxides or (b) formed by the development of authigenic hematite- and goethite-rich pisoliths and nodules in sediments. Goethite in the cement typically has low Al substitution, so Fe is probably derived hydromorphically by absolute accumulation or by Fe migration in a strongly reducing environment. The common occurrence of ferruginised wood fragments may suggest formation in a swamp or bog environment.

A

Oolitic ferricrete (LF201) This oolitic ferricrete forms a ridge crest and unconformably overlies saprolite developed over mafic bedrock. The ferricrete shows the hetrogeneous nature of the components which include ooliths (1) and lithic fragments (2) set in a goethite-rich matrix. Ooliths have a variety of cores ranging from hematite to ferruginised wood.

Sample 07-1390. Brilliant, Lawlers. *Photograph of the polished surface of a hand specimen taken in oblique reflected light.*

B

The core of an oolith comprising goethite replaced woody tissue.

Sample 07-1390. *Photomicrograph of a polished block taken in normally reflected light.*

C

Pisolitic ferricrete (LF202) This pisolitic ferricrete is overlain by about 3 m of hardpanised sediments and is underlain by mottled sediments. It comprises authigenic hematite-rich pisoliths set in a kaolinite-hematite matrix that is variably bleached due to the removal of Fe.

Sample 07-6498. Bulloak Pit, Sandstone. *Photograph of the polished surface of a hand specimen taken in oblique reflected light.*

D

A quartz-rich pisolith set in kaolinitic clays. The black core of the pisolith (1) is encased by both hematitic (2) and goethitic (3) cutans. Poorly sorted angular quartz (4) occurs in both the matrix and the pisolith.

Sample 07-6497. Bulloak Pit, Sandstone. *Photomicrograph of a polished thin section taken in transmitted light with crossed polarisers and oblique reflected light.*

E

Pisolitic ferricrete (LF202) Pisolitic ferricrete showing cutanic pisoliths, some of which contain goethite replaced wood fragments cores (1). The internal structure of some of these fragments suggests that they are from a monocotyledon-type plant. Other cores are red-brown to black and hematite-rich (2). Most pisoliths have a series of alternating yellow to brown cutans. The matrix is dominated by a dark brown goethite cement (3) and yellow, void-filling clays occur (4).

Sample 02-5062. Madoonga. *Photograph of the polished surface of a hand specimen taken in oblique reflected light.*

F

Goethite replaced wood fragments (1) form the core of some pisoliths. The cores of others are ferruginous clays (2). Some pisoliths show fragmentation and truncation of their inner cutans (3) which have been subject to transportation and encased by goethite-rich concentric cutan accretion (4). The pisoliths have been cemented by brown goethite (5) and yellow goethite stained clays fill many of the voids (6).

Sample 02-5062. *Photomicrograph of a polished thin section taken in transmitted light with crossed polarisers and oblique reflected light.*

Ferricrete (LF200) (Consolidated)
Oolitic ferricrete (LF201)
Pisolitic ferricrete (LF202)
Pisolitic-nodular ferricrete (LF203)
Nodular ferricrete (LF204)
Conglomeratic ferricrete (LF206)
Vermiform ferricrete (LF231)
Vesicular ferricrete (LF233)
Mottled ferricrete (LF241)
Massive ferricrete (LF242)
Slabby ferricrete (LF243))

Ferricrete (LF200)

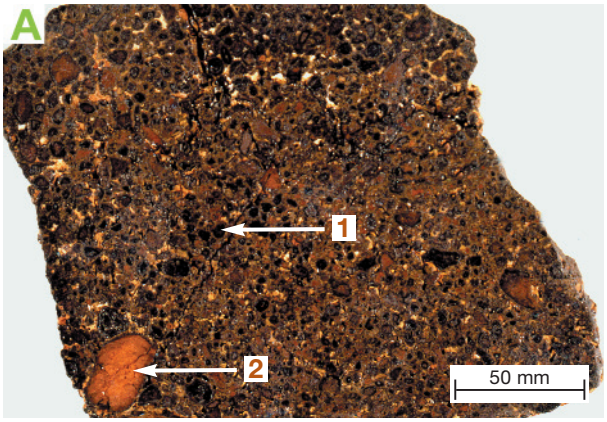

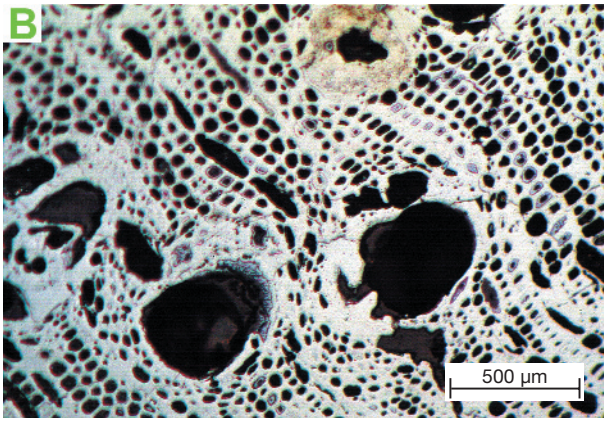

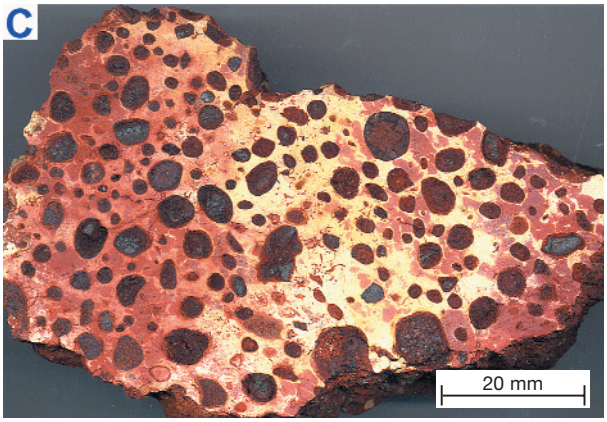

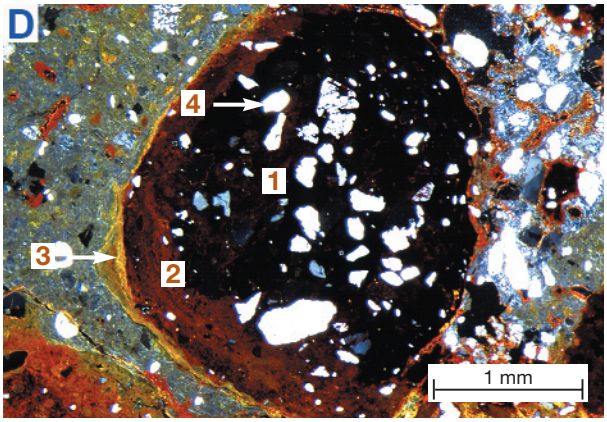

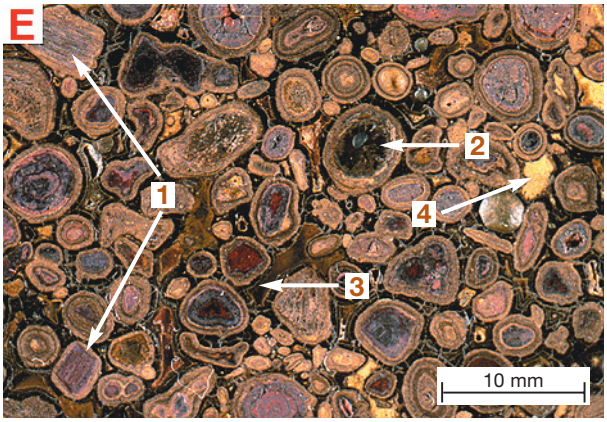

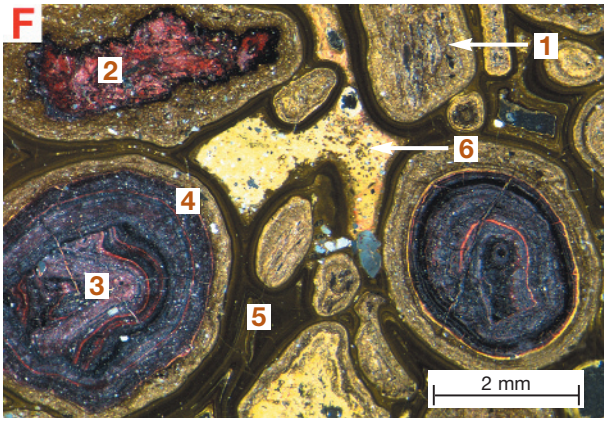

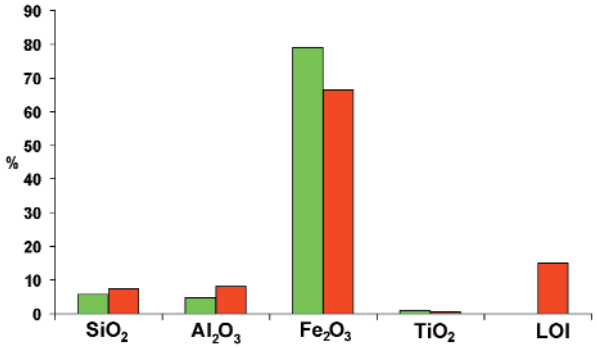

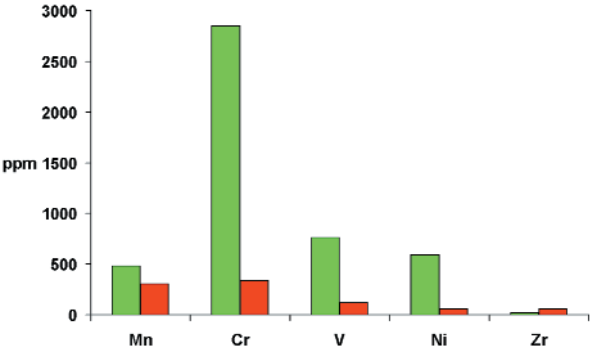

Ferricrete (LF200)

A

Pisolitic-nodular ferricrete (LF203) This ferricrete forms low mesas within a valley in the Weld Range. The sample comprises a variety of goethite-rich pisoliths and nodules, many of which have ferruginised woody fragments as their cores (1) (After Von Perger, 1991).

Madoonga, Weld Range. *Photograph of the polished surface of a hand specimen taken in oblique reflected light.*

B

A goethitised wood fragment the structure of which suggests that the precursor was a monocotyledonous plant (After Von Perger, 1991).

Madoonga, Weld Range. *Photograph of the polished surface of a hand specimen taken in oblique reflected light.*

C

Pisolitic-nodular ferricrete (LF203) This pisolitic ferricrete forms a ridge crest and unconformably overlies a mottled zone. Pisoliths exhibit a variety of cores ranging from massive dark red to black hematite-rich (1) to ferruginised clastic material (2). They have been coated and incompletely cemented by goethite (3). Irregular cavities (4) occur where the matrix has either been removed or never existed. Cavities within the cement are commonly filled with ferruginous clay (5).

Sample 07-3581. Ora Banda. *Photograph of the polished surface of a hand specimen taken in oblique reflected light.*

D

Packed rounded pisoliths with hematitic cores (1) surrounded by a series of cutans, some of which become more reflective towards the core (2). The goethitic layer that follows is slightly dehydrated showing minimal cracking (3). The outermost cutans commonly merge to cement pisoliths together (4).

Sample 07-3581. *Photomicrograph of a polished thin section taken in normally reflected light.*

E

Nodular ferricrete (LF204). Authigenic nodules in sandy sediments overlying a weathering profile formed on mafic rocks. The nodules are massive, red and are hematite- and kaolinite-rich. They are sub-angular to sub-rounded (1) and are set in a yellow to orange sandy kaolinitic matrix (2). All nodules and pisoliths have thin, yellow cutans (3). The matrix contains pale goethite-stained kaolinite spherules (4).

Sample 07-0303. C Pit, Mt Gibson. *Photograph of the polished surface of a hand specimen taken in oblique reflected light.*

F

Opaque nodules (1) with quartz grains scattered in their cores (2) have thin, yellow to orange goethitic cutans (3). The matrix contains goethitic clay clasts (4) in a goethitic sandy clay matrix (5).

Sample 07-0303. *Photomicrograph of a polished thin section taken in transmitted light and oblique reflected light.*

Ferricrete (LF200)
(Consolidated)

Oolitic ferricrete (LF201)
Pisolitic ferricrete (LF202)
Pisolitic-nodular ferricrete (LF203)
Nodular ferricrete (LF204)
Conglomeratic ferricrete (LF206)

Vermiform ferricrete (LF231)
Vesicular ferricrete (LF233)

Mottled ferricrete (LF241)
Massive ferricrete (LF242)
Slabby ferricrete (LF243)

Ferricrete (LF200)

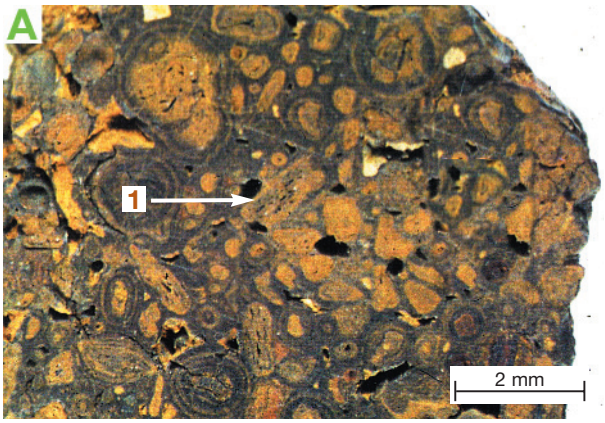

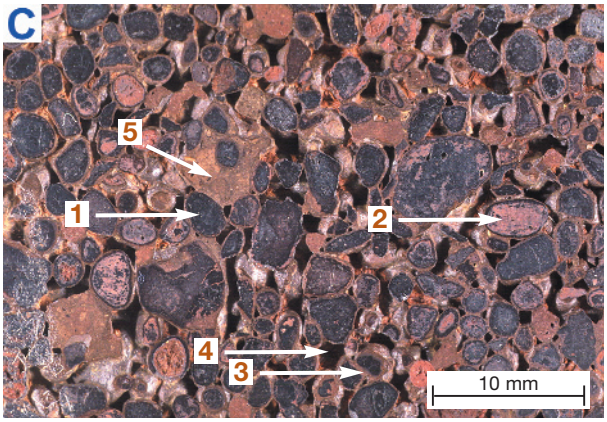

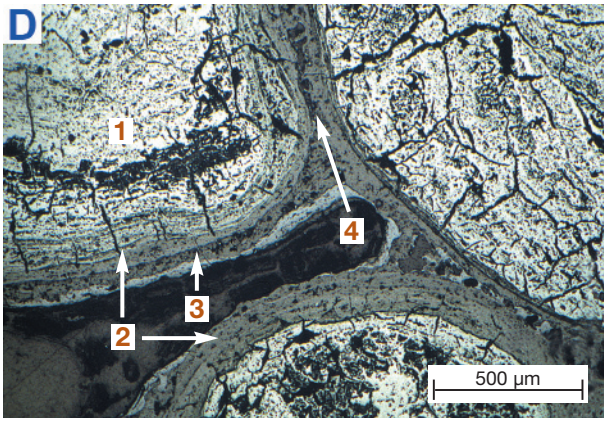

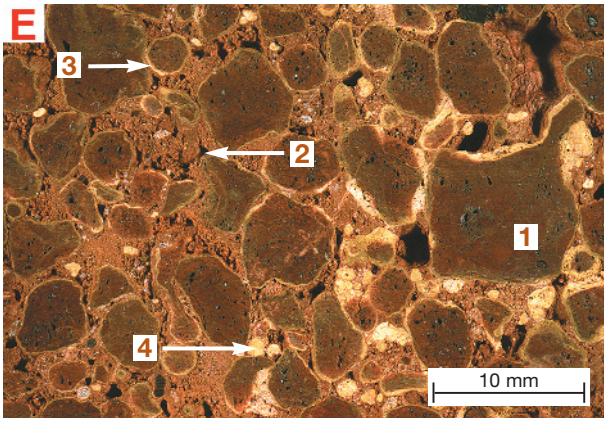

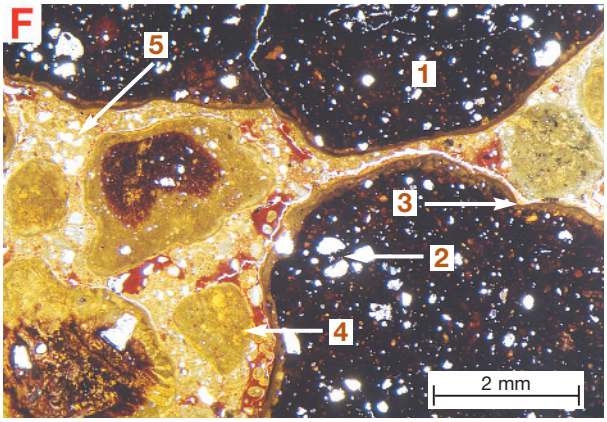

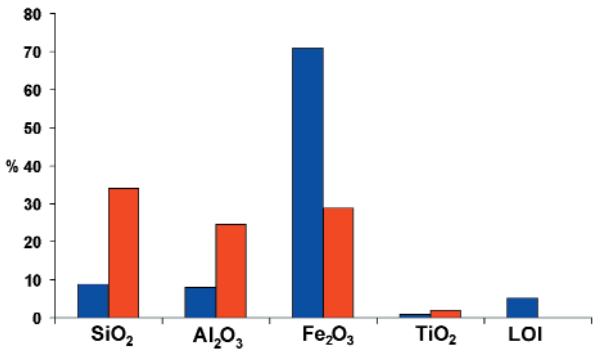

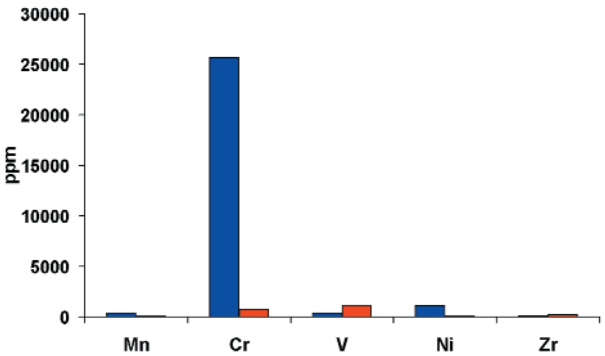

Ferricrete (LF200)

A

Conglomeratic ferricrete (LF206). This ferricrete was deposited on a weathered ultramafic bedrock and now forms a ridge crest. The outer surfaces of this sample have a marked pebbly appearance. It contains a variety of clasts from hematite-maghemite-rich ferruginous lithic fragments (1) to nodules (2) and pisoliths (3) set in a goethite-hematite-rich matrix (4). Dissolution of the matrix has left cavities (5).

Sample 07-1524. Near Cawse Find, Ora Banda. *Photograph of the polished surface of a hand specimen taken in oblique reflected light.*

B

Sub-rounded hematite-goethite-rich pisoliths (1) with goethitic cutans (2) are cemented by goethite (3). A few quartz grains occur in the matrix (4) and within the cutans (5).

Sample 07-1524. *Photomicrograph of a polished block taken in normally reflected light.*

C

Vesicular ferricrete (LF233) This ferricrete occurs on the edge of a valley floor and consists of sand cemented by goethite (1) and hematite (2). Harder, more hematite-rich areas (3) occur along with angular to rounded quartz grains in both the goethite- and hematite-rich matrix.

Sample 07-4619. Cobiac Pit, Darling Range. *Photograph of the surface of a hand specimen taken in oblique reflected light.*

D

Poorly sorted subangular to rounded quartz grains (1) embedded in a goethite-rich matrix.

Sample 07-4619. *Photomicrograph of a polished thin section taken in transmitted light with crossed polarisers.*

E

Slabby ferricrete (LF243) This outcrop of slabby ferricrete occurs on the edge of a lake at Black Flag. The ferricrete has a subhorizontal fabric that reflects the bedding in the original sediment. It consists of goethite, hematite and quartz. Small pod-shaped cavities represent ancient root channels.

Black Flag, Ora Banda.

Ferricrete (LF200) **(Consolidated)**
Oolitic ferricrete (LF201)
Pisolitic ferricrete (LF202)
Pisolitic-nodular ferricrete (LF203)
Nodular ferricrete (LF204)
Conglomeratic ferricrete (LF206)
Vermiform ferricrete (LF231)
Vesicular ferricrete (LF233)
Mottled ferricrete (LF241)
Massive ferricrete (LF242)
Slabby ferricrete (LF243))

Ferricrete (LF200)

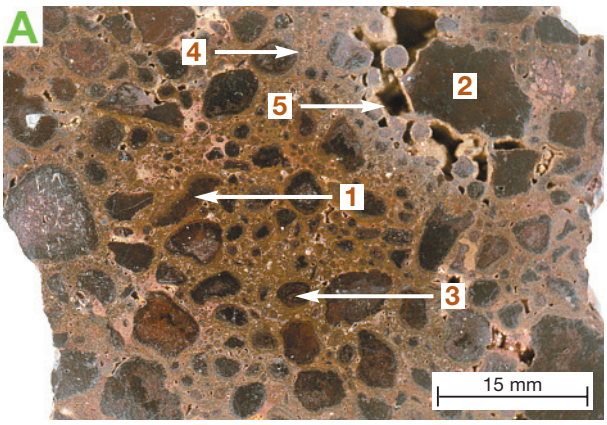

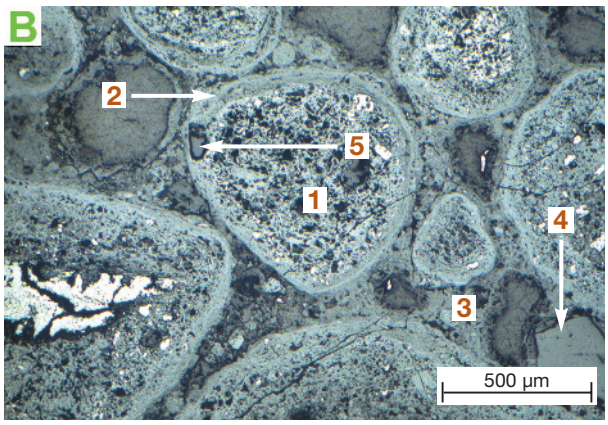

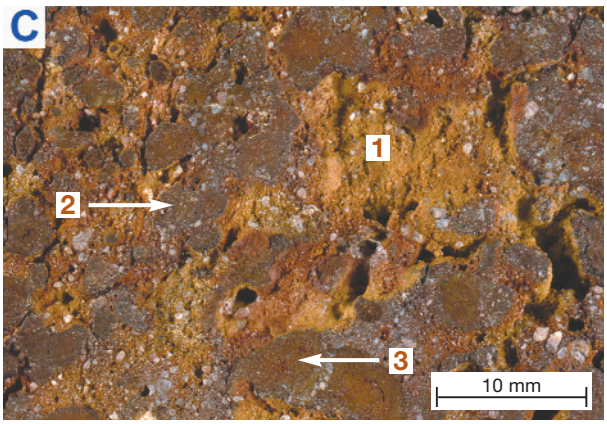

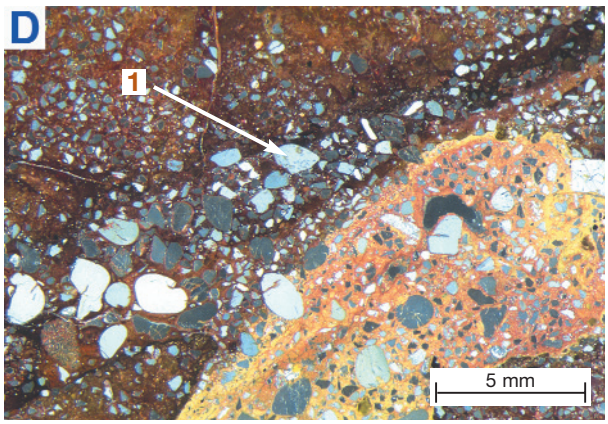

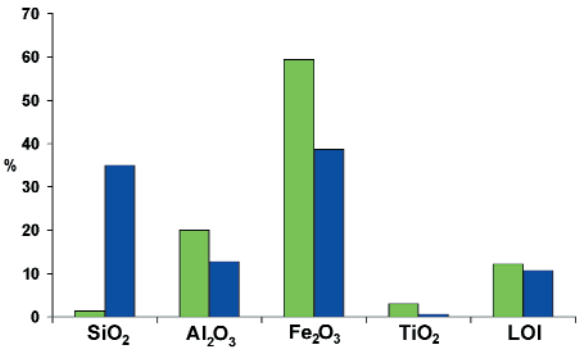

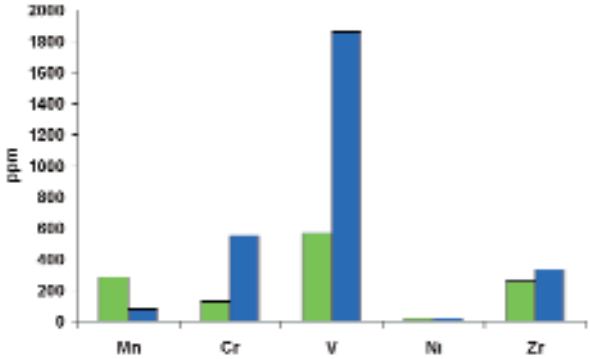

10.7 IRON SEGREGATIONS

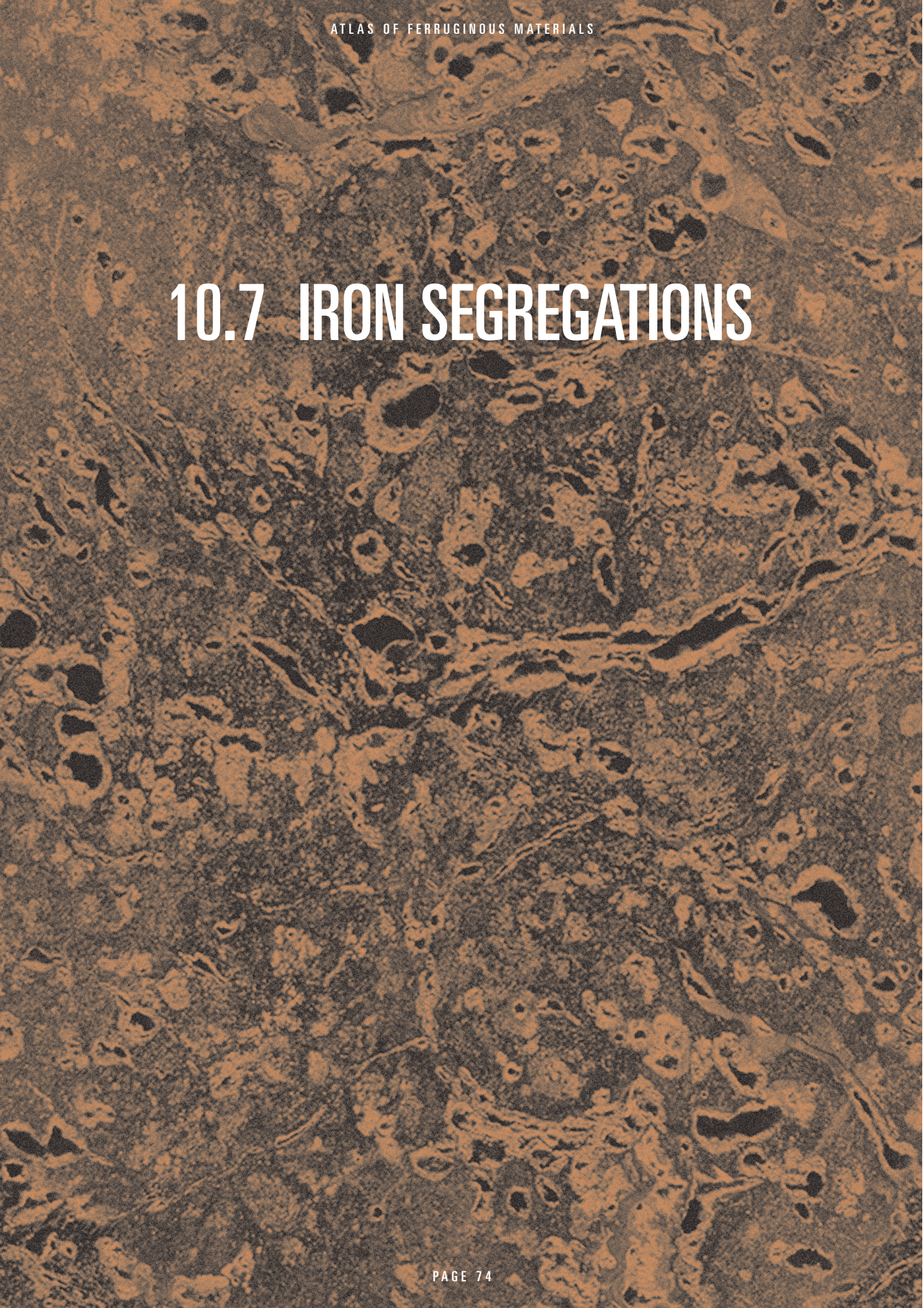

Iron segregations (IS)

A

Vesicular goethite pod (IS101). Vesicular textured goethite pod resembling an oblate spheroid. The vesicles vary from rounded to funnel-like or lenticular and irregular ranging from 1 to 7 mm (1). The voids are coated by wart-like protuberances of yellow ocherous goethite. Fracture surfaces in goethite are sub-conchoidal to hackly with a sub metallic to resinous lustre. Thin (1-3 mm across) veins of laminated earthy hematite-goethite traverse the goethite mass (2).

Sample 07-0719. S Pit, Mt Gibson. *Photograph of the polished surface of a hand specimen taken in oblique reflected light.*

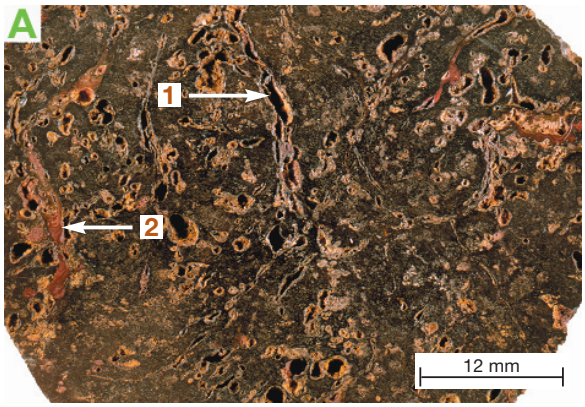

B

Vesicular goethite pod (IS101). Massive goethite (1) which is transgressed by a laminated goethite/hematite vein (2). Goethite pseudomorphs after mica also occur (3).

Photomicrograph of a polished thin section taken in transmitted light.

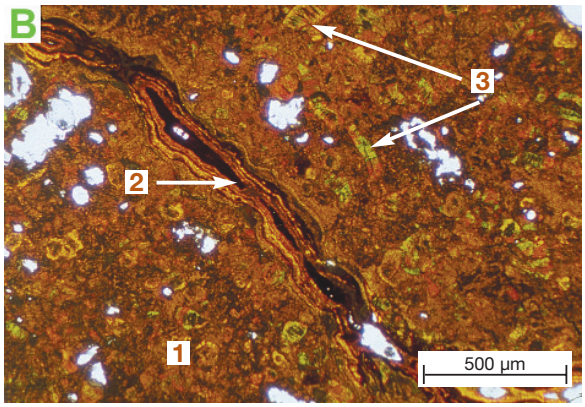

C

Discordant hematite-goethite body (IS102). This sample is from the core of a discordant, 3 m thick, sheet-like pod of goethite that is hosted by ferruginous saprolite. Crystalline goethite mesh veining (1) (the thicker veins having an internal laminar structure) are truncated by the hematite vein on the left margin of the sample (2). The latter grades from a crystalline blue grey hematite to an earthy red form (3). Fragments of white quartz (4) are included in goethite on the upper and right hand margins of the sample.

Sample 07-1164. McCaffery Pit, Lawlers*. Photograph of the polished surface of a hand specimen taken in oblique reflected light.*

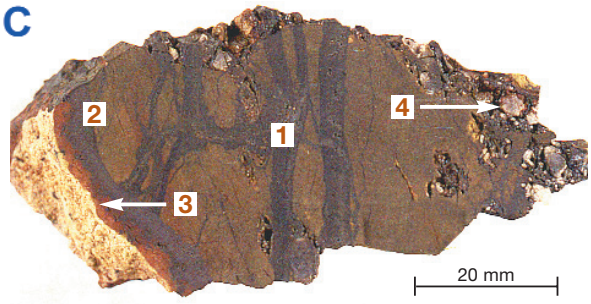

D

Stratabound hematite layer (IS201). This sample represents part of a series of 1-5 cm thick hematite layers interbanded on the decimeter scale with bleached mafic saprolite; the later displays relict porphyritic fabric. Rouge to reddish-brown porous hematite and fine-grained brown goethite appear to have replaced thin, sheared clay-rich units in a layered sequence of mafic volcanics and interflow sediments.

Sample 07-1189. McCaffery Pit, Lawlers. *Photograph of the surface of a hand specimen taken in oblique reflected light.*

Goethite-hematite segregations (IS 100)
Vesicular goethite pod (IS101)
Discordant hematite-goethite body (IS102)
Stratabound hematite-goethite body (IS103)
Goethite selvage to quartz veins (IS111)
Hematite segregations (IS200)
Strata bound hematite layer (IS201)

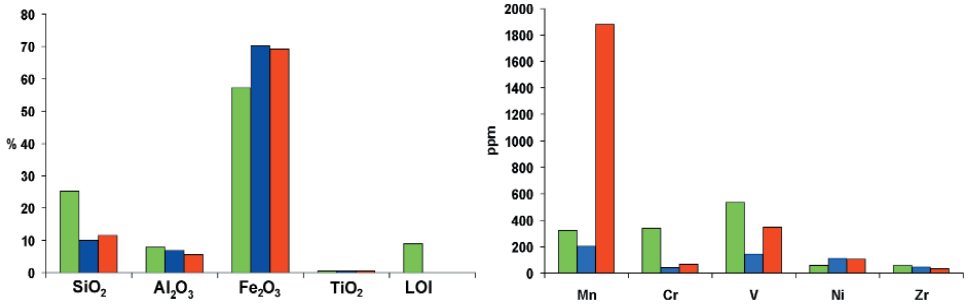

10.8 LAG

Lag (LG)

Lag is the residual accumulation of coarse, usually hard, fragments at the surface. They have been left after physical and chemical dismantling of the upper horizons of the regolith and removal of finer materials in solution, by sheetwash, wind or by churning.

A

Lag of ooliths (LG101). Handpicked ooliths from the surface. Ooliths typically have yellowish goethite-gibbsite coatings on their outer surfaces and range from 0.25-2 mm in diameter. The cores of pisoliths consist of hematite, maghemite, goethite, quartz and gibbsite. The lag is underlain by 50-100 cm thick gravelly soil which in turn overlies pisolitic duricrust.

Sample 07-1301. Jarrahdale, Darling Ranges.

B

Lag of pisoliths (LG102) Handpicked loose pisoliths with well developed yellow gibbsite-goethite cutans. The cores of the pisoliths consist of hematite, gibbsite, maghemite, quartz and goethite. The lag is underlain by 50-100 cm thick gravelly soil.

Sample 07-1302. Jarrahdale, Darling Ranges.

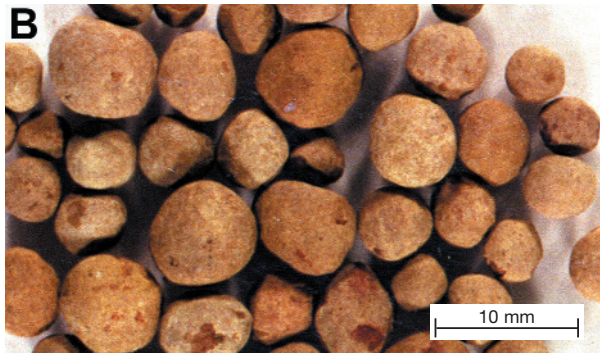

C

Lag of pisoliths (LG102). Loose fine, black, magnetic hematite-maghemite-rich ferruginous pisoliths without cutans characteristic of the lower slopes of breakaways. Lithic fragments and angular quartz clasts also occur. The lag overlies a reddish brown sandy clay loam developed in colluvium. Lateritic residuum or mottled zone is an extensive substrate to the soil. It is here suggested that pisoliths without cutans were eroded from upslope and subsequently lost their cutans during transportation.

Meatoa prospect, Lawlers.

D

Lag of nodules and pisoliths (LG103) This unit occurs on the upper backslopes of breakaways. It comprises pisoliths and nodules containing hematite, goethite and kaolinite with yellowish to reddish brown hematite-kaolinite cutans. Black pisoliths are generally magnetic. The lag is underlain by a gravelly soil which in turn overlies lateritic gravels.

Agnew, Lawlers

Lateritic Lag (LG100)
Ooliths (LG101)
Pisoliths (LG102)
Nodules and pisoliths (LG103)
Nodules (LG104)
Hardened mottles (LG105)
Nodules and hardened mottles (LG106)
Nodules, hardened mottles and pisoliths (LG107)
Lag, other (LG200)
Ferruginous saprolite (LG231)
Iron segregation fragments LG241)
Gossan fragments (LG261)

Lag (LG)

A

Lag of hardened mottles (LG105). Monomictic coarse fragments of goethite-kaolinite-hematite mottles with yellowish brown goethitic cutans characteristic of broad crests. The lag is derived from a weathering profile developed on gabbro and overlies mottled saprolite.

Agnew, Lawlers.

B

Lag of ferruginous saprolite (LG231SF). Monomictic coarse fragments of ferruginous saprolite on low hill. Their angular appearance is reflective of a preserved schistocity, and their gloss indicates intense ferruginisation and silicification. The lag is formed from the weathering of basalt and overlies ferruginous saprolite or saprolite.

Agnew, Lawlers.

C

Lag of iron segregations (LG241)
Goethite-rich iron segregations after sulphide-rich rocks. Inset shows close up of brown-black goethite-rich cobbles. The lag overlies ferruginous saprolite.

Jundee.

Lateritic Lag (LG100)
Ooliths (LG101)
Pisoliths (LG102)
Nodules and pisoliths (LG103)
Nodules (LG104)
Hardened mottles (LG105)
Nodules and hardened mottles (LG106)
Nodules, hardened mottles and pisoliths (LG107)
Lag, other (LG200)
Ferruginous saprolite (LG231)
Iron segregation fragments LG241)
Gossan fragments (LG261)

10.9 MODIFICATIONS TO FERRUGINOUS MATERIALS

Modifications of ferruginous materials (CF, HP, SF)

During arid conditions, the weathering regime changes from one favouring the export of weathering products to one in which weathering products are concentrated. Soil forming processes became dominated by calcification and silicification. The examples shown here demonstrate the affects of these modification on ferruginous materials.

A

Calcified pisolitic duricrust (LT202CF). Calcified duricrust showing ferruginous pisoliths (1) in a calcite matrix (2).

Sample 07-0304. S Pit, Mt Gibson. *Photograph of the polished surface of a hand specimen taken in oblique reflected light.*

B

Calcified pisolitic duricrust (LT202CF). Sparite (1) with interlocking calcite grains forming external hypo-coatings on subangular ferruginous pisoliths (2). The crystalline birefringent groundmass consists of calcite crystals and clays (3). (C. Phang, pers comm. 2001).

Sample 07-3828. Discovery Pit, Bronzewing. *Photomicrograph of a polished thin section taken in transmitted light with crossed polarisers.*

C

Calcified ferruginous nodule (LT104CF). A ferruginous nodule (1) with complete infilling of cracks and voids by calcite (2). Cracking results from the replacement of hematite and kaolinite by calcite.

Sample 07-1525. Ora Banda. *Photomicrograph of a polished thin section taken in transmitted light.*

D

Calcified ferruginous nodule (LT104CF). Partial replacement of hematite and kaolinite by calcite (1) leaving islands of remnant hematite (2).

Sample 07-1525. Ora Banda. *Photomicrograph of a polished thin section taken in transmitted light.*

E

Hardpanised pisolitic-nodular duricrust (LT203HP). This outcrop displays pervasive hardpanisation of a pisolitic-nodular duricrust. Sub-horizontal laminations are lined with hyalite, kaolinite and manganese oxides.

S Pit, Mt Gibson.

F

Hardpanised nodular ferricrete (LF204HP). This sample is overlain by hardpanised colluvium and underlain by ferricrete. It has a laminated matrix, nodules and pisoliths, and comprises irregular, well-rounded, hematite-rich, red, earthy nodules (1) that are typically rimmed by a yellow goethite cutan. Smaller, irregular metallic black nodules (2) are less abundant. These nodules are cemented in a yellow and red sandy clay kaolinite-rich matrix (3) that is bleached in some places. The hardpanised matrix (4) is characteristically porous, red and consists of hyalite, kaolinite, quartz and goethite.

Sample 07-556. N Pit, Mt Gibson. *Photograph of the polished surface of a hand specimen taken in oblique reflected light.*

Modifications of ferruginous materials (CF, HP, SF)

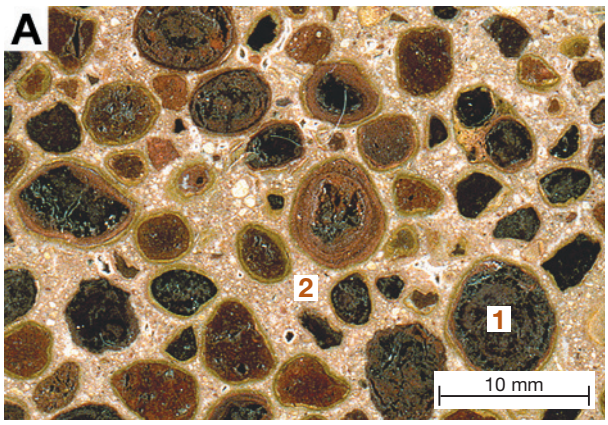

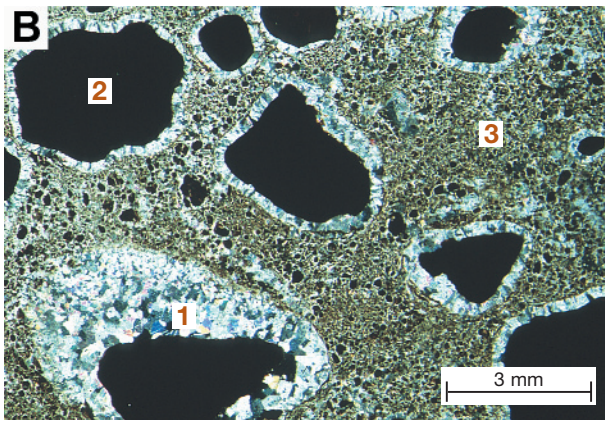

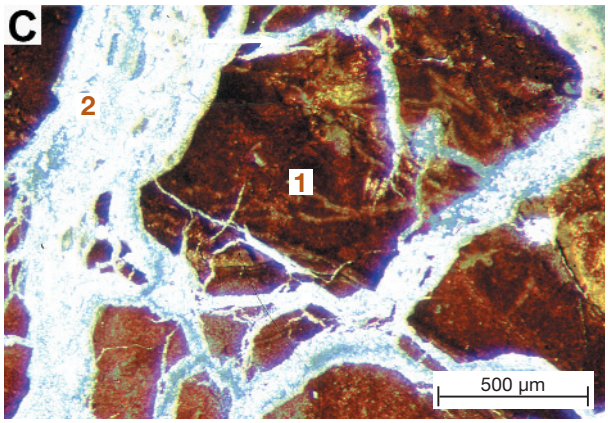

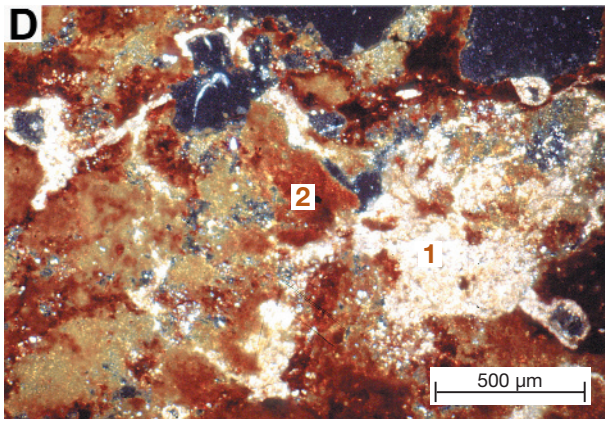

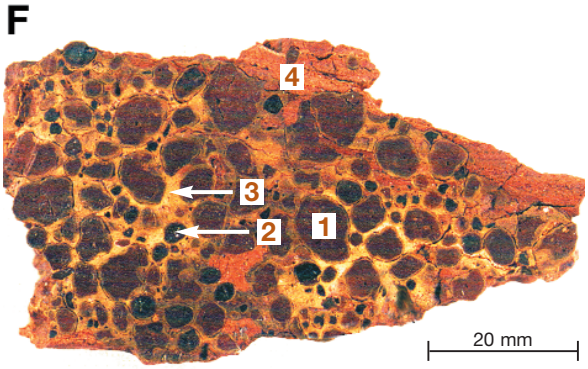

11.0 ACKNOWLEDGEMENTS

Much of the work summerised in this report was originally part of a series of large, multidisciplinary projects conducted by CSIRO and CRC LEME through the Australian Minerals Research Association (AMIRA). Acknowledgement is made to the numerous mining and exploration companies that have supported the research.

Thin and polished sections were prepared by R.J. Biltz and D. Winchester. Geochemical analyses were by M.K.W. Hart. Artwork was prepared by T. Naughton, A.D. Vartesi and C.R. Steel. P.Agnew, I.D.M. Robertson and M. F. Killick reviewed the manuscript. C. Phang and P. Phillips provided technical assistance during the production of the atlas. All this is acknowledged with appreciation. The work was supported by the Australian Government's Cooperative Research Centres' Program.

12.0 REFERENCES

Aleva, G.J.J., 1986. Classification of laterites and their textures. In: P.K. Banerjee (Editor), Lateritisation Processes, Geological Survey of India, Memoirs Vol. 120, pp 8-28.

Aleva, G.J.J., 1994. Laterite - Concepts, geology, morphology and chemistry. International Soil Reference and Information Centre (ISRIC) Wageningen. 169pp.

Anand, R.R. and Butt, C.R.M., 1988. The terminology and classification of the deeply weathered regolith. CSIRO Australia, Division of Exploration Geoscience, Perth. Discussion paper. 29 pp.

Anand, R.R., Smith, R.E., Innes, J., Churchward, H.M., Perdrix, J.L. and Grunsky, E.C., 1989. Laterite types and associated ferruginous materials, Yilgarn Block, WA: terminology, classification and atlas. CSIRO Australia, Division of Exploration Geoscience, Perth. Report 60R. CSIRO/AMIRA Project 240: Laterite Geochemistry. 90 pp.

Anand, R.R., Churchward, H.M., Smith, R.E. and Grunsky, E.C., 1991. Regolith-landform development and consequences on the characteristics of regolith units, Lawlers District, Western Australia. CSIRO Division of Exploration Geoscience. Restricted Report 166R, (Reissued as Open File Report 62, CRC LEME, Perth, 1998), 167 pp.

Anand, R.R., Smith, R.E., Phang, C., Wildman, J.E., Robertson, I.D.M. and Munday, T.J., 1993. Geochemical exploration in complex lateritic environments of the Yilgarn Craton, Western Australia. Volume 1, Volume 2 & Volume 3. CSIRO Division of Exploration and Mining. Restricted Report 442R, (Reissued as Open File Report 58, CRC LEME, Perth, 1998), 307pp., 119., 143 pp.

Anand, R.R., 1995. Genesis and classification of ferruginous regolith materials in the Yilgarn Craton: implications for mineral exploration. CSIRO Australia, Division of Exploration and Mining Research News, 3: 3-5.

Anand, R.R., 1998. Distribution, classification and evolution of ferruginous materials over greenstones on the Yilgarn Craton - implications for mineral exploration. In: R. A. Eggleton (Editor), The State of the Regolith. Proceedings of the Second Australian Conference on Landscape Evolution and Mineral Exploration, Conference Publications, Springwood, NSW. pp. 175-193.

Anand, R.R., 2000. Regolith and geochemical synthesis of the Yandal greenstone belt. In: G. Neil Phillips and Ravi R. Anand (Editors), Yandal Greenstone Belt - Regolith, Geology and Mineralisation. Australian Institute of Geoscientists Bulletin 31: 79-112.

Anand, R.R., 2001. Evolution, classification and use of ferruginous regolith materials in exploration, Yilgarn Craton. Geochemistry: Exploration, Environment, Analysis. 1, pp. 221-236.

Anand, R.R. and Paine, M. Regolith geology of the Yilgarn Craton, Western Australia: implications for exploration. Australian Journal of Earth Sciences. 49 (1) 162pp.

Bardossy, G. and Aleva, G.J.J., 1990. Lateritic Bauxites. Elsevier, Amsterdam, 624pp.

Bourman, R.P., Milnes, A.R. and Oades, J.M., 1987. Investigations of ferricretes and related surficial ferruginous materials in parts of southern and eastern Australia. Zeitschrift Fuer Geomorphologie 64: 1-24.

Bourman, R.P., 1993. Perennial problems in the study of laterite: A review. Australian Journal of Earth Sciences 40: 387-401.

Brimhall, G.H, Lewis, C., Ford, C., Bratt, J., Taylor, G., and Warin, O., 1991. Quantitative geochemical approach to pedogenesis: Importance of parent material reduction, volumetric expansion, and eolian influx in laterization. Geoderma, 51: 51-91.

Buchanan, F., 1807. A journey from Madras though the countries of Mysore, Canara and Malabar etc. (in 1800-1807). The East India Co., London, Vol 3, 1500pp.

Chan, R.A., Craig, M.A., Hazzel, M.S. and Ollier, C.D., 1992. Kalgoorlie Regolith Terrain Map and Commentary, Sheet SH51, Western Australia, 1:1000000 Regolith Series, AGSO Record, 1992/8.

Charman, J.H., 1988. Laterite in road pavements. Construction Industry Researh and Information Association (CIRIA) Special Publication 47, London, 71pp.

Clark, J.D.A. and Chenworth, L., 1995. Classification, genesis and evolution of ferruginous surface grains. AGSO Journal of Geology and Geophysics 16: 213-221.

Costa, M.L., 1993. Gold distribution in lateritic profiles in South America, Africa and Australia: applications to geochemical exploration in tropical regions. Journal of Geochemical Exploration 47: 143-163.

Costa, M.L., Romulo, S. and Costa, A.N., 1999. The geochemical association Au-As-B-(Cu)-Sn-W in latosols, colluvium, lateritic iron crust and gossan in Carajas, Brazil: importance for primary ore identification. Journal of Geochemical Exploration 67: 33-49.

Davy, R., 1979. A study of laterite profiles in relation to bedrock in the Darling Range, near Perth, W.A. Geological Survey of Western Australia Report 8, 87 pp.

Dury, G.H., 1969. Rational descriptive classification of duricrusts. Earth Sciences J13: 77-86.

Dusci, M.E., 1994. Regolith-landform evolution of the Black Flag area with emphasis on the upper reaches of the Roe Palaeochannel System, Western Australia. Honours Thesis, Curtin University of Technology, Perth, 134 pp. (unpublished).

Eggleton, R.A., 2001 (Editor). Glossary of Regolith - Surficial Geology, Soils and Landscapes. CRC LEME Publication, 144pp.

Eggleton, R.A. and Taylor, G., 1998. Selected thoughts on 'laterite'. In G. Taylor and C.Pain (Editors), New Approaches to an Old Continent Proceedings, Regolith 98, 209-226 pp.

Finkl, C.W. and Fairbridge, R.W., 1979. Paleogeographic evolution of a rifted cratonic margin: S.W. Australia. Palaeogeography, Palaeoclimatology, Palaeoecology 26: 221-52.

Freyssinet, Ph., Lecomte, P. and Edima, A. 1989. Dispersion of gold and base metals in the Mborguene lateritic profile, East Cameron. Journal of Geochemical Exploration 32: 99-116.

Glassford, D.K. and Semenuik, V., 1995. Desert-aeolian origin of Late Cainozoic regolith in arid and semi-arid South-western Australia. Palaeogeography, Palaeoclimatology, Palaeoecology 114: 131-66.

Lamplugh, G.W., 1902. Calcrete. Geological Magazine 9: 75.

Maignien, R., 1966. Review of research on laterites. United Nations Educational Scientific and Cultural Organisation, Paris, 148pp.

Mann, A.W., 1983. Hydrogeochemistry and weathering on the Yilgarn Block, Western Australia-ferrolysis and heavy metals in continental brines. Geochemistry Cosmochimica Acta 47: 181-90.

Mann, A.W. and Ollier, C.D., 1985. Chemical diffusion and ferricrete formation. Soils and Geomorphology, Catena Supplement 62: 151-57.

Martin, F. J. and Doyne, H.C., 1932. Soil Survey of Sierra Leone. Department of Agriculture, Freetown, Sierra Leone.

McFarlane, M.J., 1976. Laterite and Landscape. Academic Press, London, 151 pp.

Millot, G., 1964. Geologie des argiles. Masson, Paris, 499 pp.

Milnes, A.R., Bourman, R.P. and Northcote, K.M., 1985. Field relationships of ferricretes and weathered zones in southern South Australia: a contribution to 'laterite' studies in Australia. Australian Journal of Soil Research 23: 441-65.

Nahon, D., 1986. Evolution of iron crusts in tropical landscapes. In: M. Colman and X. Dethiver (Editors), Rates of Chemical Weathering of Rocks and Minerals. Academic Press, London, pp. 169-191.

Nahon, D.B., 1991. Introduction to the Petrology of Soils and Chemical weathering. Wiley, New York, 313pp.

Nahon, D. and Tardy, Y., 1992. The ferruginous laterites. In: C. R. M. Butt and H. Zeegers (Editors), Regolith Exploration Geochemistry in Tropical and Subtropical Terrains. Elsevier, Amsterdam, pp. 41-55.

Nair, N.G.K., Santosh, M. and Mahadevan, R., 1987. Lateritisation as a possible contributor to gold placers in the Nilambur Valley, Southwest India. Chemical Geology 60: 309-315.

Ollier, C.D., Chan, R.A., Craig, M.A. and Gibson, D.L., 1988. Aspects of landscape history and regolith in the Kalgoorlie region, Western Australia. BMR Journal of Australian Geology and Geophysics 10: 309-21.

Ollier, C.D. and Galloway, R.W., 1990. The laterite profile, ferricrete and unconformity. Catena 17: 97-109.

Ollier, C.D., 1991. Laterite profiles, ferricrete and landscape evolution. Zeitschrift Fur Geomorphologie 35: 165-73.

Ollier, C.D. and Rajaguru, S.N., 1991. Laterite of Kerala (India). Geografia Fisica e Dinamica Quaternaria 12: 27-33.

Ollier, C.D., and Pain, C.F., 1996. Regolith, Soils and Landforms. John Wiley and Sons, Chichester, 316pp.

Ostwald, J., 1990. The biogeochemical origin of the Groote Eylandt manganese oxide pisoliths and ooliths, northern Australia. Ore Geology Reviews 5: 469-490.

Pain, C.F., 1998. Landforms and regolith. In: R. A. Eggleton (Editor), The State of the Regolith. Proceedings of the Second Australian Conference on Landscape Evolution and Mineral Exploration, Conference Publications, Springwood, NSW. pp. 54-62.

Pettijohn, F.J., 1975. Sedimentary Rocks. Harper and Row, New York, 628pp.

Phang, C., Anand, R.R., Wildman, J.E. and Robertson, I.D.M., 1998. Atlas of ferruginous and siliceous materials, North Queensland. CSIRO Australia, Division of Exploration and Mining, Perth. Report 66R. CSIRO/AMIRA Project P417: Geochemical Exploration in regolith dominated terrain of North Queensland. pp 63.

Prescott, J.A. and Pendleton, R.L., 1952. Laterite and lateritic soils. Commonwealth Bureau of Soil Science. Technical Communication. Report, No. 47. Farnham Royal, Bucks, 51 pp.

Pullan, R.A., 1967. A morphological classification of lateritic ironstones and ferruginised rocks in Northern Nigeria. Nigerian Journal of Science 1: 161-73.

Robertson, I.D.M. and Butt, C.R.M., 1997. Atlas of Weathered Rocks. CSIRO Division of Exploration Geoscience, Perth. Restricted Report 390. (Reissued as Open File Report 1, CRC LEME, Perth, 1998).

Schellmann, W., 1981. Considerations on the definition and classification of laterites. In: Proceedings of the International Seminar on Lateritisation Processes, Trivandrum, India, A. A. Balkema, Rotterdam, pp.1-10.

Schellmann, W., 1983. A new definition of laterite. Natural Resources and Development 18: 7-21.

Sivarajasingham, S., Alexander, L.T., Cady, J.G. and Cline, M.G., 1962. Laterite. Advances in Agronomy 14: 1-60.

Smith, R.E. and Perdrix, J.L., 1983. Pisolitic laterite geochemistry in the Golden Grove massive sulphide district, Western Australia. Journal of Geochemical Exploration 18:131-164.

Smith, R.E., Anand, R.R., Churchward, H.M., Robertson, I.D.M., Grunsky, E.C., Gray, D.J., Wildman, J.E. and Perdrix, J.L., 1992. Laterite geochemistry for detecting concealed mineral deposits, Yilgarn Craton, Western Australia. CSIRO Division of Exploration Geoscience. Restricted Report 236R, (Reissued as Open File Report 50, CRC LEME, Perth, 1998), 181 pp.

Tardy, Y. and Nahon, D., 1985. Geochemistry of laterites, stability of Al-goethite, Al-hematite and Fe+-kaolinite in bauxites and ferricretes: an approach to the mechanism of concretion formation. American Journal of Science 285: 865-903.

Tardy, Y. and Roquin, C., 1992. Geochemistry and evolution of lateritic landscapes. In: I. P. Martini and W. Chesworth (Editors), Weathering, Soils and Paleosols. Amsterdam: Elsevier, pp. 407-43.

Trendall, A.F., 1962. The formation of apparent peneplains by a process of combined lateritisation and surface wash. Zeitschrift Fur Geomorphologie (Annals of Geomorphology) 6: 183-197.

Trescases, J.J., 1992. Chemical weathering. Regolith exploration geochemistry in tropical and subtropical terrains. In: C.R.M. and H. Zeegers (Editor), Handbook of Exploration Geochemistry 4: 25-39. Elsevier, Amsterdam.

Von Perger, A.D., 1992. Regolith development and geochemistry of the Madoonga Area, W.A. Honours Thesis, School of Applied Geology Curtin University, Perth. (unpublished).

Walther, J., 1915. Laterit in Westaustralien. Zeitschrift Deutschlands Geologie Gessellschaft 67B: 113-140.